Cytoskeleton Associated Proteins in Neurons:
The Eml family and Synaptopodin

Simone Hendrika Houtman

Cytoskeleton Associated Proteins in Neurons: The Eml family and Synaptopodin

ISBN: 978-90-9023040-5

The studies represented in this thesis were performed in the Department of Neuroscience of the Erasmus MC in Rotterdam, The Netherlands.

Cover: The microtubule network in Cos7 cells

Printed by PrintPartners Ipskamp BV, Enschede

Cytoskeleton Associated Proteins in Neurons: The Eml family and Synaptopodin

Eiwitten geassocieerd met het cytoskelet in neuronen:

De Eml familie en Synaptopodin

Proefschrift

ter verkrijging van de graad van doctor aan de
Erasmus Universiteit Rotterdam
op gezag van de
rector magnificus
Prof.dr. S.W.J. Lamberts

en volgens besluit van het College voor Promoties.

De openbare verdediging zal plaatsvinden op
woensdag 7 mei 2008 om 13.45 uur

door

Simone Hendrika Houtman

geboren te Gorinchem

ERASMUS UNIVERSITEIT ROTTERDAM

Promotiecommissie

Promotor: Prof.dr. C.I. de Zeeuw

Overige leden: Dr. C.C. Hoogenraad

Prof.dr. F.G. Grosveld

Prof.dr. P.A.E. Sillevis Smitt

Copromotor: Dr. P.J. French

Voor Jullie

Table of Contents

Chapter 5

Chapter 1

General Introduction

1.1 Brain

Humans (and animals) are able to learn (remembering events or skills) and to forget. This ability of the brain has been a subject of interest for neuroscientists, psychologists and philosophers for many decades. Already 387 B.C. Plato describes that the brain is the seat of the mental process. In 1664 Thomas Willis publishes *Cerebri anatome* (in Latin) and in 1681 he coins the term *Neurology*. With the use of a silvernitrate staining method developed by Camillo Golgi in 1873, Santiago Ramon y Cajal described that neurons are independent elements. He proposed that memories might be formed by strengthening the connections between existing neurons to improve the effectiveness of their communication. Both Camillo Golgi and Santiago Ramon y Cajal received a Nobel prize in 1906 for their contribution to the field.

1.1.1 Gross anatomy

The human nervous system can anatomically be divided into the peripheral nervous system (PNS) and the central nervous system (CNS). The PNS is the information source of the CNS and can be divided into a somatic and an autonomic part. The somatic PNS is associated with voluntary control of body movement and consist of 12 pairs of cranial nerves and 31 pairs of spinal nerves. These sensory and motor neurons innervate the skin, muscles and joints. The cell bodies of these neurons lie in the dorsal root ganglia and the cranial ganglia. Receptors associated with dorsal root and cranial ganglion cells provide sensory information to the CNS about muscle and limb positions and about touch and pressure at the body surface. The autonomic division of the PNS mediates sensation and motor control of the viscera, smooth muscles and exocrine glands. It consists of the sympathetic (response to stress), parasympathetic (restore homeostasis) and enteric system (smooth muscles of the gut).

The CNS can anatomically be divided into the spinal cord, medulla oblongata, pons, midbrain, cerebellum, diencephalon and the cerebral hemispheres (figure 1). The spinal cord is the most caudal part of the CNS. It receives sensory information from the skin, joints and muscles and contains motor neurons responsible for movement (voluntary and reflex). Rostral to the spinal cord lies the brain stem, containing the medulla oblongata, pons and midbrain. The brainstem is involved in the regulation of blood pressure and respiration, sensations (e.g. taste, hearing, vision), balance, movement, sleep and control of the facial and neck muscles.

The cerebellum contains the highest number of neurons in the CNS. Partly because the types of neurons in the cerebellum are limited, its circuitry is well understood. It receives somatosensory input from the spinal cord, motor information from the cerebral cortex, and input about balance from the

vestibular organs of the inner ear. The cerebellum is important for maintaining posture and for coordinating head and eye movement, in fine tuning of the muscle movement and for learning motor skills. The cerebellum is also involved in language and other cognitive functions.

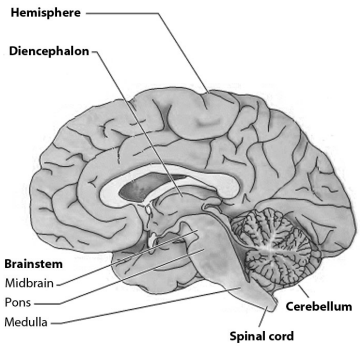

Figure 1 Sagital midsection of a human brain.

The diencephalon is formed by the thalamus and hypothalamus. The thalamus plays a gating and modulation role in relaying sensory information to the neocortex. The thalamus is also involved in modulating information from the cerebellum and basal ganglia to the cerebral cortex and is thought to influence levels of attention and consciousness. The hypothalamus regulates hormonal secretion of the pituitary gland and thus is essential for homeostasis and reproduction. The hypothalamus is also a component of the motivation system of the brain and regulates circadian rhythms.
The largest part of the brain is formed by the cerebral hemispheres. These consist of the cerebral cortex, basal ganglia, amygdala and hippocampus. Within these structures lie our perceptual, motor and cognitive functions, including memory, emotion, social behavior and fine movement.

1.1.2 Neurons

In 1836 Gabriel Gustav Valentin was the first anatomist to describe a neuron. Years later, in 1891 Wilhem von Waldeyer first introduces the term neuron. A neuron, like cells in all tissues, has a cell body with a nucleus and other subcellular components that synthesize proteins. In addition, neurons contain an axon, the function of which is to conduct signals away from the cell body (soma), and dendrites that conduct signals toward the cell body. Dendrites are extensively arborized to enlarge the surface area onto which they receive afferent input from axons of other neurons.
Over 50 distinct types of neurons have been described (figure 2). Apart from two limited regions in the adult brain (the subventricular zone and the inner

blade of the dentate gyrus) neurons no longer divide. This indicates that unlike e.g. liver cells, one neuron cannot simply be replaced by another.

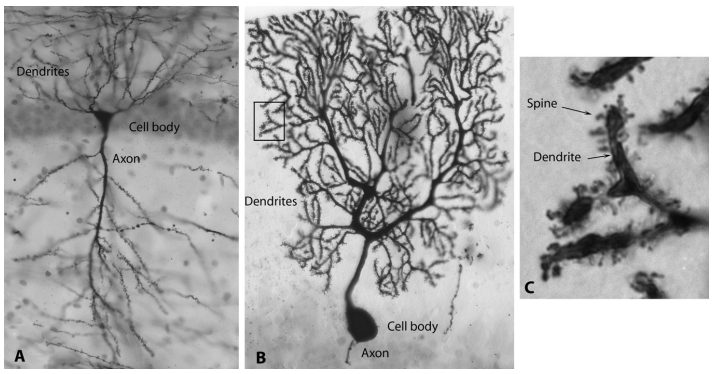

gure 2 Golgi staining of (A) Hippocampal CA1 pyramidal neuron, ith dendrites, cell body and axon. (B) Cerebellar Purkinje cell with endritic tree, a cell body and axon. (C) Enlargement of the

One of the great things of neurons is that they can communicate with each other using electrical or chemical signals. The structure where this communication between neurons takes place is called synapse. Here the membrane contains specialized proteins, like ion channels and receptors, permitting influx and efflux of inorganic ions.

1.1.3 Neuroglial cells

Supporting cells in the CNS are the neuroglial cells, also called glial cells or glia, that outnumber the number of neurons. The functions of glial cells include maintainance of the ionic milieu of nerve cells, modulation of the rate of nerve signal propagation, modulation of synaptic transmission by controlling the uptake of neurotransmitters, providing a scaffold for some aspects of neural development, formation of the blood brain barrier. Glial cells also aid in recovering from neural injury.

Three types of glial cells are described in the CNS: astrocytes, oligodendrocytes and microglial cells. A number of morphological distinct types of astrocytes can be found in the CNS. These include protoplasmic astrocytes in the gray matter, fibrous astrocytes in the white matter, radial glia in the cerebellum and sub-ependymal astrocytes adjacent to the cerebral ventricles (Eng *et al.*, 2000). As a result of trauma, neurodegenerative disorders or neurotoxicity astrocytes in the CNS proliferate and become hypertrophic. This process is called astrogliosis (Cotrina and Nedergaard, 2002; Eddleston and Mucke, 1993; Eliasson *et al.*, 1999; Eng and Ghirnikar, 1994; Rutka *et al.*, 1997).

Oligodendrocytes in the CNS, like Schwann cells in the PNS, form a myelin sheet around some axons. This myelin sheet electrically insulates the axons and so markedly increases the speed of electrical signal transmission.
Microglial cells are derived primarily form hematopoietic precursor cells. They share many properties with macrophages found in other tissues, and are primarily scavenger cells that remove cellular debris from sites of injury or normal cell turnover. In addition, they secrete signaling molecules that can modulate local inflammation and influence cell survival or death. Similar to astrocytes, the number of microglia following brain damage at the site of injury increases.

1.2 Neuronal Development

The development of human and other species starts with the fusion of the oocyte and sperm, the zygote is born. After approximately eight days two primitive cell layers (germ layers) are formed: the primary ectoderm and primary endoderm. At day 16 the primitive streak, is formed. The primitive streak evolves into a primitive groove, pit and node. The future head will be formed near the primitive pit, and the cranial/caudal, left/right, and ventral/dorsal axes of the body are established. From this primitive streak flattened cells migrate into the space between the primary ectoderm and primary endoderm forming the third primitive cell layer, the mesoderm. These flattened cells also migrate to the primary endoderm to replace cells and form the definitive endoderm, or entoderm. This process is called gastrulation. One key consequence of gastrulation is the formation of the notochord within the mesoderm. The ectoderm that lies immediately above the notochord, is called the neuroectoderm. The neuroectoderm will give rise to the entire nervous system.
The notochord signals the neuroectodermal cells to differentiate into neuronal precursor cells and so form the neural plate. The neuronal plate folds inward to form the neural tube, a structure that will give rise to the brain and spinal cord. Thickenings in the neural tube at the rostral end are formed that are the forerunners of the major brain regions. These thickenings are called the prosencephalon (forebrain), mesenchephalon (midbrain), rhombencephalon (hindbrain) and spinal cord. The prosencephalon will be divided in the telencephalon (eventually forming the cerebral cortex, hippocampus and basal ganglia) and the diencephalon (forming the thalamus and hypothalamus). The mesencephalon will form the superior and inferior colliculi whereas the rhombencephalon will be divided into the metencephalon (forming the cerebellum and pons) and the myelencephalon (forming the medulla).

During development, synaptic connections between neurons have to be made between the appropriate pre- and postsynaptic neuron. In fact, it is remarkable that axons are able to find the way to their appropriate synaptic partner, sometimes over many centimeters. Axons find their way to their postsynaptic neuron through a complex mechanism involving attractive and repulsive signaling molecules. The growth cone at the tip of the axon detects and responds to such signaling molecules. The growth cone is a sheetlike expansion of the growing axon at its tip, called a lamellipodium. Numerous fine processes called filopodia rapidly form and disappear from the lamellipodium. Growth cones are highly motile, which is mediated by rapid, controlled rearrangement of cytoskeletal elements.

1.3 Neuronal Plasticity

The nervous system can change in response to a variety of intrinsic or extrinsic inputs. This adaptation is called neuronal plasticity; the flexibility of neurons to change their neuronal network. Neuronal plasticity is obvious during the development of neural circuits. However, the adult brain must also be able to adapt to changes in the external environment e.g. to learn new skills and establish new memories. Novel information is presumed to be stored within neuronal networks. One obvious place to change neuronal network properties is at the site of communication between two neurons, the synapse. Changes in the strength of communication between neurons is therefore called synaptic plasticity. Two cellular models of synaptic plasticity have been described: long-term potentiation (LTP) and long-term depression (LTD) resulting in increases and decreases in synaptic strength respectively. LTP and LTD have extensively been studied as cellular models for learning and memory formation.

1.3.1 LTP and LTD

LTP and LTD can be induced in different ways and depend on the developmental state and the brain area. In the hippocampus, both LTP and LTD depend on the NMDA-receptor, which is a specific type of glutamate receptor. In the hippocampus LTP can be induced by a variety of protocols, which result in de activation of the NMDA receptor, resulting in an influx of Ca^{2+}. This elevation of the internal Ca^{2+} concentration is necessary for the induction of LTP. LTP can be divided into an early phase and a late phase (Malenka and Bear, 2004; Massey and Bashir, 2007). The early phase of LTP, lasting 1 to 3 hours, does not depend on protein synthesis, while the late phase, lasting at least 24 hours, of LTP requires *de novo* RNA and protein synthesis. One of the proteins that is upregulated after LTP in the hippocampus is Synaptopodin (Chapter 4).

1.4 Cytoskeleton

Cells are dynamic, they grow, divide and change shape. These dynamics requires cells to be able to rearrange their internal components. Morphological changes of all cells are directed by a filamentous system of interconnected proteins called the cytoskeleton. In eukaryotic cells the cytoskeleton consists of three different types of filaments: microtubules (1.5), intermediate filaments (1.6) and actin (1.7).

1.5 Microtubules

Microtubules are hollow filaments with a diameter of ~24 nm, each filament is built up of 13 protofilaments which are laterally bound to each other (figure 3A). Each protofilament is a chain made up of α- and β-tubulin dimers (Molodtsov *et al.*, 2005; Nogales, 2000). Within the cytoplasm heterodimers of α- and β-tubulin are present, and can bind the existing filaments. Microtubules are highly dynamic, with a slow growing minus end and a fast growing plus end (Wade and Hyman, 1997). In non-neuronal cells, almost all microtubule minus-ends are attached to the centrosome or microtubule organizing centre (MTOC), whereas in neurons few microtubules are bound to the centrosome. The centrosome or MTOC is a ring-like structure where nucleation of the microtubule takes place. γ-Tubulin, a protein with high homology to α- and β-tubulin, plays an essential role in microtubule nucleation in providing a template for the 13-protofilament microtubule structure (Bornens, 2002; Nogales, 2000).

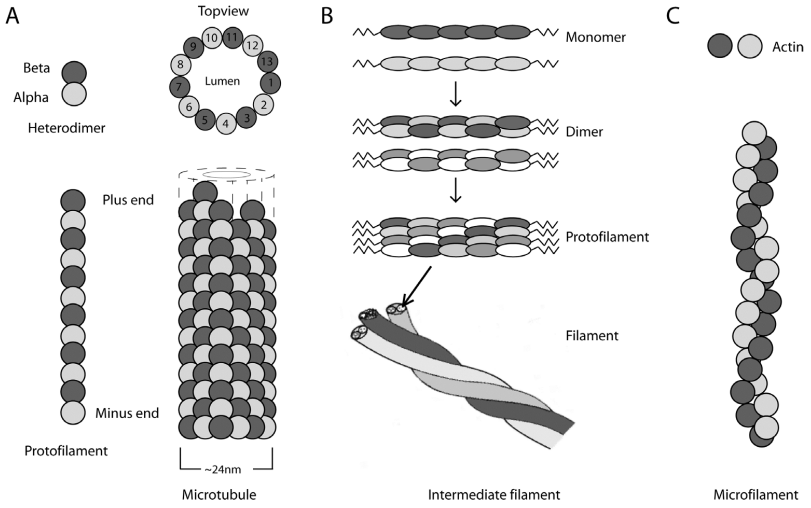

Figure 3 The cytoskeleton consists of microtubules (A), intermediate filaments (B) and actin microfilaments (C).

Both α- and β-tubulin monomers bind a GTP molecule at the nucleotide exchangeable site (E-site). During microtubule polymerization, GTP-bound tubulin heterodimers are added to the exposed ends. The GTP bound to the tubulin heterodimers is not immediately hydrolyzed because β-tubulin is a weak GTPase. As the polymer continues to assemble, GTP is hydrolyzed to GDP. As result of GTP hydrolysis, the plus end generally has a multilayer GTP cap of approximately five or more tubulin layers (Schek *et al.*, 2007). However, if dimer addition is faster than that of GTP hydrolysis, the size of the GTP cap will increase. In contrast, if GTP hydrolysis exceeds microtubule assembly, GDP-tubulin subunits will appear at the microtubule tip. GDP bound β-tubulin can assume a curved conformation. This conformation will break up the lateral interactions between protofilaments. This results in microtubule disassembly at the plus-end. Because all of the tubulin inside the microtubule filament is in the GDP conformation, depolymerization is a rapid process (Nogales, 2000; Schek *et al.*, 2007).

1.5.1 Microtubule binding proteins

The stability of microtubules is regulated by microtubule associated proteins (MAPs). MAPs can be divided into a number of distinct subgroups based on their site of binding to the microtubule (e.g. the microtubule lattice or the plus ends so called +TIPs proteins). MAPs can also be categorized based on their functional properties: those that stabilize the microtubule (e.g. MAP2, tau) and those that destabilize the microtubule (e.g. MCAK, Op18/Stathmin, XKLP2). Whether MAPs stabilize or destabilize MTs is a sum of the overall dynamics of microtubules: their growth and collapse rate and their frequency of switching between polymerization and depolymerization (catastrophe and rescue). Examples of each are stated below.

1.5.2 Microtubule stabilizing proteins

Archetypical stabilizing MAPs are MAP2 and tau in neurons and MAP4 in non-neuronal cells. These MAPs bind to the surface of microtubules, interacting with multiple tubulins with their C-terminus, stabilize them and promote assembly (Heald and Nogales, 2002). The N-terminal part is thought to project out of the microtubule surface and interacts with other cytoplasmic components. In neurons, the microtubule stabilizing effect of MAP2 and tau is observed as an increase in the polymerization and rescue rate and a decreased rate of catastrophes (Desai and Mitchison, 1997). MAP2 does not only bind to microtubules, it can also associate with actin microfilaments, membrane organelles and the post-synaptic density in dendritic spines (Caceres *et al.*, 1984; Dehmelt and Halpain, 2005; Farah *et al.*, 2005).

	Polymerization	Depolymerization	Frequency of rescue	Frequency of catastrophe
MAP2	↑		↑	↓
Tau	↑		↑	↓
XMAP215	↑↑	↑	↑	
EB-1				↓

Table 1 Microtubule stabilizing proteins. ↑ increase, ↓ decrease.

Several splice-variants of MAP2 are expressed in brain tissue, some of which show developmentally regulated expression (Shafit-Zagardo and Kalcheva, 1998). For example, MAP2A is expressed only in mature brain whereas MAP2B is expressed both in the developing brain and the mature brain. MAP2C is highly expressed during development and down-regulated during maturation. Glial cells abundantly express MAP2D.
MAP2 can be phosphorylated by cAMP-dependent protein kinases (e.g. CamKII, PKA, PKC, cdc2 kinase) and dephosphorylated by protein phosphatases (PP1, PP2A, PP2B). The binding efficiency of MAP2 to tubulin depends on its phosphorylation status (Avila *et al.*, 1994; Itoh *et al.*, 1997).
Several distinct Tau splice-variants have been described. One class of Tau isoforms contains three tubulin-binding motifs and is mainly expressed in the developing brain. Another class of Tau isoforms contains four tubulin-binding motifs and is mainly expressed in the mature brain. Tau is predominantly localized to the neuronal axon, where it is required for its elongation. Tau can be phosphorylated by kinases like CamKII, PKC and Cdk5 and dephosporylated by protein phosphatases like PP2A and PP2B. Phosphorylated and dephosphorylated Tau exhibit decreased and increased affinity for tubulin respectively. A hyperphosphorylation of Tau proteins is found in several neurodegenerative disorders, like Alzheimer's disease (Avila *et al.*, 1994).

TOGp (XMAP215) was first discovered in Xenopus eggs and is expressed in ectodermal and neuroectodermal tissue during development. XMAP215 strongly increases the polymerization rate of pure tubulin, but only the plus ends, thereby affecting the dynamics of microtubules in a different manner compared to the classical MAPs (Becker and Gard, 2000; Charrasse *et al.*, 1998). XMAP215 binds to the microtubule plus-end and stabilizes weakly attached tubulin dimers (Brouhard *et al.*, 2008). XMAP215 also increases the rate of rapid depolymerization and decreases the rescue frequency, increasing the microtubule turnover (Kinoshita *et al.*, 2002). In the brain TOGp

is abundantly expressed in the Purkinje cells of the cerebellum (Charrasse *et al.*, 1996).

EB1 binds to the tips of growing microtubules and is therefore called an +TIP protein. In mitosis EB1 stabilizes the tubulin polymer by preventing catastrophes (Tirnauer *et al.*, 2002). EB1 is highly expressed in the distal axon of neurons. EB1 can interact with most other +TIPs (e.g. APC, CLASPs, CLIPs) (Akhmanova and Hoogenraad, 2005; Gu *et al.*, 2006).

1.5.3 Microtubule destabilizing proteins

The high frequency of catastrophe in cells compared to the frequency of catastrophe observed with pure tubulin in vitro suggested the existence of factors that promoted catastrophes. It was hypothesized that these factors underlie rapid changes in microtubule dynamics, for example during interphase-mitosis transition.

	Polymerization	Depolymerization	Frequency of rescue	Frequency of catastrophe
Op18/stathmin	↓			↑
Katanin				↑
MCAK		↑		↑

Table 2 Microtubule destabilizing proteins. ↑ increase, ↓ decrease.

The first microtubule destabilizing protein identified was Op18/stathmin, which is expressed in the cytosol of neurons (Belmont and Mitchison, 1996; Curmi *et al.*, 2000; Hanash *et al.*, 1988; Himi *et al.*, 1994; Ohkawa *et al.*, 2007; Price *et al.*, 2000). Op18/stathmin sequesters tubulin dimers, which leads to lower tubulin dimer concentrations. Lower tubulin concentrations have two effects, it slows microtubule growth and induces catastrophe by promoting the hydrolysis of microtubules by removal of the stabilizing GTP cap (Cassimeris, 2002; Heald and Nogales, 2002).
Katanin is a distinct microtubule destabilizing protein. It destabilizes polymers by removing the GTP-cap, generating new ends (Hartman *et al.*, 1998; McNally and Thomas, 1998; McNally and Vale, 1993). In effect, katanin severs microtubules and is essential for releasing microtubules from the neuronal centrosome (Ahmad *et al.*, 1999). The releasing from the centrosome is necessary for the transport of microtubules into the axon (Ahmad *et al.*, 1994).

Tradionally kinesins are proteins that move along the microtubule lattice, however some kinesin-like proteins cause destabilization of microtubules. An

example of such "catastrophe kinesin" is MCAK. MCAK uses ATP to destabilize both microtubule ends and causes a conformational change, which results in protofilament ´peeling´ (Desai *et al.*, 1999; Howard and Hyman, 2003; Hunter *et al.*, 2003; Kinoshita *et al.*, 2006; Walczak *et al.*, 1996).

1.5.4 EMAP family

The most abundant MAP in dividing sea urchin eggs and embryos is the echinoderm microtubule associated protein (EMAP) (Li and Suprenant, 1994; Suprenant *et al.*, 1993). EMAP is a 77 kDa polypeptide with almost no homology to other MAPs (Li *et al.*, 1998). Five EMAP homologs have been identified in mammals (EML1-5)(Eudy *et al.*, 1997; Heidebrecht *et al.*, 2000; Jin *et al.*, 2004; Lepley *et al.*, 1999; O'Connor *et al.*, 2004; Pozuelo Rubio *et al.*, 2004).

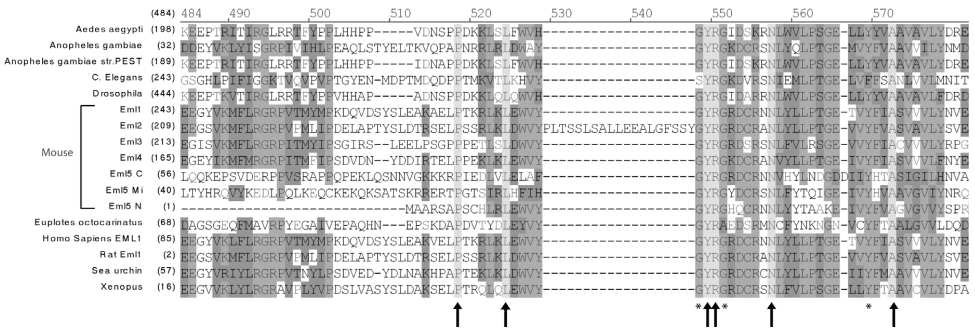

Figure 4. HELP domain evolutionary conserved. The HELP domain of all mouse Emls compared with Emls from e.g. drosophila, c. elegans and xenopus. Arrows: conserved amino acid; * conserved amino acid except for one specie.

The sequence of EMAP is highly conserved during evolution. Several distinct domains are present within the primary protein structure. The hydrophobic EMAP-like protein (HELP) domain is unique for this family and is localized at the N-terminal end of the protein (figure 4). The HELP domain is a hydrophobic domain that is thought to be involved in microtubule binding (Eichenmuller *et al.*, 2001; Li and Suprenant, 1994).

Multiple WD40 domains are present at the C-terminal end of the protein. These domains are putative protein-protein interaction domains that can form a blade of a propeller-like structure. A coiled-coil domain is present in most of the mammalian EMAPs. This domain is a putative dimerization domain, suggesting Emls can form homo- or heterodimers (Lupas *et al.*, 1991).

In vitro EMAP binds with a high affinity to both microtubules and tubulin dimers. It effects microtubule dynamics as microtubules are slightly longer in the presence of EMAP. EMAP reduces the frequency of rescue (Eichenmuller

et al., 2001; Hamill *et al.*, 1998; Nogales, 2000). Similar to other MAPs, EMAP can be phopshorylated. EMAP is, on average, constitutively phosphorylated on 5 serine residues (Brisch *et al.*, 1996; Li and Suprenant, 1994). $p34^{cdc2}$ phosphorylates EMAP in a cell-cycle dependent manner.

Mammalian homologs

Eml1 (ELP79/HuEMAP-1) was isolated as a protein product within the Usher1a locus (Eudy *et al.*, 1997). Usher syndrome is an autosomal recessive disorder that manifests as congenital deafness, retinitis pigmentosa and balance problems. So far at least 13 distinct loci have been associated with Usher syndrome. Three types of Usher syndrome have been described, children with Usher type I are born deaf and have balance problems. During childhood, around the age of 10, these children develop retinitis pigmentosa and become blind. Children with type II have hearing disabilities, no balance problems and the retinitis pigmentosa starts around puberty. Usher syndrome type III is characterized by a normal hearing and vision at birth with varying onset of hearing disability and blindness (Sankila *et al.*, 1995; Smith *et al.*, 1994). Eml1 is also found as a fusion protein with ABL1 in T-cell acute lymphoblastic leukemia. Normally Eml1 is not expressed in leukemic cells (De Keersmaecker *et al.*, 2005).

Eml2 (ELP70/HuEMAP-2) is localized to chromosome 19 and is mainly expressed in heart, brain, placenta pancreas, colon, thyroid, spinal cord and adrenal gland (Lepley *et al.*, 1999). Within the brain, Eml2 is expressed in the inferior and superior colliculi and in nuclei of the brainstem. A relatively low expression of Eml2 is found in cortex, hippocampus and cerebellum (Ly *et al.*, 2002). Eml2 is a microtubule destabilizing protein, it decreases the nucleation, decreases the elongation length and increased the catastrophe rate (Eichenmuller *et al.*, 2002). Eml2 is also described as a binding partner of the delta1 and delta2 glutamate receptor (Ly *et al.*, 2002).

Eml3 (ELP95) is localized to chromosome 11, and interacts with 14-3-3 in HeLa cells (Jin *et al.*, 2004; Pozuelo Rubio *et al.*, 2004).

Eml4 (ELP120/ROPP120/C2ORF2) is localized to chromosome 2, was found to be "overexpressed" during mitosis (Heidebrecht *et al.*, 2000). Eml4 binds to microtubules and is essential for the formation of a microtubule network (Pollmann *et al.*, 2006). Eml4 is also found as a fusion protein in lung cancer where Eml4 is fused N-terminally to the ALK tyrosine kinase. Both the basic, HELP and WD40 domains are necessary for the formation of the tumor (Meyerson, 2007; Soda *et al.*, 2007).

Eml5 was first described by our group (O'Connor *et al.*, 2004) and contains a 2.5 fold repeat of the complete EMAP protein. Eml5 is also found as a

quantitative trait loci for intramuscular fat content (Sato *et al.*, 2006). The role of any Eml in neurons is not yet described.

1.6 Intermediate filaments

Intermediate filaments have a diameter of approximately 10 nm (figure 3B). All intermediate filaments contain (1) a N-terminal head domain, which is important for self-assembly by phosphorylation; (2) a highly conserved central a-helical rod domain, essential for the packing of the a-helical coil and for co-assembly; and (3) a C-terminal tail domain needed for self-assembly and important for interaction with other cytoskeleton elements (Rutka *et al.*, 1997).
The intermediate filaments can be divided into at least five distinct types encoded by approximately 65 human genes. Type I and II are, respectively, the acidic and basic keratins, type III include desmin, vimentin, glial fibrillary acidic protein and peripherin. The neuron specific intermediate filaments NF-L, NF-M and NF-H form the type IV together with nestin, a internexin, syncoilin and synemin. In type V intermediate filaments are the lamins, which have a structural function in the nucleus. Filensin and Phakinin are intermediate filaments that are not yet divided into any type of intermediate filaments (Barry *et al.*, 2007; Oshima, 2007).

1.7 Actin

Actin is the most abundant cytoskeletal protein in the cell and is encoded by 6 genes (three alpha, one beta and two gamma actin). The total pool of actin consists of polymerized, filamentous (F) actin and unpolymerized, globular (G) actin. Only a small portion of the globular actin is not in a complex with other proteins. G-actin is essential for rapid reorganization of the network when motility is needed. ATP-bound actin monomers polymerize head-to-tail to form filamentous actin. Two parallel F-actins form a rod-like helical filament (microfilament) with a diameter of 5-7 nm (figure 3C).
Actin filaments have an intrinsic polarity, both in their structure and in their way of assembly. The two ends of the filament polymerize at different rates resulting in a fast growing plus (or barbed) end and a slower growing minus (or pointed) end (Wegner, 1976).
Polymerization starts with the formation of a nucleation site. Nucleation sites can be formed *de novo*, from the sides of existing filaments or by severing of an existing filament. Once nucleated, rapid polymerization occurs and ATP-bound monomers are added to the exposed ends of the growing polymer. As the filaments matures, the ATP is hydrolyzed and ADP-actin is released from the pointed end. Nucleotide exchange regenerates ATP-actin monomers that can again be added to the growing end of the filament. After the initial fast polymerization, an equilibrium phase is reached when the growth of polymer

due to monomer additions is precisely balanced by the shrinkage due to monomer loss. At this point, the net length of the filament remains constant, even though polymer addition and loss continues. This process is called 'treadmilling' (Margolis et al., 1978).
Actin filaments form short polymers: they are concentrated at the cell's periphery in the cortical cytoplasm lying just underneath the plasmalemma, where, together with a large number of actin-binding proteins (e.g. secrin-fodrin, ankyrin, talin and actinin), they form a dense network. This matrix plays a key role in the dynamic function of the cell's periphery, such as the motility of growth cones during development, generation of specialized microdomains on the cell surface, and the formation of pre- and postsynaptic morphologic specializations.

1.7.1 Actin binding proteins

The dynamics of the actin cytoskeleton is regulated by actin binding proteins (ABPs). The molecular mechanism ABPs use to influence the actin microfilament on the molecular level are diverse (figure 5). Their net result on actin polymerization determines whether ABPs stabilize or destabilize actin filaments. Different approaches can be used by an ABP, namely nucleating, capping, severing, crosslinking, bundling, sequestering, delivering monomers or promoting monomer nucleotide exchange.

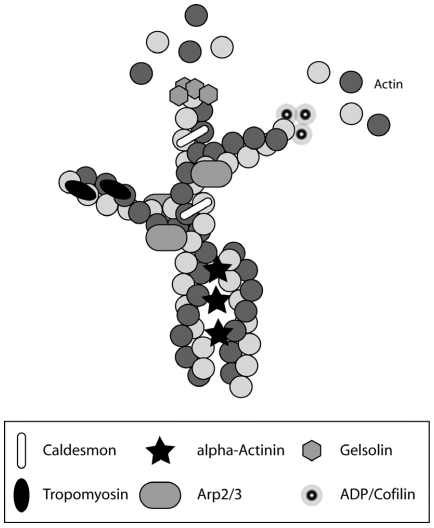

Figure 5. A model of an actin filament with divers ABP

Examples of ABP with different approaches to stabilize or destabilize the actin filaments are given below.
1) a-Actinin, an actin cross-linking protein, that does not bind to G-actin, but binds reversibly to F-actin (McGough *et al.*, 1994; Miyata *et al.*, 1996). a-

Actinin organizes actin filaments in a parallel fashion, like in a contracting network (Biron and Moses, 2004; Nakagawa *et al.*, 2004).
2) the Arp2/3 complex consist of 7 polypeptides and was first identified based on its affinity to profilin. The Arp2/3 complex is activated by the nucleation-promoting factor (NPF) resulting in the formation of new filaments from the existing filament with a regular angle of 70˚ (Goley and Welch, 2006).
3) Caldesmon, an ABP with two actin binding sites within its C-terminus. Both sites bind with adjacent actin microfilaments forming interstrand interactions. The net result of these interstrand "crossbridges" is an increase in filament length by 1.6 fold (Greenberg *et al.*, 2007).
4) Tropomyosin, an ABP that forms a cable along the actin microfilament lattice. By forming this cable, Tropomyosin strengthens the monomer-monomer intrastrand interaction within one F-Actin filament. As a result of this stabilization, the actin filament remains 1.5-2.0 times its 'normal' length (Greenberg *et al.*, 2007).
5) ADP/cofilin is a small protein of about 15-20 kDa. It binds preferentially to GDP-F-actin, causing a twist of the microfilament of 5˚. As a result, the actin filament depolymerizes. ADP/cofilin can be regulated by phosphorylation. Phosphorylation causes a reduced affinity to actin though the physiological effects of this remains to be investigated (Paavilainen *et al.*, 2004).
6) The gelsolin family of ABPs consists of seven different proteins: gelsolin, adseverin, villin, capG, advillin, supervillin and flightless I. Gelsolin, the founding member of this family, can bind actin filaments and severs them, cap the plus end and assist in the formation of polymerization nucleation sites. Gelsolin, is a calcium activated ABP.(Silacci *et al.*, 2004; Sun *et al.*, 1999).

1.7.2 Synaptopodin

Synaptopodin is a proline-rich actin associated protein, expressed in differentiated renal podocytes, in the spine neck of telencephalic neurons, and in the axonal initial segment (Bas Orth *et al.*, 2007; Mundel *et al.*, 1997). In the spine neck Synaptopodin associates with F-actin, a-actinin and the spine apparatus. In the axonal initial segment Synaptopodin associates with the cisternal organelle (Bas Orth *et al.*, 2007; Bas Orth *et al.*, 2005; Deller *et al.*, 2003; Deller *et al.*, 2000a; Deller *et al.*, 2000b; Deller *et al.*, ; Kremerskothen *et al.*, 2005).

Synaptopodin has two 'close' homologs: Myopodin and Fesselin (Leinweber *et al.*, 1999; Schroeter and Chalovich, 2005; Weins *et al.*, 2001).
Myopodin shares significant sequence homology to Synaptopodin and is expressed as a 80 kDa protein in skeletal muscles, colon, stomach, uterus and lung and as a 95 kDa protein in the heart. These two different protein sizes are

either due to splice variants or post-translational modifications. Within the muscle cells Myopodin localizes with the Z-disc, a line that divides the sacromeres (Weins *et al.*, 2001). Fesselin, a 103 kDa protein, is expressed in smooth muscle cells (Leinweber *et al.*, 1999). Furthermore it is known that Fesselin is regulated by Calmodulin, through this pathway the Ca^{2+} levels affect the polymerization of actin (Kolakowski *et al.*, 2004; Schroeter and Chalovich, 2004).

Synaptopodin can bind to the actin cytoskeleton and rearrange the microfilaments (Asanuma *et al.*, 2005). In addition, Synaptopodin interacts with a-actinin (an actin binding protein), MAGI (a member of the MAGUK scaffolding proteins) and, RhoA (a Ras homologue known to regulate stress fiber formation) (Asanuma *et al.*, 2005; Asanuma *et al.*, 2006; Kremerskothen *et al.*, 2005). Although Synaptopodin associates with actin, and other proteins its functional domains remain to be characterized.
Synaptopodin expression is upregulated after neuronal activity (Deller *et al.*, 2007; Fukazawa *et al.*, 2003; Kikuno *et al.*, 1999; Matsuo *et al.*, 1998; Matsuo *et al.*, 2000; Roth *et al.*, 2001; Yamazaki *et al.*, 2001) and Synaptopodin knock out mice show loss of LTP, impaired spatial learning, and loss of spines with a spine apparatus.
In conclusion, these data suggest a role for Synaptopodin and the spine apparatus in synaptic plasticity. However, the underlying mechanism still has to be unraveled.

1.8 Scope of this thesis

The cytoskeleton of neurons is highly dynamic. Therefore detailed analysis of cytoskeletal proteins in the mammalian brain is essential to understand the role of the cytoskeleton during development and neuronal plasticity.
In **Chapter 2** we describe Eml4, a member of the echinoderm microtubule associated protein (EMAP) family that shows developmentally regulated expression. We show that Eml4 expression is maintained at low levels in the adult mouse olfactory bulb, hippocampus and cerebellum. Functional analysis demonstrates that Eml4 is a microtubule stabilizing protein. In **Chapter 3** we describe the cloning and expression of a novel member of the EMAP family, Eml5. We concluded that rat Eml5 is expressed in rat olfactory bulb, hippocampus and cerebellum. Eml5 is unusual because it contains tandem repeats of the typical EMAP domains. In **Chapter 4** we functionally characterized Synaptopodin, a protein that bundles the actin cytoskeleton in neurons. We provide evidence for the presence of at least two Synaptopodin splice variants in rat brain. Only one of these isoforms shows activity

associated expression. Functionally, the activity associated Synaptopodin isoform can modify the actin cytoskeleton perhaps by recruitment of other actin bundling proteins like a-Actinin.

1.9 References

Ahmad, F.J., H.C. Joshi, V.E. Centonze, and P.W. Baas. 1994. Inhibition of microtubule nucleation at the neuronal centrosome compromises axon growth. *Neuron*. 12:271-80.

Ahmad, F.J., W. Yu, F.J. McNally, and P.W. Baas. 1999. An essential role for katanin in severing microtubules in the neuron. *J Cell Biol*. 145:305-15.

Akhmanova, A., and C.C. Hoogenraad. 2005. Microtubule plus-end-tracking proteins: mechanisms and functions. *Curr Opin Cell Biol*. 17:47-54.

Asanuma, K., K. Kim, J. Oh, L. Giardino, S. Chabanis, C. Faul, J. Reiser, and P. Mundel. 2005. Synaptopodin regulates the actin-bundling activity of alpha-actinin in an isoform-specific manner. *J Clin Invest*. 115:1188-98.

Asanuma, K., E. Yanagida-Asanuma, C. Faul, Y. Tomino, K. Kim, and P. Mundel. 2006. Synaptopodin orchestrates actin organization and cell motility via regulation of RhoA signalling. *Nat Cell Biol*. 8:485-91.

Avila, J., J. Dominguez, and J. Diaz-Nido. 1994. Regulation of microtubule dynamics by microtubule-associated protein expression and phosphorylation during neuronal development. *Int J Dev Biol*. 38:13-25.

Barry, D.M., S. Millecamps, J.P. Julien, and M.L. Garcia. 2007. New movements in neurofilament transport, turnover and disease. *Exp Cell Res*. 313:2110-20.

Bas Orth, C., C. Schultz, C.M. Muller, M. Frotscher, and T. Deller. 2007. Loss of the cisternal organelle in the axon initial segment of cortical neurons in synaptopodin-deficient mice. *J Comp Neurol*. 504:441-9.

Bas Orth, C., A. Vlachos, D. Del Turco, G.J. Burbach, C.A. Haas, P. Mundel, G. Feng, M. Frotscher, and T. Deller. 2005. Lamina-specific distribution of Synaptopodin, an actin-associated molecule essential for the spine apparatus, in identified principal cell dendrites of the mouse hippocampus. *J Comp Neurol*. 487:227-39.

Becker, B.E., and D.L. Gard. 2000. Multiple isoforms of the high molecular weight microtubule associated protein XMAP215 are expressed during development in Xenopus. *Cell Motil Cytoskeleton*. 47:282-95.

Belmont, L.D., and T.J. Mitchison. 1996. Identification of a protein that interacts with tubulin dimers and increases the catastrophe rate of microtubules. *Cell*. 84:623-31.

Biron, D., and E. Moses. 2004. The effect of alpha-actinin on the length distribution of F-actin. *Biophys J*. 86:3284-90.

Bornens, M. 2002. Centrosome composition and microtubule anchoring mechanisms. *Curr Opin Cell Biol*. 14:25-34.

Brisch, E., M.A. Daggett, and K.A. Suprenant. 1996. Cell cycle-dependent phosphorylation of the 77 kDa echinoderm microtubule-associated protein (EMAP) in vivo and association with the p34cdc2 kinase. *J Cell Sci*. 109 (Pt 12):2885-93.

Brouhard, G.J., J.H. Stear, T.L. Noetzel, J. Al-Bassam, K. Kinoshita, S.C. Harrison, J. Howard, and A.A. Hyman. 2008. XMAP215 is a processive microtubule polymerase. *Cell*. 132:79-88.

Caceres, A., L.I. Binder, M.R. Payne, P. Bender, L. Rebhun, and O. Steward. 1984. Differential subcellular localization of tubulin and the microtubule-associated protein MAP2 in brain tissue as revealed by immunocytochemistry with monoclonal hybridoma antibodies. *J Neurosci*. 4:394-410.

Cassimeris, L. 2002. The oncoprotein 18/stathmin family of microtubule destabilizers. *Curr Opin Cell Biol*. 14:18-24.

Charrasse, S., P. Coubes, S. Arrancibia, and C. Larroque. 1996. Expression of the tumor over-expressed ch-TOG gene in human and baboon brain. *Neurosci Lett*. 212:119-22.

Charrasse, S., M. Schroeder, C. Gauthier-Rouviere, F. Ango, L. Cassimeris, D.L. Gard, and C. Larroque. 1998. The TOGp protein is a new human microtubule-associated protein homologous to the Xenopus XMAP215. *J Cell Sci*. 111 (Pt 10):1371-83.

Cotrina, M.L., and M. Nedergaard. 2002. Astrocytes in the aging brain. *J Neurosci Res*. 67:1-10.

Curmi, P.A., C. Nogues, S. Lachkar, N. Carelle, M.P. Gonthier, A. Sobel, R. Lidereau, and I. Bieche. 2000. Overexpression of stathmin in breast carcinomas points out to highly proliferative tumours. *Br J Cancer*. 82:142-50.

De Keersmaecker, K., C. Graux, M.D. Odero, N. Mentens, R. Somers, J. Maertens, I. Wlodarska, P. Vandenberghe, A. Hagemeijer, P. Marynen, and J. Cools. 2005. Fusion of EML1 to ABL1 in T-cell acute lymphoblastic leukemia with cryptic t(9;14)(q34;q32). *Blood*. 105:4849-52.

Dehmelt, L., and S. Halpain. 2005. The MAP2/Tau family of microtubule-associated proteins. *Genome Biol*. 6:204.

Deller, T., M. Korte, S. Chabanis, A. Drakew, H. Schwegler, G.G. Stefani, A. Zuniga, K. Schwarz, T. Bonhoeffer, R. Zeller, M. Frotscher, and P. Mundel. 2003. Synaptopodin-deficient mice lack a spine apparatus and show deficits in synaptic plasticity. *Proc Natl Acad Sci U S A*. 100:10494-9.

Deller, T., T. Merten, S.U. Roth, P. Mundel, and M. Frotscher. 2000a. Actin-associated protein synaptopodin in the rat hippocampal formation: localization in the spine neck and close association with the spine apparatus of principal neurons. *J Comp Neurol*. 418:164-81.

Deller, T., P. Mundel, and M. Frotscher. 2000b. Potential role of synaptopodin in spine motility by coupling actin to the spine apparatus. *Hippocampus*. 10:569-81.

Deller, T., C.B. Orth, D. Del Turco, A. Vlachos, G.J. Burbach, A. Drakew, S. Chabanis, M. Korte, H. Schwegler, C.A. Haas, and M. Frotscher. 2007. A role for synaptopodin and the spine apparatus in hippocampal synaptic plasticity. *Ann Anat*. 189:5-16.

Desai, A., and T.J. Mitchison. 1997. Microtubule polymerization dynamics. *Annu Rev Cell Dev Biol*. 13:83-117.

Desai, A., S. Verma, T.J. Mitchison, and C.E. Walczak. 1999. Kin I kinesins are microtubule-destabilizing enzymes. *Cell*. 96:69-78.

Eddleston, M., and L. Mucke. 1993. Molecular profile of reactive astrocytes--implications for their role in neurologic disease. *Neuroscience*. 54:15-36.

Eichenmuller, B., D.P. Ahrens, Q. Li, and K.A. Suprenant. 2001. Saturable binding of the echinoderm microtubule-associated protein (EMAP) on microtubules, but not filamentous actin or vimentin filaments. *Cell Motil Cytoskeleton*. 50:161-72.

Eichenmuller, B., P. Everley, J. Palange, D. Lepley, and K.A. Suprenant. 2002. The human EMAP-like protein-70 (ELP70) is a microtubule destabilizer that localizes to the mitotic apparatus. *J Biol Chem*. 277:1301-9.

Eliasson, C., C. Sahlgren, C.H. Berthold, J. Stakeberg, J.E. Celis, C. Betsholtz, J.E. Eriksson, and M. Pekny. 1999. Intermediate filament protein partnership in astrocytes. *J Biol Chem*. 274:23996-4006.

Eng, L.F., and R.S. Ghirnikar. 1994. GFAP and astrogliosis. *Brain Pathol*. 4:229-37.

Eng, L.F., R.S. Ghirnikar, and Y.L. Lee. 2000. Glial fibrillary acidic protein: GFAP-thirty-one years (1969-2000). *Neurochem Res*. 25:1439-51.

Eudy, J.D., M. Ma-Edmonds, S.F. Yao, C.B. Talmadge, P.M. Kelley, M.D. Weston, W.J. Kimberling, and J. Sumegi. 1997. Isolation of a novel human homologue of the gene coding for echinoderm microtubule-associated protein (EMAP) from the Usher syndrome type 1a locus at 14q32. *Genomics*. 43:104-6.

Farah, C.A., D. Liazoghli, S. Perreault, M. Desjardins, A. Guimont, A. Anton, M. Lauzon, G. Kreibich, J. Paiement, and N. Leclerc. 2005. Interaction of microtubule-associated protein-2 and p63: a new link between microtubules and rough endoplasmic reticulum membranes in neurons. *J Biol Chem*. 280:9439-49.

Fukazawa, Y., Y. Saitoh, F. Ozawa, Y. Ohta, K. Mizuno, and K. Inokuchi. 2003. Hippocampal LTP is accompanied by enhanced F-actin content within the dendritic spine that is essential for late LTP maintenance in vivo. *Neuron*. 38:447-60.

Goley, E.D., and M.D. Welch. 2006. The ARP2/3 complex: an actin nucleator comes of age. *Nat Rev Mol Cell Biol*. 7:713-26.

Greenberg, M.J., C.L. Wang, W. Lehman, and J.R. Moore. 2007. Modulation of actin mechanics by caldesmon and tropomyosin. *Cell Motil Cytoskeleton*.

Gu, C., W. Zhou, M.A. Puthenveedu, M. Xu, Y.N. Jan, and L.Y. Jan. 2006. The microtubule plus-end tracking protein EB1 is required for Kv1 voltage-gated K+ channel axonal targeting. *Neuron*. 52:803-16.

Hamill, D.R., B. Howell, L. Cassimeris, and K.A. Suprenant. 1998. Purification of a WD repeat protein, EMAP, that promotes microtubule dynamics through an inhibition of rescue. *J Biol Chem*. 273:9285-91.

Hanash, S.M., J.R. Strahler, R. Kuick, E.H. Chu, and D. Nichols. 1988. Identification of a polypeptide associated with the malignant phenotype in acute leukemia. *J Biol Chem*. 263:12813-5.

Hartman, J.J., J. Mahr, K. McNally, K. Okawa, A. Iwamatsu, S. Thomas, S. Cheesman, J. Heuser, R.D. Vale, and F.J. McNally. 1998. Katanin, a microtubule-severing protein, is a novel AAA ATPase that targets to the centrosome using a WD40-containing subunit. *Cell*. 93:277-87.

Heald, R., and E. Nogales. 2002. Microtubule dynamics. *J Cell Sci*. 115:3-4.

Heidebrecht, H.J., F. Buck, M. Pollmann, R. Siebert, and R. Parwaresch. 2000. Cloning and localization of C2orf2(ropp120), a previously unknown WD repeat protein. *Genomics*. 68:348-50.

Himi, T., T. Okazaki, H. Wang, T.H. McNeill, and N. Mori. 1994. Differential localization of SCG10 and p19/stathmin messenger RNAs in adult rat brain indicates distinct roles for these growth-associated proteins. *Neuroscience*. 60:907-26.

Howard, J., and A.A. Hyman. 2003. Dynamics and mechanics of the microtubule plus end. *Nature*. 422:753-8.

Hunter, A.W., M. Caplow, D.L. Coy, W.O. Hancock, S. Diez, L. Wordeman, and J. Howard. 2003. The kinesin-related protein MCAK is a microtubule depolymerase that forms an ATP-hydrolyzing complex at microtubule ends. *Mol Cell*. 11:445-57.

Itoh, T.J., S. Hisanaga, T. Hosoi, T. Kishimoto, and H. Hotani. 1997. Phosphorylation states of microtubule-associated protein 2 (MAP2) determine the regulatory role of MAP2 in microtubule dynamics. *Biochemistry*. 36:12574-82.

Jin, J., F.D. Smith, C. Stark, C.D. Wells, J.P. Fawcett, S. Kulkarni, P. Metalnikov, P. O'Donnell, P. Taylor, L. Taylor, A. Zougman, J.R. Woodgett, L.K. Langeberg, J.D. Scott, and T. Pawson. 2004. Proteomic, functional, and domain-based analysis of in vivo 14-3-3 binding proteins involved in cytoskeletal regulation and cellular organization. *Curr Biol*. 14:1436-50.

Kikuno, R., T. Nagase, K. Ishikawa, M. Hirosawa, N. Miyajima, A. Tanaka, H. Kotani, N. Nomura, and O. Ohara. 1999. Prediction of the coding sequences of unidentified human genes. XIV. The complete sequences of 100 new cDNA clones from brain which code for large proteins in vitro. *DNA Res*. 6:197-205.

Kinoshita, K., B. Habermann, and A.A. Hyman. 2002. XMAP215: a key component of the dynamic microtubule cytoskeleton. *Trends Cell Biol*. 12:267-73.

Kinoshita, K., T.L. Noetzel, I. Arnal, D.N. Drechsel, and A.A. Hyman. 2006. Global and local control of microtubule destabilization promoted by a catastrophe kinesin MCAK/XKCM1. *J Muscle Res Cell Motil*. 27:107-14.

Kolakowski, J., A. Wrzosek, and R. Dabrowska. 2004. Fesselin is a target protein for calmodulin in a calcium-dependent manner. *Biochem Biophys Res Commun*. 323:1251-6.

Kremerskothen, J., C. Plaas, S. Kindler, M. Frotscher, and A. Barnekow. 2005. Synaptopodin, a molecule involved in the formation of the dendritic spine apparatus, is a dual actin/alpha-actinin binding protein. *J Neurochem*. 92:597-606.

Leinweber, B.D., R.S. Fredricksen, D.R. Hoffman, and J.M. Chalovich. 1999. Fesselin: a novel synaptopodin-like actin binding protein from muscle tissue. *J Muscle Res Cell Motil*. 20:539-45.

Lepley, D.M., J.M. Palange, and K.A. Suprenant. 1999. Sequence and expression patterns of a human EMAP-related protein-2 (HuEMAP-2). *Gene*. 237:343-9.

Li, Q., M. Callaghan, and K.A. Suprenant. 1998. The 77-kDa echinoderm microtubule-associated protein (EMAP) shares epitopes with the mammalian brain MAPs, MAP-2 and tau. *Biochem Biophys Res Commun*. 250:502-5.

Li, Q., and K.A. Suprenant. 1994. Molecular characterization of the 77-kDa echinoderm microtubule-associated protein. Homology to the beta-transducin family. *J Biol Chem*. 269:31777-84.

Lupas, A., M. Van Dyke, and J. Stock. 1991. Predicting coiled coils from protein sequences. *Science*. 252:1162-1164.

Ly, C.D., K.W. Roche, H.K. Lee, and R.J. Wenthold. 2002. Identification of rat EMAP, a delta-glutamate receptor binding protein. *Biochem Biophys Res Commun*. 291:85-90.

Malenka, R.C., and M.F. Bear. 2004. LTP and LTD: an embarrassment of riches. *Neuron*. 44:5-21.

Margolis, R.L., L. Wilson, and B.I. Keifer. 1978. Mitotic mechanism based on intrinsic microtubule behaviour. *Nature*. 272:450-2.

Massey, P.V., and Z.I. Bashir. 2007. Long-term depression: multiple forms and implications for brain function. *Trends Neurosci*. 30:176-84.

Matsuo, R., A. Kato, Y. Sakaki, and K. Inokuchi. 1998. Cataloging altered gene expression during rat hippocampal long-term potentiation by means of differential display. *Neurosci Lett*. 244:173-6.

Matsuo, R., A. Murayama, Y. Saitoh, Y. Sakaki, and K. Inokuchi. 2000. Identification and cataloging of genes induced by long-lasting long-term potentiation in awake rats. *J Neurochem*. 74:2239-49.

McGough, A., M. Way, and D. DeRosier. 1994. Determination of the alpha-actinin-binding site on actin filaments by cryoelectron microscopy and image analysis. *J Cell Biol*. 126:433-43.

McNally, F.J., and S. Thomas. 1998. Katanin is responsible for the M-phase microtubule-severing activity in Xenopus eggs. *Mol Biol Cell*. 9:1847-61.

McNally, F.J., and R.D. Vale. 1993. Identification of katanin, an ATPase that severs and disassembles stable microtubules. *Cell*. 75:419-29.

Meyerson, M. 2007. Cancer: broken genes in solid tumours. *Nature*. 448:545-6.

Miyata, H., R. Yasuda, and K. Kinosita, Jr. 1996. Strength and lifetime of the bond between actin and skeletal muscle alpha-actinin studied with an optical trapping technique. *Biochim Biophys Acta*. 1290:83-8.

Molodtsov, M.I., E.A. Ermakova, E.E. Shnol, E.L. Grishchuk, J.R. McIntosh, and F.I. Ataullakhanov. 2005. A molecular-mechanical model of the microtubule. *Biophys J*. 88:3167-79.

Mundel, P., H.W. Heid, T.M. Mundel, M. Kruger, J. Reiser, and W. Kriz. 1997. Synaptopodin: an actin-associated protein in telencephalic dendrites and renal podocytes. *J Cell Biol*. 139:193-204.

Nakagawa, T., J.A. Engler, and M. Sheng. 2004. The dynamic turnover and functional roles of alpha-actinin in dendritic spines. *Neuropharmacology*. 47:734-45.

Nogales, E. 2000. Structural insights into microtubule function. *Annu Rev Biochem*. 69:277-302.

O'Connor, V., S.H. Houtman, C.I. De Zeeuw, T.V. Bliss, and P.J. French. 2004. Eml5, a novel WD40 domain protein expressed in rat brain. *Gene*. 336:127-37.

Ohkawa, N., K. Fujitani, E. Tokunaga, S. Furuya, and K. Inokuchi. 2007. The microtubule destabilizer stathmin mediates the development of dendritic arbors in neuronal cells. *J Cell Sci*. 120:1447-56.

Oshima, R.G. 2007. Intermediate filaments: a historical perspective. *Exp Cell Res*. 313:1981-94.

Paavilainen, V.O., E. Bertling, S. Falck, and P. Lappalainen. 2004. Regulation of cytoskeletal dynamics by actin-monomer-binding proteins. *Trends Cell Biol*. 14:386-94.

Pollmann, M., R. Parwaresch, S. Adam-Klages, M.L. Kruse, F. Buck, and H.J. Heidebrecht. 2006. Human EML4, a novel member of the EMAP family, is essential for microtubule formation. *Exp Cell Res*. 312:3241-51.

Pozuelo Rubio, M., K.M. Geraghty, B.H. Wong, N.T. Wood, D.G. Campbell, N. Morrice, and C. Mackintosh. 2004. 14-3-3-affinity purification of over 200 human phosphoproteins reveals new links to regulation of cellular metabolism, proliferation and trafficking. *Biochem J*. 379:395-408.

Price, D.K., J.R. Ball, Z. Bahrani-Mostafavi, J.C. Vachris, J.S. Kaufman, R.W. Naumann, R.V. Higgins, and J.B. Hall. 2000. The phosphoprotein Op18/stathmin is differentially expressed in ovarian cancer. *Cancer Invest*. 18:722-30.

Roth, S.U., C. Sommer, P. Mundel, and M. Kiessling. 2001. Expression of synaptopodin, an actin-associated protein, in the rat hippocampus after limbic epilepsy. *Brain Pathol*. 11:169-81.

Rutka, J.T., M. Murakami, P.B. Dirks, S.L. Hubbard, L.E. Becker, K. Fukuyama, S. Jung, A. Tsugu, and K. Matsuzawa. 1997. Role of glial filaments in cells and tumors of glial origin: a review. *J Neurosurg*. 87:420-30.

Sankila, E.M., L. Pakarinen, H. Kaariainen, K. Aittomaki, S. Karjalainen, P. Sistonen, and A. de la Chapelle. 1995. Assignment of an Usher syndrome type III (USH3) gene to chromosome 3q. *Hum Mol Genet*. 4:93-8.

Sato, S., H. Hasebe, S. Sato, Y. Asahi, T. Hayashi, E. Kobayashi, and Y. Sugimoto. 2006. High-resolution physical mapping and construction of a porcine contig spanning the intramuscular fat content QTL. *Anim Genet*. 37:113-20.

Schek, H.T., 3rd, M.K. Gardner, J. Cheng, D.J. Odde, and A.J. Hunt. 2007. Microtubule assembly dynamics at the nanoscale. *Curr Biol*. 17:1445-55.

Schroeter, M., and J.M. Chalovich. 2004. Ca2+-calmodulin regulates fesselin-induced actin polymerization. *Biochemistry*. 43:13875-82.

Schroeter, M.M., and J.M. Chalovich. 2005. Fesselin binds to actin and myosin and inhibits actin-activated ATPase activity. *J Muscle Res Cell Motil*. 26:183-9.

Shafit-Zagardo, B., and N. Kalcheva. 1998. Making sense of the multiple MAP-2 transcripts and their role in the neuron. *Mol Neurobiol*. 16:149-62.

Silacci, P., L. Mazzolai, C. Gauci, N. Stergiopulos, H.L. Yin, and D. Hayoz. 2004. Gelsolin superfamily proteins: key regulators of cellular functions. *Cell Mol Life Sci*. 61:2614-23.

Smith, R.J., C.I. Berlin, J.F. Hejtmancik, B.J. Keats, W.J. Kimberling, R.A. Lewis, C.G. Moller, M.Z. Pelias, and L. Tranebjaerg. 1994. Clinical diagnosis of the Usher syndromes. Usher Syndrome Consortium. *Am J Med Genet*. 50:32-8.

Soda, M., Y.L. Choi, M. Enomoto, S. Takada, Y. Yamashita, S. Ishikawa, S. Fujiwara, H. Watanabe, K. Kurashina, H. Hatanaka, M. Bando, S. Ohno, Y. Ishikawa, H. Aburatani, T. Niki, Y. Sohara, Y. Sugiyama, and H. Mano. 2007. Identification of the transforming EML4-ALK fusion gene in non-small-cell lung cancer. *Nature*. 448:561-6.

Sun, H.Q., M. Yamamoto, M. Mejillano, and H.L. Yin. 1999. Gelsolin, a multifunctional actin regulatory protein. *J Biol Chem*. 274:33179-82.

Suprenant, K.A., K. Dean, J. McKee, and S. Hake. 1993. EMAP, an echinoderm microtubule-associated protein found in microtubule-ribosome complexes. *J Cell Sci*. 104:445-50.

Tirnauer, J.S., S. Grego, E.D. Salmon, and T.J. Mitchison. 2002. EB1-microtubule interactions in Xenopus egg extracts: role of EB1 in microtubule stabilization and mechanisms of targeting to microtubules. *Mol Biol Cell*. 13:3614-26.

Wade, R.H., and A.A. Hyman. 1997. Microtubule structure and dynamics. *Curr Opin Cell Biol*. 9:12-7.

Walczak, C.E., T.J. Mitchison, and A. Desai. 1996. XKCM1: a Xenopus kinesin-related protein that regulates microtubule dynamics during mitotic spindle assembly. *Cell*. 84:37-47.

Wegner, A. 1976. Head to tail polymerization of actin. *J Mol Biol*. 108:139-50.

Weins, A., K. Schwarz, C. Faul, L. Barisoni, W.A. Linke, and P. Mundel. 2001. Differentiation- and stress-dependent nuclear cytoplasmic redistribution of myopodin, a novel actin-bundling protein. *J Cell Biol*. 155:393-404.

Yamazaki, M., R. Matsuo, Y. Fukazawa, F. Ozawa, and K. Inokuchi. 2001. Regulated expression of an actin-associated protein, synaptopodin, during long-term potentiation. *J Neurochem*. 79:192-9.

Chapter 2

Eml4, a member of the echinoderm microtubule associated protein family, stabilizes microtubules

S.H. Houtman[1], M. Rutteman[1], C.I. De Zeeuw[1], P.J. French[2]

[1]Department of Neuroscience, Erasmus MC, Rotterdam, the Netherlands
[2]Department of Neurology, Erasmus MC, Rotterdam, the Netherlands

Neuroscience 144 (2007) 1373-1382

Abstract
Echinoderm microtubule-associated protein (EMAP) is the major microtubule binding protein in dividing sea urchin (*Strongylocentrotus purpuratus*) eggs. Echinoderm microtubule-associated protein like protein 4 (Eml4, restrictedly overexpressed proliferation-associated protein 120 kDa (Ropp120)) is one of the five mammalian EMAP homologues, the cellular function of which remains to be elucidated. In our first set of experiments we determined the spatio-temporal expression pattern of *Eml4* in mouse brain. Our results demonstrate that *Eml4* is a highly developmentally regulated gene with high expression levels in the developing nervous system of E11 embryos declining to low levels in adult. Spatially, *Eml4* expression becomes restricted to the olfactory bulb, hippocampus and cerebellum. Transient transfection of a fusion construct of full-length mouse Eml4 with green fluorescent protein (GFP-Eml4) into Cos7 and HeLa cells resulted in colocalization of GFP-Eml4 with microtubules. This colocalization was observed both with microtubules of non-dividing cells and with the mitotic spindle of dividing cells. In addition, transient overexpression of GFP-Eml4 in Cos7 cells resulted in microtubules that were resistant to nocodazole treatment suggesting that Eml4 stabilizes microtubules. A consequence of microtubule stabilization is a net reduction in the amount of free tubulin. Microtubule stabilizing proteins therefore are expected to indirectly decrease the microtubule growth rate. Indeed, transient transfection of GFP-Eml4 resulted in a marked decrease in the microtubule growth rate, which is in line with our hypothesis that Eml4 functions as a microtubule stabilizing protein. In summary, our results suggest that Eml4 is a developmentally regulated protein that colocalizes with and stabilizes microtubules.

Introduction
Microtubules are polymers made up of alpha- and beta-tubulin subunits that provide the architectural structure of eukaryotic cells (Nogales, 2000). They play a role in various cellular processes, such as cell division, intracellular transport and cell motility. Microtubules are bipolar structures with their minus-end anchored in the microtubule-organizing center (MTOC) and their plus-ends directed toward the cell membrane. In neurons however, the microtubule network is slightly different from other eukaryotic cells: in the axon, microtubules are oriented with their plus ends away from the soma, while in the dendrites the microtubules are oriented in both directions (Baas, 1999).
Microtubules are highly dynamic structures that can switch between growing and shrinking phases (Heald and Nogales, 2002; Howard and Hyman, 2003; Nogales, 2000). Microtubule dynamics are regulated by their interaction with

microtubule-associated proteins (MAPs) of which many have been identified (Desai and Mitchison, 1997; Itoh and Hotani, 2004; Nogales, 2000). The MAPs can generally be classified into two categories, microtubule-stabilizing proteins (e.g. MAP2, cytoskeleton-associated protein 2 (CKAP2) and tau) and microtubule-destabilizing proteins (e.g. stathmin, katanin) (Ahmad *et al.*, 1999; Cassimeris, 2002; Kalcheva *et al.*, 1998).

In dividing sea urchin eggs the most abundant MAP is echinoderm microtubule-associated protein (EMAP) (Suprenant *et al.*, 1993). Interestingly, several mammalian homologs of EMAP, EMLs (EMAP-like proteins) have been identified. These include: 1) EML1 (echinoderm microtubule-associated protein-like protein (ELP)79/HuEMAP-1), a candidate for Usher-1a (Eudy *et al.*, 1997), 2) EML2 (ELP70/HuEMAP-2) (Lepley *et al.*, 1999), 3) EML3 (ELP95) (Jin *et al.*, 2004; Pozuelo Rubio *et al.*, 2004), 4) EML4 (ELP120/restrictedly overexpressed proliferation-associated protein 120 kDa (ROPP120)/chromosome 2 open reading frame 2 (C2ORF2)) (Heidebrecht *et al.*, 2000; Pollmann *et al.*, 2006), a member that was found to be "overexpressed" during mitosis and, 5) Eml5, recently cloned in our group from adult rat brain (O'Connor *et al.*, 2004).

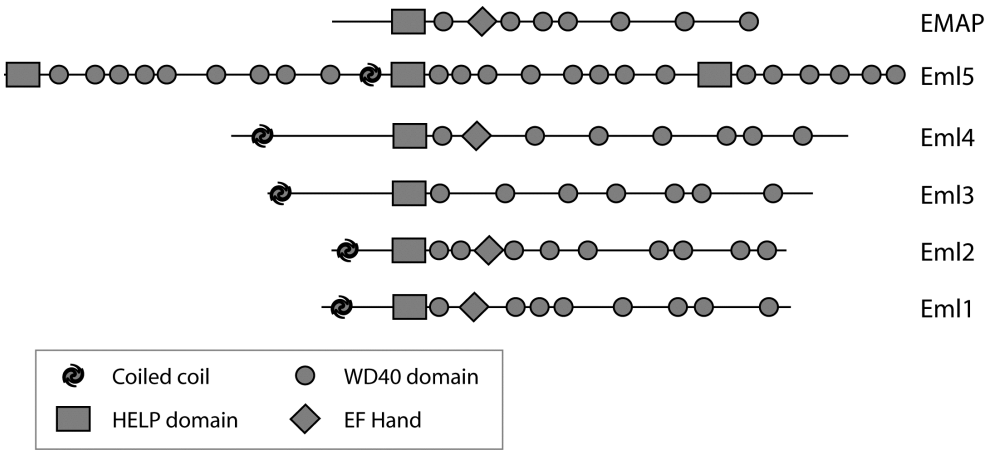

Figure 1. Schematic drawing of Eml proteins showing conserved HELP- and WD40 domains, an EF-hand and helical coiled-coil region.

The protein sequences of all five EMLs are highly conserved (Figure 1). They all contain a hydrophobic EMAP like (HELP; hydrophobic echinoderm microtubule-associated protein-like protein) domain that is unique to this family and multiple WD40 domains (Hamill *et al.*, 1998; Li *et al.*, 1998; Pollmann *et al.*, 2006; Suprenant *et al.*, 2000). Although evidence suggests that EMAP and EML2 associate with microtubules and regulate their dynamics (Eichenmuller *et al.*, 2002; Hamill *et al.*, 1998; Suprenant *et al.*, 1993), the

cellular function of other EMAP family members remains to be determined. We therefore set out to examine the cellular function of one of the murine members of the EMAP protein family, Eml4. In this study we examine its spatio-temporal expression pattern, alternative splicing and, provide evidence that Eml4 associates with and stabilizes microtubules.

Materials and Methods

Tissues

Whole embryos (embryonic day (E) 11, 15 or 18) or brains from postnatal day (P) 1, 10 or adult mice (C57/Bl6, Harlan, Horst, The Netherlands) were carefully removed, frozen on dry ice and stored at −80 °C; 14 µm sections were cut on a cryostat, mounted onto superfrost plus (Menzel-Glaser, Braunschweig, Germany) glass slides and stored at −80 °C. The housing of the mice was in filter-top units, with extra nesting material for pregnant mice. All animal experiments were performed in accordance with the recommendations of the European Communities Council Directive of 24 November 1986 (86/609/EEC) and were conducted with the approval of the Dutch Ethical Committee for animal experiments. All efforts were made to minimize animal suffering.

In situ hybridization (ISH)

Radioactive and non-radioactive ISHs were performed essentially as described (French *et al.*, 2001). For radioactive ISH, sections were thawed, fixed in 4% paraformaldehyde, acetylated in 1.4% triethanolamine and 0.25% acetic anhydride, dehydrated through graded ethanol solutions and delipidated in chloroform. Sections were hybridized overnight at 42 °C in 100 µl buffer containing 50% formamide, 4× SSC, 10% dextran sulfate, 5× Denhardt's solution, 200 mg/ml acid alkali cleaved salmon testis DNA, 100 mg/ml long-chain polyadenylic acid, 25 mM sodium phosphate (pH 7.0), 1 mM sodium pyrophosphate and 100,000 CPM radiolabeled probe (approx. 1ng/ml) under parafilm coverslips. Sections were subsequently washed in 1× SSC at 55 °C (30 min), 0.1× SSC at room temperature (5 min) and dehydrated in ethanol. Hybridized sections were then exposed to autoradiographic film. ^{35}S-ATP end-labeled probes (Amersham, Munich, Germany) were generated using terminal deoxynucleotidyl transferase (Promega, Leiden, The Netherlands) according to manufacturer's instructions. A 50-fold excess of unlabeled antisense oligonucleotide was used as negative control. Sequence of the Eml4 antisense oligonucleotide (Invitrogen, Paisley, UK) was 5'-GCGGTCTTGAACGTCAGAGGTACTTGCAGCAGAAATACTATCATC-3' corresponding to amino acids 9–23 (AAH70427). Sections were counterstained with hematoxylin and eosin. For non-radioactive ISHs, sections

were fixed in 4% paraformaldehyde, acetylated in 1.4% triethanolamine, 0.25% acetic anhydride and washed in phosphate-buffered saline (PBS). Sections were then prehybridized (1 h) in buffer containing 50% formamide (Sigma, Zwijndrecht, The Netherlands), 5× SSC, 5× Denhardt's (Sigma), 250 µg/ml yeast tRNA (Roche, Almere, The Netherlands) and 500 µg/ml acid-alkali cleaved salmon testis DNA (Sigma). Hybridization was performed overnight at 65 °C in prehybridization buffer containing 100 ng/ml digoxigenin–UTP-labeled cRNA probes. Antisense and sense probes directed against bp 2139–2719 (amino acids: 714–907 of AAH70427) were generated using DIG RNA labeling kit (Roche) according to manufacturer's instructions. Following hybridization, sections were washed in 0.2× SSC at 65 °C and blocked in 0.1M Tris pH 7.5, 0.15 M NaCl and 10% heat-inactivated sheep serum (Sigma) for 1 h at RT. Alkaline phosphatase conjugated anti-digoxigenin antibodies (Roche) were added to the sections in a dilution of 1:5000 in 0.1 M Tris pH 7.5, 0.15 M NaCl and 1% heat-inactivated sheep serum and incubated overnight at 4 °C. Following washing of the sections, color reactions were performed in 0.1 M Tris pH 9.5, 0.1 M NaCl, 50 mM $MgCl_2$, 2 mM levamisole (Sigma), 0.35 mg/ml nitro-blue tetrazolium (Roche) and 0.18 mg/ml 5-bromo-4-chloro-3-indolylphosphate (Roche). Reactions were terminated upon visual inspection (~18 h) and mounted in Permount (Fisher Scientific, Loughborough, UK).

Reverse transcriptase–polymerase chain reaction (RT-PCR)

Total RNA from adult mouse brain was isolated using Trizol (Invitrogen) according to manufacturer's guidelines. cDNA was synthesized from 2 µg isolated RNA using a T18 oligonucleotide in the presence of 200U Superscript III (Invitrogen), 10 mM dNTPs, 40 U RNasin (Promega), 0.01 M DTT for 1 h at 50 °C. Full-length *Eml4* constructs were amplified from the cDNA using 5′-GCAAGCTCCCGTTAGACATCTGAG-3′ and 5′-GCAAGATGGACGGGTTTC-3′ oligonucleotides. The fragment was cloned into pEGFP-C2 vector (Invitrogen), in which EGFP is fused N-terminally to full length Eml4, and sequence verified. For the splicing PCR we used the following primers: 131: 5′-AAGATGGACGGTTTCGCCGG-3′, 134: 5′-TTTTTCACTGAGGCTACATGATC-3′; 135: 5′-CGAGAAGCTATTTCTATGTCCTG-3′; 140: 5′-GATTGACGATGACATCTTTATG-3′; 139: 5′-CATAAAGATGTCATCGTCAATC-3′; 143: 5′-AGGAATGAACATTGTAATTGGCC-3′.

Antibodies

We generated a peptide-antibody (1139) against amino acids 118–132 of Eml4 (primary sequence IKRPPTAEKSHNSWE). Adult New Zealand White rabbits were immunized with 50–100 µg peptide using Freund's complete adjuvant (Eurogentec, Seraing, Belgium). The immunization was followed by four boosts

of 50–100 µg administered every 2 or 3 weeks in Freund's incomplete adjuvant. Serum was taken 24 days after the final boost.

Western blot

Proteins were isolated from mouse E11 embryos, E15 brain, E18 brain, adult brain (olfactory bulb, cortex, hippocampus, cerebellum and brainstem) and transiently transfected Cos7 cells. Isolations were performed in ice-cold PBS containing 1% SDS and protease inhibitor cocktail (Sigma). Homogenized tissues or lysed cells were incubated on ice for 20 min and centrifuged to eliminate protein insoluble fractions. Protein concentrations were measured using BCA (Pierce, Perbio Science, Etten-Leur, The Netherlands) according to the manufacturer's guidelines. Samples diluted in Laemmli sample buffer (LSB; 50 mM Tris–HCl, pH 6.8, 2.5% v/v SDS, 12.5% v/v glycerol, 0.01% w/v Bromophenol Blue, 100 mM DTT, β-mercaptoethanol) were denatured for 5 min at 95 °C, after which 20 µg of protein was transferred to 10% or 6% acrylamide gels. Following electrophoresis, gels were wet-blotted on either PVDF (Bio-rad, Veenendaal, The Netherlands) or nitrocellulose (Bio-rad) overnight and blocked in TBS containing 5% milk (Nutricia, Cuijk, The Netherlands) and 1% Tween. Serum 1139 (1:500), pre-immune serum (1:500) or anti-green fluorescent protein (GFP) (Abcam, Cambridge, UK; 1:5000) was added to the blots in TBS containing 2% milk and 1% Tween (TBS-T). Next day the blots were washed and incubated with secondary antibody (swine-anti-rabbit-HRP or rabbit-anti-mouse-HRP, 1:5000 Dako, Glostrup, Denmark) in TBS-T. The blots were then washed in TBS/1% Tween following which we measured signals on the blot using chemiluminescence (Amersham) according to the manufacturer's instructions.

Transient transfection

Cos7 cells, grown in two-well chambered coverglasses (NalgeNunc, Naperville, IL, USA) were transfected using DEAE-dextran (O'Connor *et al.*, 2004). In brief, cells were incubated for 30 s in serum free medium containing 0.5 mg/ml DEAE-dextran (Sigma). Cells were then exposed to GFP-Eml4 and/or end-binding protein (EB)3–monomeric red fluorescent protein (mRFP) (kindly donated by A. Akhmanova, Erasmus MC, Rotterdam, The Netherlands) expression vectors (total DNA amount per well of 1 µg) in the presence of 0.1 mM chloroquine for 2–4 h. Cells were then incubated in 10% dimethyl sulfoxide in PBS for 90 s and returned to normal medium (10% fetal calf serum, 45% DMEM and 45% F-10, 500 U/ml penicillin and 500 U/ml streptomycin). HeLa cells, grown in two-well chambered coverglasses (NalgeNunc) were transfected using DNA/Ca^{2+}-phosphate co-precipitation as described by Kohrmann et al. (1999). Briefly, fresh serum free culture medium (Cos7 culture

medium) was added to HeLa cells 1–4 h before transfection. The cells were then incubated for 0.5–2 h with 120 µl containing 5–10 µg DNA, 125 µM $CaCl_2$, 140 mM NaCl, 0.75 mM Na_2HPO_4 and 25 mM BES pH 7.1, which was added to the medium. The forming of the calcium phosphate precipitates was visually inspected. Cells were then washed twice with prewarmed HBS (135 mM NaCl, 4 mM KCl, 1 mM Na_2HPO_4, 2 mM $CaCl_2$, 1 mM $MgCl_2$, 10 mM glucose, 20 mM Hepes, pH 7.35) and returned to normal medium. Eighteen hours to 48 h after transfection, cells were fixed in ice-cold methanol (100%), 1 mM EGTA (10 min) followed by 4% paraformaldehyde in PBS (10 min). Cells were permeabilized in 0.1% saponin/PBS, and blocked with PBS containing 1% BSA, 10% fetal calf serum before being incubated (overnight) with beta-tubulin antibodies (Sigma tub clone 2.1; 1:300). Following washing in PBS, cells were incubated (1 h) with the secondary antibody (Alexa-fluor goat-anti-mouse 594, dilution 1:300; Molecular Probes, Invitrogen). Slides were mounted in Vectashield mounting medium (Vector Laboratories, Burlingame, CA, USA) containing DAPI. For nocodazole treatment: Cos7 cells were incubated for 20 min with 10 µM nocodazole (Sigma) 18 or 48 h post-transfection with GFP-Eml4.

Imaging

Fluorescence images where made using a Leica (Wetzlar, Germany) DMRBE microscope with a 40× oil immersion objective coupled to a Hamamatsu (Hamamatsu Photonics K.K.; Hamamatsu City, Japan) C4880 CCD camera or using a Zeiss (Jena, Germany) LSM510 confocal laser-scanning microscope using a 63× oil immersion objective. For live imaging, cells were analyzed on the confocal microscope at 37 °C, under 5% CO_2 in culture medium. In our experiments we used an optical slice of ~1 µm, images were taken every second. Microtubule growth was measured as the traveled distance of EB3–mRFP (kindly donated by A. Akhmanova), a plus-end microtubule binding protein fused to RFP (Akhmanova and Hoogenraad, 2005; Nakagawa *et al.*, 2000; Stepanova *et al.*, 2003). Analysis was performed using LSM510 software, 18 h post-transfection. N=16±5 growing microtubule plus-ends were counted per cell on microtubules that were visual on at least three consecutive frames. Statistical analysis was performed using the Student's *t*-test.

Results

Eml4 expression is developmentally regulated

We first determined the spatio-temporal expression pattern of *Eml4* using ISH (Figure 2). Our results show that *Eml4* is highly expressed in most regions in mouse E11 embryos. High expression levels are observed in developing nervous system, in fore- and hindbrain regions. Many other tissues also express *Eml4*. In E15 embryos, *Eml4* is also highly expressed in the developing CNS (e.g.

neopallial cortex, ventricular zone, roof of midbrain, cerebellar primordium and spinal cord) and peripheral nervous system (e.g. ganglions).

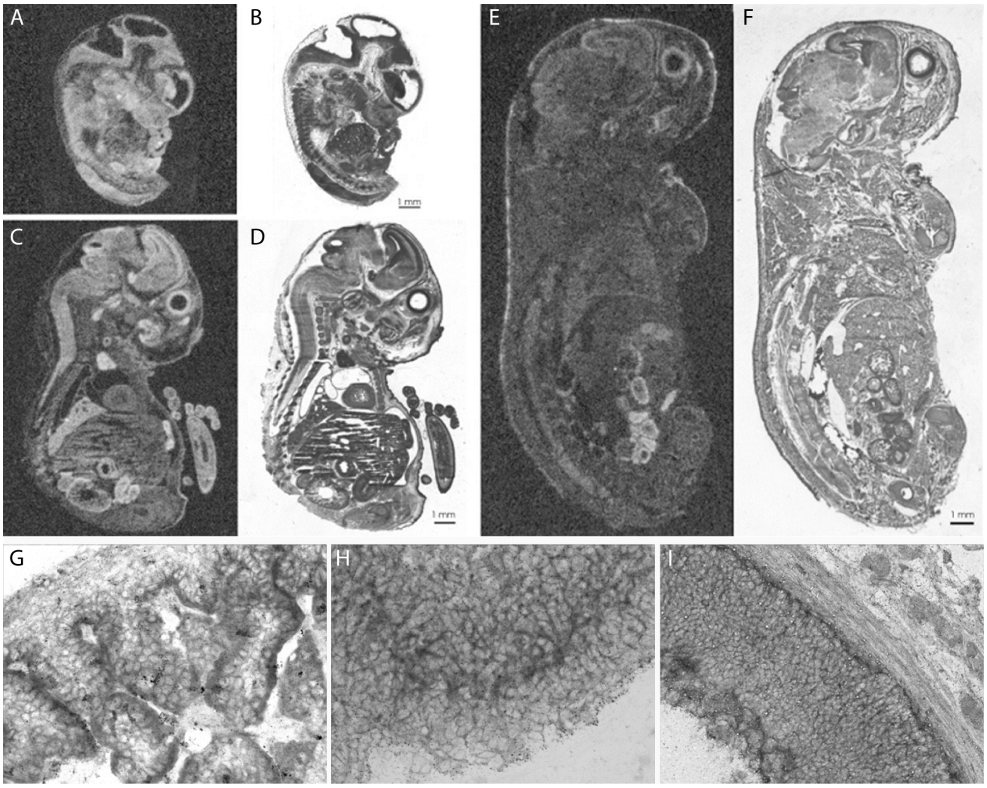

Figure 2. Developmental expression of *Eml4*. (A) At E11, *Eml4* is expressed throughout the whole embryo; (B) HE staining of E11 embryo. (C) *Eml4* expression at E15 is more restricted to the developing nervous system, the intestines and the eye; (D) HE staining of E15 embryo. (E) At E18, *Eml4* is expressed at lower levels compared with E11 and E15 embryos, and expression is restricted to the intestines, the eye and the nervous system; (F) HE staining of E18. (G–I) Non-radioactive ISH confirming *Eml4* expression in E18 intestines (G), cerebellum (H) and eye (I).

Other regions in which *Eml4* is expressed include, liver, thymus, intestines, eye, kidney, salivary gland and paws. In E18 embryos, *Eml4* expression is mainly restricted to regions of the developing nervous system e.g. in neopallial cortex (the future cerebral cortex), hippocampus, diencephalon, roof of midbrain, cerebellum and spinal cord. Expression of *Eml4* is also observed within the developing intestine and eye.

Because our results indicate that *Eml4* expression is predominantly expressed within the developing nervous system, we performed ISH on brain sections of

P1, P10 and adult mice (Figure 3). In P1 mouse brains, virtually all brain regions express *Eml4*. Highest expression levels are observed in cortex, olfactory bulb, hippocampus and cerebellum (data not shown). In P10 mouse brain *Eml4* is expressed at lower levels compared with P1 mouse brain (data not shown). At this stage expression is mainly restricted to cortex, olfactory bulb, hippocampus and cerebellum (Figure 3A). In adult mouse brain *Eml4* is expressed albeit at low level in olfactory bulb, hippocampus and cerebellum (Figure 3C).

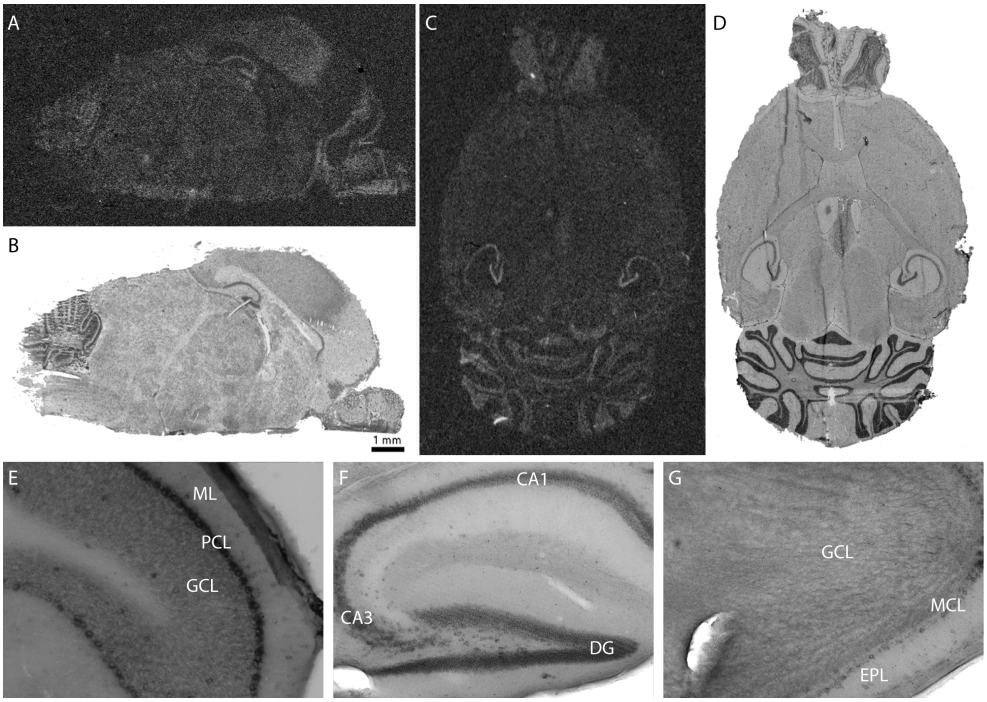

Figure 3. Eml4 expression shown in P10 and adult mouse brain. (A) *Eml4* expression in P10 sagital mouse slice, with expression in olfactory bulb, hippocampus, cortex and cerebellum. (B) HE staining of the same slice as A. (C) Horizontal section of adult mouse brain, with Eml4 expression in olfactory bulb, hippocampus and cerebellum. (D) HE staining of slice in C. E, F and G are non-radioactive ISH sections showing the cellular resolution of *Eml4* expression of adult mouse cerebellum (E), hippocampus (F) and olfactory bulb (G). ML, molecular layer; PCL, Purkinje cell layer; GCL, granule cell layer; CA1, cornu ammonis 1; CA3, cornu ammonis 3; DG, dentate gyrus; MCL, mitral cell layer; EPL, external plexiform layer.

We confirmed the *Eml4* expression pattern at all stages during development using an independent, digoxigenin-labeled cRNA probe (Figure 2G–I). The cellular resolution obtained with this technique indicates that in adult mouse olfactory bulb, the granule cell layer and mitral cell layer express *Eml4* (Figure 3G). In the hippocampus, the subventrical zone and the granule cell layers of

the dentate gyrus are labeled as well as the CA1-3 pyramidal cell layers of the Ammon's horn (Figure 3F). In the cerebellum, *Eml4* expression if found predominantly in the Purkinje cell layer (Figure 3E). Because the granule cell layers of the dentate gyrus, the mitral cell layer of the olfactory bulb, the Purkinje cell layer of the cerebellum and the CA1-3 pyramidal cell layers of the hippocampus predominantly contain cells of neuronal origin, our data indicate that *Eml4* expression persists in postmitotic neurons.
In summary, our ISH data indicate that *Eml4* expression is highly developmentally regulated and that *Eml4* expression becomes predominantly restricted to regions of the developing CNS. In addition, *Eml4* expression persists in adult mouse brain in neurons of olfactory bulb, hippocampus and cerebellum.

Eml4 splice variants

In order to determine the cellular function of Eml4, we cloned the full-length mouse Eml4 by RT-PCR using total RNA, isolated from adult mouse brain. The RT-PCR product was sequence verified, and was most similar to accession number AAH70427. However, we observed that our sequence (database accession number DQ230326) contained 174 additional base pairs suggesting that Eml4 may be subjected to alternative splicing. Furthermore other submitted Eml4 sequences (NM199466 and BC067011) also slightly differ in their primary sequence. When our sequence and the sequences AAH70427, NM199466 and BC067011 are plotted onto the mouse genome, it can be hypothesized that exons 2, 5, 6 and 8 are alternatively spliced. To confirm alternative splicing we performed RT-PCR on cDNA derived from E11, E15 and E18 embryos and different areas from adult mouse brain (olfactory bulb, cortex, hippocampus, cerebellum and brainstem). Indeed, RT-PCR on adult and developing mouse brain confirms that exons 5, 6 and 8 are subject to alternative splicing (Figure 4).

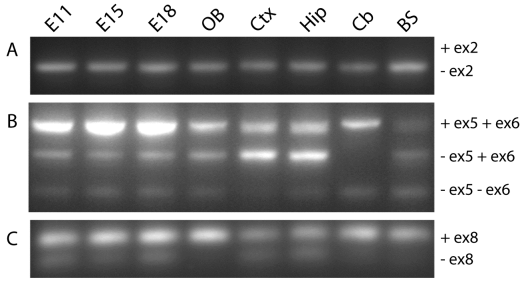

Figure 4. RT-PCR on embryos and regions of adult mouse brain. (A) RT-PCR using exon 2 spanning primers. Our experiments failed to identify expression of this exon. (B) RT-PCR using primers spanning exons 5 and 6 demonstrating regulated splicing of exon 5/6 in adult cerebellum. (C) Exon 8 is always present in olfactory bulb, cerebellum and brainstem. OB, olfactory bulb; Ctx, cortex; Hip, Hippocampus; Cb, cerebellum; BS, brainstem.

We were unable to confirm alternative splicing of exon 2. Although exons 5, 6 and 8 are found at the examined developmental stages, the abundance of individual splice variants differs between specific brain areas. For example, adult cerebellum does not express an isoform with only exon 5 or exon 6.

Protein expression of Eml4

We performed Western blot analysis to examine specific Eml4 protein expression. To determine specificity of our antibody we first fused our Eml4 construct C-terminally to eGFP (GFP-Eml4). We observed a distinct band at ~150 kDa on Western blot of transiently transfected Cos7 cells (Figure 5A). Such size can be expected based on the molecular mass of the fusion construct: 120 kDa of Eml4+30 kDa of GFP. This band was recognized both by our Eml4 antibody (1139) and by an anti-eGFP antibody. However, this band was not detected in control, GFP transfected cells indicating that antibody 1139 can recognize Eml4 fusion proteins.

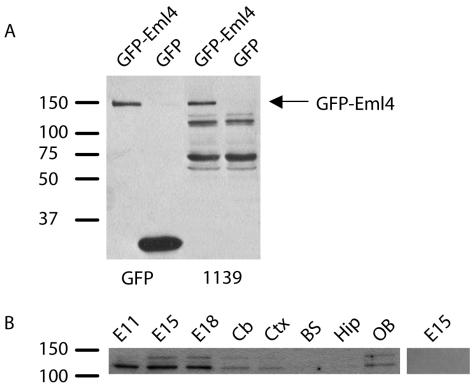

Figure 5. (A) Specificity of serum 1139 demonstrated by Western blot analysis. Anti-GFP antibodies recognize a distinct band of ~150 kDa denoted by the arrow in GFP-Eml4 transfected Cos7 cells (lane 1) and a band of ~30 kDa in GFP-transfected cells (lane 2). These bands correspond to the calculated molecular weights of GFP-Eml4 and GFP respectively. Serum 1139 (lanes 3 and 4) recognizes a band identical to the band identified using GFP-antibodies in GFP-Eml4-transfected cells (lane 3). No specific band with this antibody was observed in control (GFP−) transfected cells. (B) Western blot analysis of E11, E15, E18 and various brain areas of adult mouse brain using serum 1139 (left) and pre-immune serum (right). OB, olfactory bulb; Ctx, cortex; Hip, Hippocampus; Cb, cerebellum; BS, brainstem.

We next performed Western blot analysis of proteins isolated from whole E11 embryos, E15 brain, E18 brain and adult olfactory bulb, cortex, cerebellum and hippocampus (Figure 5B). Our antibody recognized distinct bands around 120 kDa, molecular weights that correspond to the calculated mass of Eml4 (and splice variants). These bands were not recognized by pre-immune serum (Figure 5B). Similar to RNA expression, the embryonic stages

show higher Eml4-protein expression levels compared with adult brain regions. Western blot analysis therefore indicates that, Eml4 protein expression is developmentally regulated and expression persists in distinct regions of the adult mouse brain.

Eml4 associates with and stabilizes microtubules

We next transiently transfected GFP-Eml4 into Cos7 and HeLa cells in order to help elucidate the molecular function of Eml4. In non-dividing cells we observed a clear filamentous staining pattern radiating from a perinuclear region 18 h post-transfection. When the transfected cells were counterstained with anti-beta tubulin antibodies, we observed a complete colocalization of GFP-Eml4 with microtubules (Figure 6A). GFP-Eml4 staining can be observed throughout the whole microtubule. This colocalization suggests that Eml4, like its archetypical family member EMAP, is a MAP.

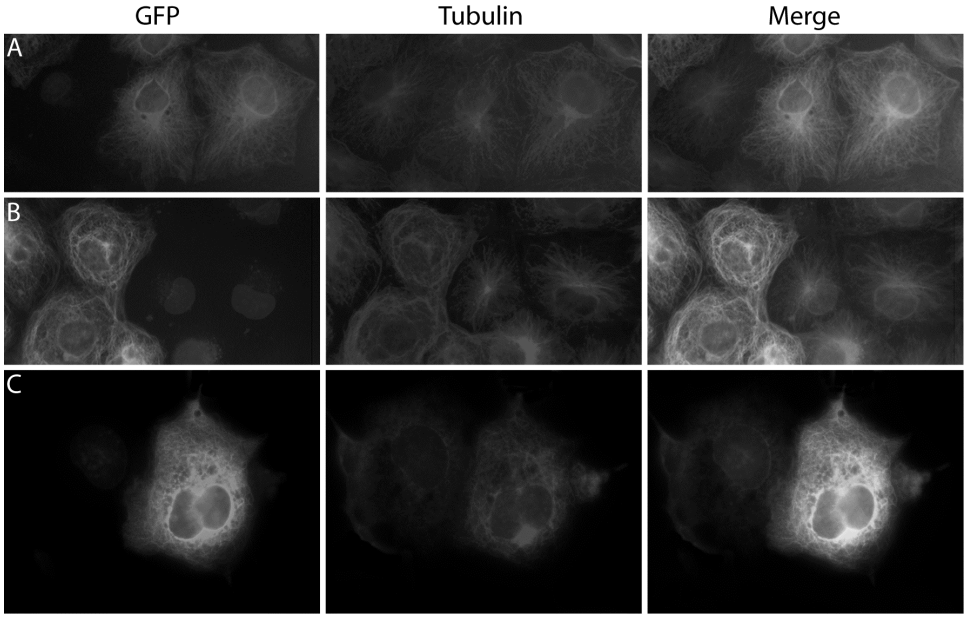

Figure 6. GFP-Eml4 transiently transfected into Cos7 cells. Transfected cells were visualized by GFP fluorescence and cells were counterstained with a tubulin antibody (red). Right panel shows merge. (A) Cos7 cells 18 h post-transfection shows radiating microtubules that colocalize with GFP-Eml4 whereas circular microtubules are observed 48 h post-transfection (B). Eighteen hours post-GFP-Eml4 transfection, transfected cells are resistant to microtubule depolymerization by nocodazole for 20 min whereas in non-transfected cells microtubules are disrupted (C).

As EMAP and Eml2 have been shown to associate with the mitotic spindle of dividing cells (Eichenmuller *et al.*, 2002; Suprenant *et al.*, 1993), we examined

whether GFP-Eml4 also colocalizes with microtubules of the mitotic spindle. Indeed, both in dividing Cos7 and HeLa cells, GFP-Eml4 shows a clear colocalization with the mitotic spindle (Figure 7). GFP-Eml4 staining appeared uniform across the spindle. We only observed colocalization with the mitotic spindle in cells expressing very low amounts of GFP-Eml4 (hence the relative high background staining in these cells). This may indicate that overexpression of GFP-Eml4 interferes with the process of cell division. We therefore quantified the dividing cell population following transient transfection. Mock transfected Cos7 cells have a dividing cell population of 4.65% ±1.03 whereas in GFP-Eml4 transfected cell, this percentage is decreased to 1.44% ±0.5 (P<0.01 using a Student's t-test). These results confirm the hypothesis that Eml4 overexpression interferes with the cell cycle.

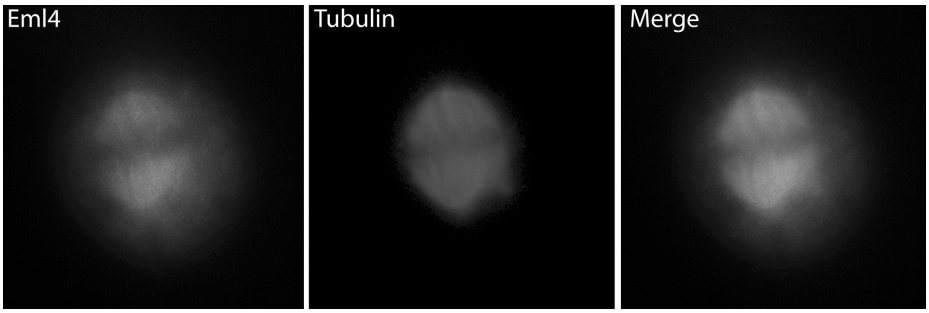

Figure 7. GFP-Eml4 transiently transfected into HeLa cells. GFP-Eml4 colocalizes with the mitotic spindle of dividing cells. Cells were counterstained with a tubulin antibody (middle panel). In the right panel GFP-Em14 and tubulin signals are overlaid, showing colocalization of GFP-Eml4 with the mitotic spindle.

Apart from a colocalization of GFP-Eml4 with microtubules in non-dividing Cos7 and HeLa cells, we also observed that cells expressing GFP-Eml4 have microtubules with a circular appearance. These circular microtubules, a result of microtubule elongation or microtubule bundling, were observed either 18 h post-transfection in cells expressing high amounts of GFP-Eml4 (as determined by the relative fluorescence intensity) or 48 h post-transfection in cells expressing low amounts of GFP-Eml4 (Figure 6B). The observation that GFP-Eml4 induces bundling or elongation of microtubules suggests that Eml4 functions as a microtubule stabilizing protein. To confirm that Eml4 is a microtubule stabilizing protein, we investigated the effect of Eml4 overexpression on microtubule stability following microtubule disruption. Eighteen hours following transient transfection with GFP-Eml4, Cos7 cells were treated with 10 µM nocodazole for 20 min. Under these conditions, virtually no polymerized microtubules were detectable in non-transfected cells. In

contrast, polymerized microtubules were readily detected in cells expressing GFP-Eml4 (Figure 6C). Because nocodazole is an effective microtubule-disrupting agent, an Eml4-associated resistance to nocodazole-induced depolymerization indicates Eml4 functions as a microtubule stabilizing protein.
In addition to nocodazole treatment, we measured the microtubule growth rate by monitoring the velocity of EB3-mRFP in transiently (co-)transfected Cos7 cells. In such experiments, microtubule-stabilizing proteins indirectly reduce the polymerization rate by reducing the concentration of non-polymerized α- and β-tubulin dimers in the cytoplasm: The concentration of unbound tubulin dimers is rate limiting for microtubule polymerization. EB3 is a plus end-tracking protein (Akhmanova and Hoogenraad, 2005; Nakagawa *et al.*, 2000; Stepanova *et al.*, 2003) and therefore only associates with the tips of growing microtubules. For *in vivo* visualization, EB3 was fused to a mRFP. Cos7 cells, transiently transfected with EB3-mRFP only, showed an average microtubule growth rate of 0.36 µm/s (range: 0.26–0.5 µm/s, *n*=200 microtubule plus-ends) as measured by the speed of movement of EB3-mRFP comet-like dashes (1 frame/s) (Figure 8). Others have reported similar microtubule growth rates. Interestingly, the microtubule growth rate in the presence of GFP-Eml4 decreases significantly ($P<0.01$) to 0.27 µm/s (range: 0.16–0.4 µm/s; *n*=200 microtubule plus-ends). This Eml4-associated decrease in microtubule growth was observed in three independent experiments, with analysis performed blind to the experimenter. In summary, GFP-Eml4 expression is associated with a decrease in microtubule growth rate and this decreased growth rate is in line with the hypothesis that GFP-Eml4 stabilizes microtubules.

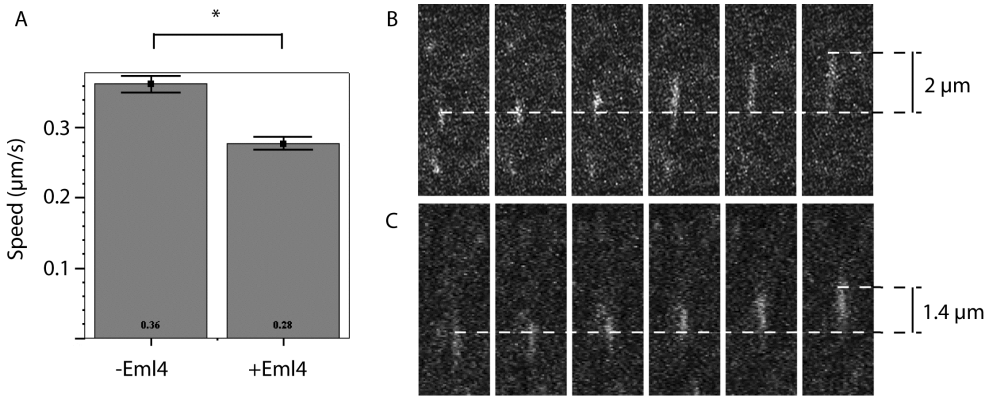

Figure 8. GFP-Eml4 cotransfection decreases microtubule growth rate. (A) Microtubule growth rate decreases significantly in the presence of Eml4. (B) EB3-mRFP (in white) comet-like structure in six successive frames, 1 s interval. The traveled distance of the comet-like structure is 2 µm whereas in the presence of Eml4 the traveled distance of the comet-like structure is 1.4 µm.

Discussion

Expression of Eml4

Our ISH experiments demonstrate that *Eml4* is highly expressed in E11 mouse embryos and expression declines throughout development. In addition, *Eml4* expression becomes restricted during maturation to the CNS, eyes and intestines. Although Eml4 is highly expressed in developing embryos, our results indicate that *Eml4* expression persists in the adult olfactory bulb, hippocampus and cerebellum. This spatio-temporal expression pattern is confirmed on the protein level by Western blot analysis. The developmentally regulated expression of Eml4 was also confirmed in a different study using differential display (Thuret *et al.*, 2004): Eml4 is differentially expressed between early embryos (E12, E14) and the adult olfactory bulb. Although the developmentally regulated expression of Eml4 is unique among other mammalian members of the EMAP protein family (O'Connor *et al.*, 2004) (S.H. Houtman, unpublished observations), other MAPs have also been reported to show developmentally regulated expression. These include mouse neuron navigator (mNAV) (*unc-53* (uncoordinated 53)) (Martinez-Lopez *et al.*, 2005) and doublecortin (Francis *et al.*, 1999; Gleeson *et al.*, 1999).

Eml4 is a member of the EMAP protein family

Our study required cloning the full length cDNA sequence of Eml4 from adult mouse brain. In comparison to mouse Eml4 sequences from the public databases (AAH70427, BC067011 and NP__199466) we identified an extra exon (exon 5) that is included in several Eml4 transcripts. Because adult cerebellum only expresses a distinct subset of splice-variants, our results provide evidence for tissue specific alternative splicing. We were unable to confirm splicing of exon 2 in any of our experiments; exon 2 was absent in all transcripts. Transcripts containing exon 2 are therefore expressed either at very low levels or expressed in areas not examined in this study. On the protein level, these splice variants do not affect the Eml4 domain structure. However, transcripts that include exon 2 do disrupt a previously unidentified alpha-helical coiled-coil (a putative dimerization domain (Lupas *et al.*, 1991; Mason and Arndt, 2004; O'Connor *et al.*, 2004)). This coiled-coil is also present in the public domain database entry of Eml4 (Heidebrecht *et al.*, 2000). Such dimerization domain has been identified in several other members of the EMAP protein family (O'Connor *et al.*, 2004). We therefore screened for and identified coiled-coil domains in all mammalian EMAP protein family members. Because alpha-helical coiled-coil domains are putative dimerization domains, it is possible that Eml4 forms either homodimers or heterodimers with other Eml family members. The expression of multiple Eml4 transcripts may result in a number of Eml4 proteins with differences in

molecular mass. Indeed, Western blot analysis identified multiple bands around the calculated molecular mass of Eml4 (120 kDa).

Microtubule association of Eml4

Our results demonstrated that GFP-Eml4 co-localizes with the microtubules of non-dividing cells. Eml4 is therefore likely to be a MAP. This hypothesis is supported by recently performed co-sedimentation assays (Pollmann *et al.*, 2006). Furthermore GFP-Eml4 co-localizes with the entire microtubules of non-dividing cells and therefore is neither a plus-end binding, like cytoplasmic linker proteins 170 kDa (Clip-170), EB1 or EB3 (Akhmanova and Hoogenraad, 2005; Perez *et al.*, 1999; Stepanova *et al.*, 2003; Tirnauer and Bierer, 2000), nor a minus-end binding protein.

In addition, we also showed that GFP-Eml4 colocalizes with the mitotic spindle of dividing cells. Such colocalization to the mitotic spindle has also been reported for other members of the EMAP protein family e.g. EMAP (Suprenant *et al.*, 1993) and Eml2 (Eichenmuller *et al.*, 2002) as well as for human EML4 (Pollmann *et al.*, 2006). The observation that Eml4 colocalizes with the mitotic spindle therefore renders Eml4 likely to play a role during cell division. This hypothesis is supported by our observation that the mitotic index of GPF-Eml4 expressing cells is reduced and the observation that down-regulation of EML4 in HeLa cells affects cell proliferation (Pollmann *et al.*, 2006). Similar to EMAP (Brisch *et al.*, 1996), the function of Eml4 may be determined in a phosphorylation dependent manner during cell cycle (Pollmann *et al.*, 2006).

Eml4 is a microtubule stabilizing protein

In our transient transfection experiments, we observed circular microtubules 18 h post-transfection in cells that express GFP-Eml4 at a high level and in virtually all cells 48 h post-transfection. These circular microtubules may be a result of microtubule bundling or microtubule elongation and are suggestive of a microtubule stabilizing function of Eml4. This stabilizing function of Eml4 was confirmed in nocodazole-induced microtubule depolymerization experiment. Cos7 cells transiently transfected with GFP-Eml4 were resistant to nocodazole induced microtubule disruption.

In a separate set of experiments we demonstrated that the microtubule growth rate is significantly decreased in cells expressing GFP-Eml4. Because the concentration of unbound tubulin dimers is rate limiting for microtubule polymerization, overexpression of microtubule-stabilizing proteins indirectly will reduce the polymerization rate due to a reduction in the cytoplasmic concentration of non-polymerized α- and β-tubulin dimers. The reduced Eml4-associated microtubule growth rate therefore confirms the hypothesis that Eml4 is a microtubule stabilizing protein. Interestingly, other members of the

EMAP protein family, Eml2 and EMAP, have been shown to destabilize microtubule. For example, Eml2 reduces growth rate and increases the frequency of catastrophe (the transition from growing to shortening microtubules) (Eichenmuller *et al.*, 2002), whereas EMAP destabilizes microtubules by reducing the frequency of rescue (the transition from shortening to growing microtubules) (Hamill *et al.*). Eml4 is therefore the first member of the EMAP protein family that stabilizes microtubules. Our results were confirmed in an independent study demonstrating EML4 is essential for microtubule formation (Pollmann *et al.*, 2006). How Eml4 stabilizes microtubules (reduction in catastrophe rate, reduction in shrinkage rate, increase in rescue frequency, increase in growth rate) requires further investigation by e.g. *in vitro* polymerization assays.

The role of Eml4 in postmitotic neurons

Our results indicate that Eml4 is highly expressed in the developing nervous system and expression persists in discrete regions of the adult mouse brain. Recently a study by Dunckley and Lukas (2003) describes Eml4 (C2ORF2) as one of the genes that are down-regulated by nicotine stimulation of a neuroblastoma cell line. This nicotine-regulated expression argues for role of Eml4 following increased neuronal activity.

Although the exact cellular function of Eml4 in postmitotic neurons remains to be determined, protein–protein interactions of other closely related proteins (i.e. other members of the EMAP protein family) might help defining the cellular function of Eml4. For example, members of the Eml family are shown to interact with δ1- and δ2-glutamate receptor (Eml2) and with 14-3-3 (Eml3) (Jin *et al.*, 2004; Ly *et al.*, 2002; Pozuelo Rubio *et al.*, 2004). The δ1- and δ2-glutamate receptors are members of a distinct protein family (Lomeli *et al.*, 1993) of which the δ2-glutamate receptor expression is restricted to cerebellar Purkinje cells (Takayama *et al.*, 1996; Yuzaki, 2003). Although Eml2 can interact with the δ2-glutamate receptor, it appears not to be expressed in these cells. Interestingly, the δ2-binding site of rat Eml2 shares a 75% similarity and 58% identity to the homologous region of mouse Eml4. Because of this high degree of homology between the δ2-binding site and because our results indicate that Eml4 is expressed in adult cerebellar Purkinje cells, it is tempting to speculate that the natural binding partner of δ2-glutamate receptor is Eml4. However, a direct association between Eml4 and δ2-glutamate receptor remains to be determined. The 14-3-3 proteins, although initially found in brain, are ubiquitously expressed and form a family of proteins that are involved in diverse cellular processes including regulation of cell cycle, signal transduction pathways and differentiation (Mackintosh, 2004; Mhawech, 2005; Muslin *et al.*, 1996). Because of the high degree of homology between

Eml3 and Eml4, it is possible that 14-3-3 proteins interact with Eml4 and/or other members of the EMAP protein family. Although such interactions and cellular functions remain to be examined, our study is the first to determine that Eml4 is a developmentally regulated protein that associates with and stabilizes microtubules.

Acknowledgments
We would like to thank A. Akhmanova for donating the EB3-mRFP construct. Supported by ZON-MW (C.I.D.Z.), NWO-ALW (C.I.D.Z.) and NWO (P.J.F.).

References

Ahmad, F.J., W. Yu, F.J. McNally, and P.W. Baas. 1999. An essential role for katanin in severing microtubules in the neuron. *J Cell Biol*. 145:305-15.

Akhmanova, A., and C.C. Hoogenraad. 2005. Microtubule plus-end-tracking proteins: mechanisms and functions. *Curr Opin Cell Biol*. 17:47-54.

Baas, P.W. 1999. Microtubules and neuronal polarity: lessons from mitosis. *Neuron*. 22:23-31.

Brisch, E., M.A. Daggett, and K.A. Suprenant. 1996. Cell cycle-dependent phosphorylation of the 77 kDa echinoderm microtubule-associated protein (EMAP) in vivo and association with the p34cdc2 kinase. *J Cell Sci*. 109 (Pt 12):2885-93.

Cassimeris, L. 2002. The oncoprotein 18/stathmin family of microtubule destabilizers. *Curr Opin Cell Biol*. 14:18-24.

Desai, A., and T.J. Mitchison. 1997. Microtubule polymerization dynamics. *Annu Rev Cell Dev Biol*. 13:83-117.

Dunckley, T., and R.J. Lukas. 2003. Nicotine modulates the expression of a diverse set of genes in the neuronal SH-SY5Y cell line. *J Biol Chem*. 278:15633-40.

Eichenmuller, B., P. Everley, J. Palange, D. Lepley, and K.A. Suprenant. 2002. The human EMAP-like protein-70 (ELP70) is a microtubule destabilizer that localizes to the mitotic apparatus. *J Biol Chem*. 277:1301-9.

Eudy, J.D., M. Ma-Edmonds, S.F. Yao, C.B. Talmadge, P.M. Kelley, M.D. Weston, W.J. Kimberling, and J. Sumegi. 1997. Isolation of a novel human homologue of the gene coding for echinoderm microtubule-associated protein (EMAP) from the Usher syndrome type 1a locus at 14q32. *Genomics*. 43:104-6.

Francis, F., A. Koulakoff, D. Boucher, P. Chafey, B. Schaar, M.C. Vinet, G. Friocourt, N. McDonnell, O. Reiner, A. Kahn, S.K. McConnell, Y. Berwald-Netter, P. Denoulet, and J. Chelly. 1999. Doublecortin is a developmentally regulated, microtubule-associated protein expressed in migrating and differentiating neurons. *Neuron*. 23:247-56.

French, P.J., V. O'Connor, M.W. Jones, S. Davis, M.L. Errington, K. Voss, B. Truchet, C. Wotjak, T. Stean, V. Doyere, M. Maroun, S. Laroche, and T.V. Bliss. 2001. Subfield-specific immediate early gene expression associated with hippocampal long-term potentiation in vivo. *Eur J Neurosci*. 13:968-76.

Gleeson, J.G., P.T. Lin, L.A. Flanagan, and C.A. Walsh. 1999. Doublecortin is a microtubule-associated protein and is expressed widely by migrating neurons. *Neuron*. 23:257-71.

Hamill, D.R., B. Howell, L. Cassimeris, and K.A. Suprenant. 1998. Purification of a WD repeat protein, EMAP, that promotes microtubule dynamics through an inhibition of rescue. *J Biol Chem*. 273:9285-91.

Heald, R., and E. Nogales. 2002. Microtubule dynamics. *J Cell Sci*. 115:3-4.

Heidebrecht, H.J., F. Buck, M. Pollmann, R. Siebert, and R. Parwaresch. 2000. Cloning and localization of C2orf2(ropp120), a previously unknown WD repeat protein. *Genomics*. 68:348-50.

Howard, J., and A.A. Hyman. 2003. Dynamics and mechanics of the microtubule plus end. *Nature*. 422:753-8.

Itoh, T.J., and H. Hotani. 2004. Microtubule dynamics and the regulation by microtubule-associated proteins (MAPs). *Biol Sci Space*. 18:116-7.

Jin, J., F.D. Smith, C. Stark, C.D. Wells, J.P. Fawcett, S. Kulkarni, P. Metalnikov, P. O'Donnell, P. Taylor, L. Taylor, A. Zougman, J.R. Woodgett, L.K. Langeberg, J.D. Scott, and T. Pawson. 2004. Proteomic, functional, and domain-based analysis of in vivo 14-3-3 binding proteins involved in cytoskeletal regulation and cellular organization. *Curr Biol*. 14:1436-50.

Kalcheva, N., J.M. Rockwood, Y. Kress, A. Steiner, and B. Shafit-Zagardo. 1998. Molecular and functional characteristics of MAP-2a: ability of MAP-2a versus MAP-2b to induce stable microtubules in COS cells. *Cell Motil Cytoskeleton*. 40:272-85.

Kohrmann, M., W. Haubensak, I. Hemraj, C. Kaether, V.J. Lessmann, and M.A. Kiebler. 1999. Fast, convenient, and effective method to transiently transfect primary hippocampal neurons. *J Neurosci Res*. 58:831-5.

Lepley, D.M., J.M. Palange, and K.A. Suprenant. 1999. Sequence and expression patterns of a human EMAP-related protein-2 (HuEMAP-2). *Gene*. 237:343-9.

Li, Q., M. Callaghan, and K.A. Suprenant. 1998. The 77-kDa echinoderm microtubule-associated protein (EMAP) shares epitopes with the mammalian brain MAPs, MAP-2 and tau. *Biochem Biophys Res Commun*. 250:502-5.

Lomeli, H., R. Sprengel, D.J. Laurie, G. Kohr, A. Herb, P.H. Seeburg, and W. Wisden. 1993. The rat delta-1 and delta-2 subunits extend the excitatory amino acid receptor family. *FEBS Lett*. 315:318-22.

Lupas, A., M. Van Dyke, and J. Stock. 1991. Predicting coiled coils from protein sequences. *Science*. 252:1162-1164.

Ly, C.D., K.W. Roche, H.K. Lee, and R.J. Wenthold. 2002. Identification of rat EMAP, a delta-glutamate receptor binding protein. *Biochem Biophys Res Commun*. 291:85-90.

Mackintosh, C. 2004. Dynamic interactions between 14-3-3 proteins and phosphoproteins regulate diverse cellular processes. *Biochem J*. 381:329-42.

Martinez-Lopez, M.J., S. Alcantara, C. Mascaro, F. Perez-Branguli, P. Ruiz-Lozano, T. Maes, E. Soriano, and C. Buesa. 2005. Mouse neuron navigator 1, a novel microtubule-associated protein involved in neuronal migration. *Mol Cell Neurosci*. 28:599-612.

Mason, J.M., and K.M. Arndt. 2004. Coiled coil domains: stability, specificity, and biological implications. *Chembiochem*. 5:170-6.

Mhawech, P. 2005. 14-3-3 proteins--an update. *Cell Res*. 15:228-36.

Muslin, A.J., J.W. Tanner, P.M. Allen, and A.S. Shaw. 1996. Interaction of 14-3-3 with signaling proteins is mediated by the recognition of phosphoserine. *Cell*. 84:889-97.

Nakagawa, H., K. Koyama, Y. Murata, M. Morito, T. Akiyama, and Y. Nakamura. 2000. EB3, a novel member of the EB1 family preferentially expressed in the central nervous system, binds to a CNS-specific APC homologue. *Oncogene*. 19:210-6.

Nogales, E. 2000. Structural insights into microtubule function. *Annu Rev Biochem*. 69:277-302.

O'Connor, V., S.H. Houtman, C.I. De Zeeuw, T.V. Bliss, and P.J. French. 2004. Eml5, a novel WD40 domain protein expressed in rat brain. *Gene*. 336:127-37.

Perez, F., G.S. Diamantopoulos, R. Stalder, and T.E. Kreis. 1999. CLIP-170 highlights growing microtubule ends in vivo. *Cell*. 96:517-27.

Pollmann, M., R. Parwaresch, S. Adam-Klages, M.L. Kruse, F. Buck, and H.J. Heidebrecht. 2006. Human EML4, a novel member of the EMAP family, is essential for microtubule formation. *Exp Cell Res*. 312:3241-51.

Pozuelo Rubio, M., K.M. Geraghty, B.H. Wong, N.T. Wood, D.G. Campbell, N. Morrice, and C. Mackintosh. 2004. 14-3-3-affinity purification of over 200 human phosphoproteins reveals new links to regulation of cellular metabolism, proliferation and trafficking. *Biochem J*. 379:395-408.

Stepanova, T., J. Slemmer, C.C. Hoogenraad, G. Lansbergen, B. Dortland, C.I. De Zeeuw, F. Grosveld, G. van Cappellen, A. Akhmanova, and N. Galjart. 2003. Visualization of microtubule growth in cultured neurons via the use of EB3-GFP (end-binding protein 3-green fluorescent protein). *J Neurosci*. 23:2655-64.

Suprenant, K.A., K. Dean, J. McKee, and S. Hake. 1993. EMAP, an echinoderm microtubule-associated protein found in microtubule-ribosome complexes. *J Cell Sci*. 104:445-50.

Suprenant, K.A., J.A. Tuxhorn, M.A. Daggett, D.P. Ahrens, A. Hostetler, J.M. Palange, C.E. VanWinkle, and B.T. Livingston. 2000. Conservation of the WD-repeat, microtubule-binding protein, EMAP, in sea urchins, humans, and the nematode C. elegans. *Dev Genes Evol*. 210:2-10.

Takayama, C., S. Nakagawa, M. Watanabe, M. Mishina, and Y. Inoue. 1996. Developmental changes in expression and distribution of the glutamate receptor channel delta 2 subunit according to the Purkinje cell maturation. *Brain Res Dev Brain Res*. 92:147-55.

Thuret, S., L. Bhatt, D.D. O'Leary, and H.H. Simon. 2004. Identification and developmental analysis of genes expressed by dopaminergic neurons of the substantia nigra pars compacta. *Mol Cell Neurosci*. 25:394-405.

Tirnauer, J.S., and B.E. Bierer. 2000. EB1 proteins regulate microtubule dynamics, cell polarity, and chromosome stability. *J Cell Biol*. 149:761-6.

Yuzaki, M. 2003. The delta2 glutamate receptor: 10 years later. *Neurosci Res*. 46:11-22.

Chapter 3

Eml5, a novel WD40 domain protein expressed in rat brain

V. O´Connor[1,2], S.H. Houtman[3], C.I. De Zeeuw[3], T.V.P. Bliss[1], P.J. French[4]

[1]Neurophysiology Division, National Institute for Medical Research, London, UK
[2]Department of Cell Sciences, University Southampton, Southampton, UK
[3]Department of Neuroscience, Erasmus MC, Rotterdam, the Netherlands
[4]Department of Neurology, Erasmus MC, Rotterdam, the Netherlands

Gene 336 (2004) 127-137

Abstract
We have isolated a novel transcript with homology to the major microtubule-associated protein in dividing sea urchin embryos, EMAP. The protein has a predicted MW of ~180 kDa and we have named it Eml5 (EMAP-like protein 5, GenBank accession no. AY445136). Eml5 contains 11 putative WD40 domains and 3 hydrophobic stretches of 43 aa, HELP domains, which have been suggested to be involved in microtubule binding. Eml5 appears to consist of two tandem repeats of the complete EMAP protein separated by a putative dimerization domain. Eml5 mRNA and protein is expressed at high levels in the hippocampus, cerebellum and olfactory bulb, as determined by in situ hybridization and immunocytochemistry. *Eml5* transcripts can be detected in fore- and hindbrain structures from embryonic day 13 onwards. Because other EMAP-like proteins are involved in regulating microtubule dynamics, it is likely that *Eml5* plays a role in the regulation of cytoskeletal rearrangements during neuronal development and in adult brain

Introduction
Microtubules are polymers made up of α- and β-tubulin subunits that provide architectural support for eukaryotic cells. In neurons, they are required for the growth and maintenance of neuronal processes (Sanchez *et al.*, 2000). Furthermore, microtubules act as pathways for transport of cytoplasmic constituents. Microtubules have an intrinsic polarity with a slow growing minus end and a fast growing plus end. In most cells, microtubules are anchored to the major microtubule-nucleating center, the centrosome (Bornens, 2002), and are oriented with their plus ends distal to the cell body (Joshi, 1998). In neurons, the microtubular network is arranged slightly different; microtubules are not anchored to the centrosome and, in dendrites, are oriented in both directions (Baas, 1999). Axonal microtubules, however, are oriented with their plus ends away from the soma (Heidemann *et al.*, 1981). It has been hypothesized that microtubules in neuronal processes may be established by mechanisms similar to those used for the formation and functioning of the mitotic spindle (Baas, 1999), which, during mitosis, become the key structural components on which chromosomes segregate.
Structural binding proteins control the dynamics of microtubules by regulating the growth and shrinkage at the plus ends (Walczak, 2000). Microtubule-stabilizing proteins like MAP2 (Sanchez *et al.*, 2000) and Tau (Buee *et al.*, 2000) promote growth by, for example, reducing the rate of catastrophe (the transition from growing to shrinking). Microtubule-destabilizing proteins like Op18/stathmin (Cassimeris, 2002) promote microtubule disassembly, or, like katanin, even cause severing of microtubules (Ahmad *et al.*, 1999).

In dividing sea urchin (*Strongylocentrotus purpuratus*) eggs, a 77-kDa echinoderm microtubule-associated protein (EMAP) is the major microtubule-binding protein (Hamill *et al.*, 1998; Suprenant *et al.*, 1993). Several mammalian homologues of EMAP, EMLs (EMAP-like proteins), have been identified. They include the Human homologue of EMAP isolated from the Usher-1a locus, EML1 (Eudy *et al.*, 1997), EML2/Huemap2 (Lepley *et al.*, 1999), and EML4/ROPP120 (Heidebrecht *et al.*, 2000). An additional EML, EML3, can be predicted from the human genomic sequence. Several EMLs have been demonstrated to associate with microtubules of the mitotic spindle in vivo and in vitro (Eichenmuller *et al.*, 2002; Hamill *et al.*, 1998; Suprenant *et al.*, 1993). Furthermore, EML proteins appear to affect the dynamics of microtubules. For example, EMAP increases microtubule dynamics and inhibits the frequency of rescue (the transition from shortening to growing microtubules; Hamill *et al.*, 1998), whereas EML2 reduces the growth rate and promotes the frequency of catastrophes (the transition from growing to shortening; Eichenmuller *et al.*, 2002). Because both EMAP and EML2 effectively cause an overall shortening of microtubules, the EML family of proteins may represent a novel class of microtubule-destabilizing proteins. Here we report the cloning and characterization of a fifth member of the EML family, Eml5 and splice variants Eml5^{a} and Eml5^{b}. Because Eml5 is expressed in post-mitotic neurons (in adult animals and during development), we hypothesize that Eml proteins play a role in the cytoskeletal rearrangements observed during neuronal development and in adult brain.

Materials and Methods

Differential display

Differential display performed primarily to identify genes regulated in LTP also identified a number of candidates whose expression and/or sequence homology warranted further investigation. The PCR-based methods used to generate fragments of hippocampal cDNA were as described previously (French *et al.*, 2001). The fragment of Eml5 described in this study was amplified using the primer combination ACGACTCACTATAGGGC$(T)_{12}$AC and ACAATTTCACACAGGATGGATTGGTC.

***In situ* hybridization**

Brains from adult rats were removed, frozen on dry ice and stored at −70 °C. Fourteen-micrometer sections were cut on a cryostat, mounted onto polylysine-coated glass slides and stored at −70 °C. In situ hybridization was performed essentially as described by French *et al*. (2001). Briefly, sections were thawed, fixed in 4% paraformaldehyde, acetylated in 1.4% triethanolamine and 0.25% acetic anhydride, dehydrated through graded

ethanol solutions and delipidated in chloroform. Sections were hybridized overnight at 42 °C in 100 µl buffer containing 50% formamide, 4× SSC, 10% dextran sulfate, 5× Denhardt's solution, 200 mg/ml acid alkali cleaved salmon testis DNA, 100 mg/ml long-chain polyadenylic acid, 25mM sodium phosphate (pH 7.0), 1 mM sodium pyrophosphate and 100,000 CPM radiolabeled probe (approximately 1 ng/ml) under parafilm coverslips. Sections were washed in 1× SSC at 55 °C (30 min), 0.1× SSC at room temperature (5 min) and dehydrated in ethanol. Sections were then exposed to autoradiographic film. ^{35}S-ATP end-labeled probes (NEN) were generated using terminal deoxynucleotidyl transferase (Promega) according to manufacturer's instructions. Either a 50-fold excess of unlabeled antisense oligonucleotide or the complementary sense oligonucleotide was used as negative controls. 45-mer oligonucleotides of unique sequence were supplied by Oswel (Southampton, UK) or Life Technologies. Sequences were: Eml5 antisense I (corresponding to aa 470–484): CTTTCCTCCTGGCATCTTGTAGAGAAG TCGTTTCCCACTGCCGTC and II (corresponding to aa 1334–1348): TGGGCGGATATTAGTTGATAAGGCTCTGATGGTGTAGCTAATTTC, and Eml5^{b} splice variant: CCCCTGTAGCTAGGACCATTTTGTCACTCCACACTGGGGATGGTT.
Control sense oligos are complementary to the antisense oligo.
For nonradioactive in situ hybridizations, sections were fixed as described above, prehybridized (1 h) in buffer containing 50% formamide, 5× SSC, 5× Denhardt's, 250 µg/ml yeast tRNA (Sigma) and 500 µg/ml acid–alkali cleaved salmon testis DNA (Sigma). Hybridization was performed overnight at 65 °C in prehybridization buffer containing 100 ng/ml digoxigenin-UTP labeled cRNA probes. Antisense and sense probes directed against bp 2929–4074 were generated using a DIG RNA labeling kit (Roche) according to manufacturer's instructions. Following hybridization, sections were washed in 0.2× SSC at 65 °C and blocked in 0.1M Tris pH 7.5, 0.15M NaCl and 10% heat inactivated sheep serum (Sigma) for 1 h at RT. Alkaline phosphatase conjugated anti-digoxigenin antibodies (Roche) were added to the sections in a dilution of 1:5000 in 0.1M Tris pH 7.5, 0.15M NaCl and 1% heat-inactivated sheep serum and incubated overnight at 4 °C. Following washing of the sections, color reactions were performed in 0.1 M Tris pH 9.5, 0.1 M NaCl, 50 mM $MgCl_2$, 2 mM Levamisole (Sigma), 0.35 mg/ml nitroblue tetrazolium (Roche) and 0.18 mg/ml 5-bromo-4-chloro-3-indolylphosphate (Roche). Reactions were terminated upon visual inspection (~18 h), counterstained in 0.1% Fast red, dehydrated and mounted in Permount (Fisher).

RT-PCR

Rat hippocampal RNA was extracted using Trizol (Invitrogen) and reverse transcribed into cDNA using SuperscriptIII (Invitrogen). To determine the

relative abundance of individual splice variants, the following PCR primers were used: Splice site 1: GTGTCCTTTCACCACAGAAAAG (fwd) and CCACTTCACTTGTCCATACC (rev). Splice site 2: GCCTTATCAACTAATATCCGCC (fwd) and CCAACACAAGGTCCTCTATG (rev).

Antibodies

A fragment of Eml5 cDNA encoding aa 468–664 was fused to a His tag using a pET30b (Novagen) plasmid. The Eml5 fusion protein was expressed in bacteria (BL21dP lys S, Stratagene) and purified under denaturing conditions over Ni-NTA columns (Qiagen) according to manufacturer's instructions. Adult New Zealand White rabbits were immunized with 80 µg of purified $Eml5_{468–664}$ using Freund's complete adjuvant. The immunization was followed by four boosts of 80 µg $Eml5_{468–664}$ administered every 3 weeks in Freund's incomplete adjuvant. Serum was collected from bleeds taken 7 days after each boost; serum from boost 3 and 4 were used in this study. Antibodies were affinity-purified over nitrocellulose filter strips containing immobilized His tagged $Eml5_{468–664}$ (transferred by Western blotting following SDS-PAGE of the affinity purified fusion protein). Bound antisera were eluted from the filter using 0.1 M glycine (pH2.3) and 1 M NaCl. After elution, the pH was quickly restored with unbuffered 1 M Tris.

Immunocytochemistry

Rats were perfused transcardially with a 4% paraformaldehyde solution in PBS. Brains were removed and stored in a 20% sucrose solution. Forty-micrometer-thick coronal sections were cut and washed in 0.1 M phosphate buffer (PB), incubated in 2% hydrogen peroxide in 0.1 M PB for 30 min and washed in PB. Sections were then incubated for 72 h with affinity-purified rabbit polyclonal Eml5 antibodies at a dilution of 1:100 in PB, 0.3% Triton and 3% normal goat serum (NGS). Next, sections were washed in PB and incubated with a biotinylated goat antirabbit antibody (Vector) at a dilution of 1:500 for 1 h. Sections were then incubated for 30 min in Advance Vector ABC Elite 0.02% in PB. Staining was performed using hydrogen peroxide (0.01–01%) in 0.15 M Tris (pH 7.4) containing 0.5 mg/ml DAB and 2 mg/ml ammonium nickel sulfate. Staining reactions were terminated upon visual inspection.

2.6. Cell culture

Cos7 cells, grown in Lab-Tek chamber slides, were transfected using DEAE-dextran. In brief, cells were incubated for 30 s in serum-free medium containing 0.5 mg/ml DEAE-dextran. Cells were then exposed to a $Eml5^b$ construct C-terminally fused to GFP (1 µg) in the presence of 0.1 mM chloroquine for 5–6 h. The $Eml5^b$ construct was generated by PCR amplification using primers AGCGGGAGAGCTTTCGTCAC (fwd) and

CTTTAGCACCAGTGTTGACC (rev) on constructs that were derived from library screens and RT-PCR reactions. Finally, cells were incubated in 10% DMSO after which they were returned to normal medium [10% fetal calf serum, 45% DMEM and 45% F-10 supplemented by antibiotics (penicillin and streptomycin)]. Eighteen to forty-eight hours after transfection, cells were fixed in ice-cold methanol (100%), 1 mM EGTA (10 min) and subsequently in 4% paraformaldehyde (10 min). Cells were permeabilized in 0.1% Saponin/PBS, containing 1% BSA, 10% fetal calf serum before being incubated (1 h) with anti-Eml5 antibodies (1:200). Following washing in PBS, cells were incubated (1 h) with the secondary antibody (Alexa-Fluor goat anti rabbit 594, dilution 1:300). Slides were mounted in Vectashield mounting medium (Vector Laboratories) containing DAPI.

Northern blot analysis

Partial Eml5 sequence corresponding to bp 1764–2052 (amino acids 458–553), isolated as a candidate LTP regulated gene from the differential display screen was used to generate radiolabeled double-stranded cDNA probes (Prime-It II Random Primer Labeling Kit, Stratagene) to screen both a hippocampal library and a rat brain Northern blot (Origene). Northern blots were prehybridized in 5× SSPE, 1% SDS, 5× Denhardt's and 0.1 mg/ml Salmon testis DNA (Sigma) for 3 h, and then, hybridized overnight in buffer containing 5× SSPE, 0.2% SDS, 5× Denhardt's, 0.1 mg/ml Salmon testis DNA (Sigma), 50% formamide and 0.8 10^6 cpm/ml probe at 68 °C. Blots were subsequently washed in 2× SSC, 0.05% SDS for 40 min at room temperature, and 0.1× SSC, 0.1% SDS at 50 °C. Blots were then exposed to X-ray film. Equivalent loading between tissues was determined by rehybridizing the blot with a 1.3-kb fragment at the 3′ end of KIAA0828, a 5.1-kb mRNA transcript expressed at high levels throughout the brain (Nagase *et al.*, 1998).

Library screen

cDNA encompassing the 3′ 3.2 kb of Eml5 was obtained by RACE-PCR (marathon cDNA amplification, Clontech) on mRNA isolated from rat cerebellum, hippocampus and olfactory bulb using oligonucleotides CAACACACGTCCATGAAGCCCAG and AAATGACGGCAGTGGGAAACGAC (corresponding to aa 497–503 and 469–475, respectively). RACE-PCR fragments were independently sequence verified following RT-PCR using primers GGTTGGTTTAGAGATCCTCAATTCAC and CCTCATTCACTTTCTGCCACTCC. The full-length Eml5 sequence was obtained by screening a rat hippocampal library that had undergone one round of amplification (a generous gift from N. Galjart, C.I. De Zeeuw and F. Grosveld). Duplicate filters containing ~10^6 clones were hybridized overnight at 60 °C with 10^6 CPM/ml hybmix (5× SSC, 5×

Denhardt's, 0.1% SDS, 100 µg/ml salmon testis DNA). Then, filters were washed at 60 °C in 2× SSC, 0.1% SDS and 0.1× SSC, 0.1% SDS. Five double-positive plaques were identified and were replated and screened to obtain single purified plaques. Purified plaques were subjected to in vivo excision according to the manufacturer's instructions (Stratagene). This identified the additional 2.8 kb situated at the 5′ end of Eml5.

Results

Cloning and sequence analysis of rat Eml5

Partial Eml5 corresponding to bp 1764–2052 (amino acids 458–553) was isolated as a false positive from a screen primarily aimed at identifying genes induced 24 h following the induction of LTP in the dentate gyrus of the hippocampus. The full-length sequence was cloned by a combination of screening a hippocampal library and 5′ and 3′ RACE PCR (GenBank accession no. AY445136). Within the sequence, a single large open reading frame was detected that encompasses a protein of 1606 amino acids with an estimated molecular mass of ~180 kDa. Stop codons can be found in all reading frames before the putative rat Eml5 translation initiation site, suggesting we indeed cloned the full-length rat Eml5 cDNA sequence. A consensus Kozak sequence (Kozak, 1987) can be identified around the putative translation initiation site.

The protein encoded by the cDNA revealed a marked homology to the 77-kDa echinoderm microtubule associated protein (EMAP) of which three other mammalian homologues have thus far been identified. A fourth homologue can be predicted from the human genomic sequence. We have therefore named this protein EMAP like protein 5 (Eml5), the largest member of the Eml family. Figure 1A shows the homology of Eml5 with the other family members. Because Eml5 appears to consist of a 2.5-fold repeat of the complete EMAP protein, we have aligned the N-terminal, middle and C-terminal parts separately. This repeat is highlighted by the similarity between individual parts of Eml5; the middle part (aa 674–1270) has 42% identity and 64% similarity with amino acids (aa) 7–599 of the N-terminal part. The homology of Eml5 to EMAP is equal at both ends of the protein; both the N-terminus (aa 7–594) and middle part (aa 674–1270) exhibit 34% identity and 53% similarity to EMAP. A phylogenetic analysis of the EML family is depicted in Figure 1B, and shows that Eml5 is more closely related to EMAP than to other members of the Eml family.

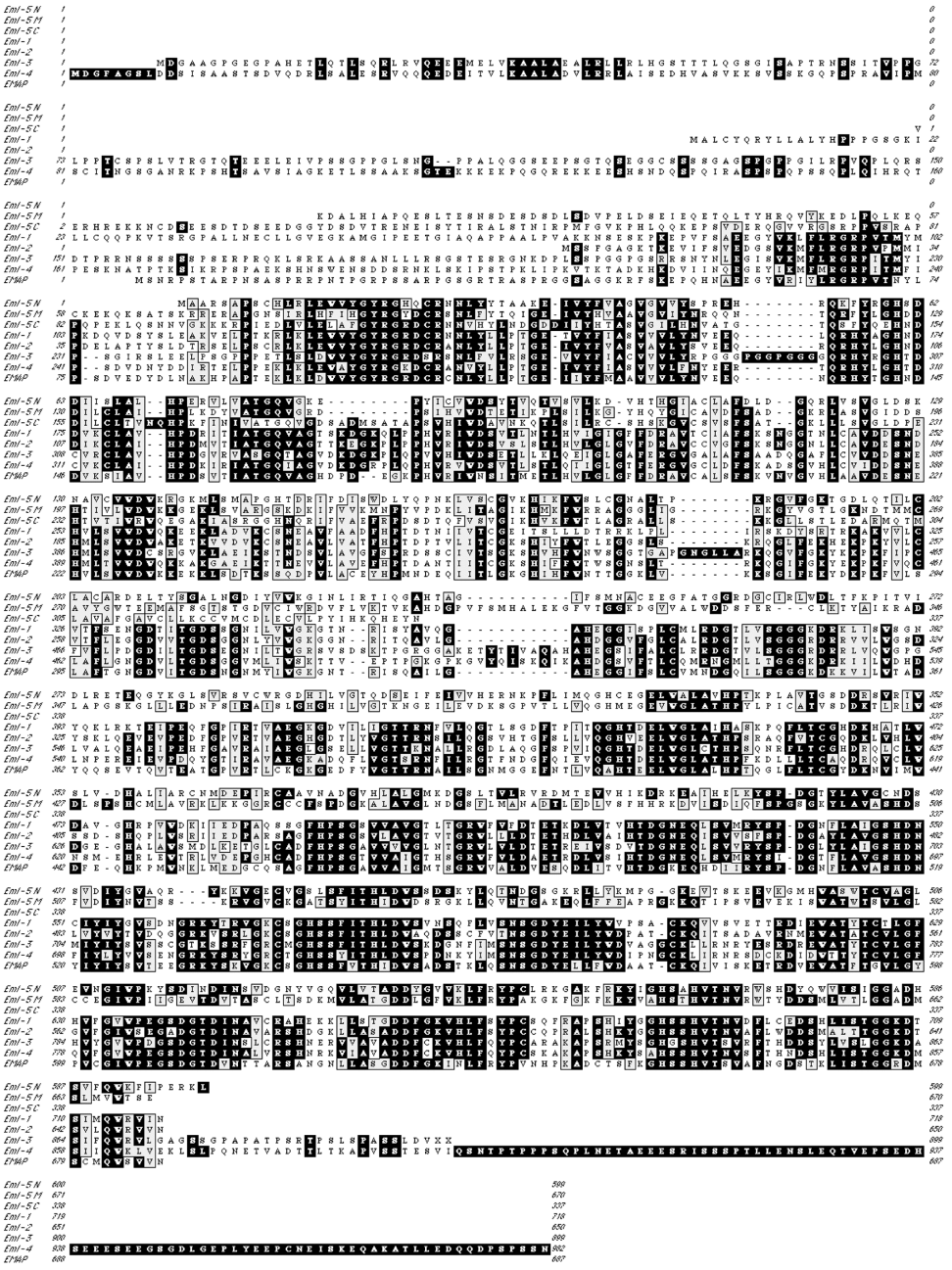

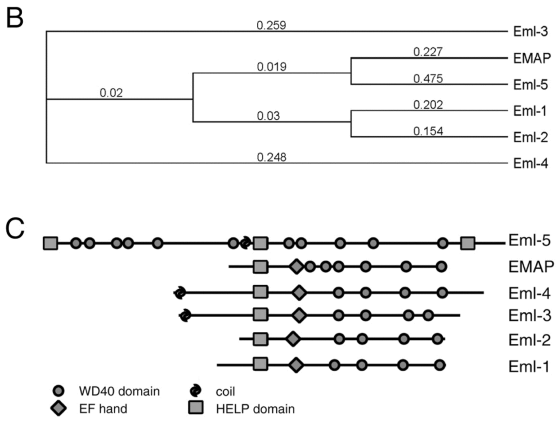

Figure 1. (A) Primary structure and sequence homologies of Eml5. The figure shows an alignment of the N-terminal middle and C-terminal parts of rat Eml5 with EMAP (derived from *S. purpuratus*) and human EML protein family members EML1/HuEMAP1, EML2/HuEmap2, EML3 (predicted) and EML4/ROPP120. (B) Phylogenetic analysis of the EML protein family. (C) Schematic drawing of EML proteins showing location of HELP- and WD40 domains, EF hands and alpha helical coiled coil region.

A schematic representation of domains present within Eml5 is shown in Figure 1C. Like other members of the EMAP family, Eml5 contains several (11) putative WD40 domains as well as three consensus HELP domains (hydrophobic EMAP-like protein domain), domains that may be required for microtubule binding (Eichenmuller *et al.*, 2002). A region that is strongly predicted to contain an alpha-helical coil, a putative dimerization domain, separates the N-terminal and middle part of Eml5 (aa 641–673). Eml4/ROPP120 and the predicted sequence of Eml3 are other family members that also contain such putative dimerization domain. Several potential sites for protein kinases can be identified within the Eml5 sequence. Although consensus phosphorylation sites have a high probability of occurrence within any given sequence, conservation of sites in all EML family members may be an indicator of functional relevance. However, none of the consensus sites for protein kinase A, cGMP-dependent protein kinase and protein kinase C appears to be conserved in all EML proteins. Besides the features mentioned, Eml5 is unique among the EML family in that it is the only member that lacks a consensus site for an EF hand, a calcium-binding domain.

A sequence homologous to EML can be found on chromosome 14q31 of the completed human genome (LOC161436). The coding sequence of EML5 described here is distributed over 33 exons, the translation–initiation site being within exon 1, and spans over 165 kb of genomic sequence. The predicted initiation site of human EML5 lies at a similar site to rat Eml5 supporting the assumption that we obtained the complete 5′ coding sequence of the mRNA.

Eml5 splice variants

Two alternative splicing products were also identified upon cloning the full-length Eml5 sequence (Figure 2). Insertions of 110 and 56 bp at position 3891 and 4397 (corresponding to aa 1166 and 1335), respectively. Omission at splice site 1 and insertion at splice sites 2 results in an insertion of an in-frame stop codon and gives rise to Eml5^{b} and Eml5^{a}, respectively. Comparison of the cDNA sequence with the human genome sequence revealed the first splice variant is likely to be caused by an alternative splice acceptor site within the 25th exon. The second variant is likely to be caused by insertion of an additional exon between exon 27 and 28.

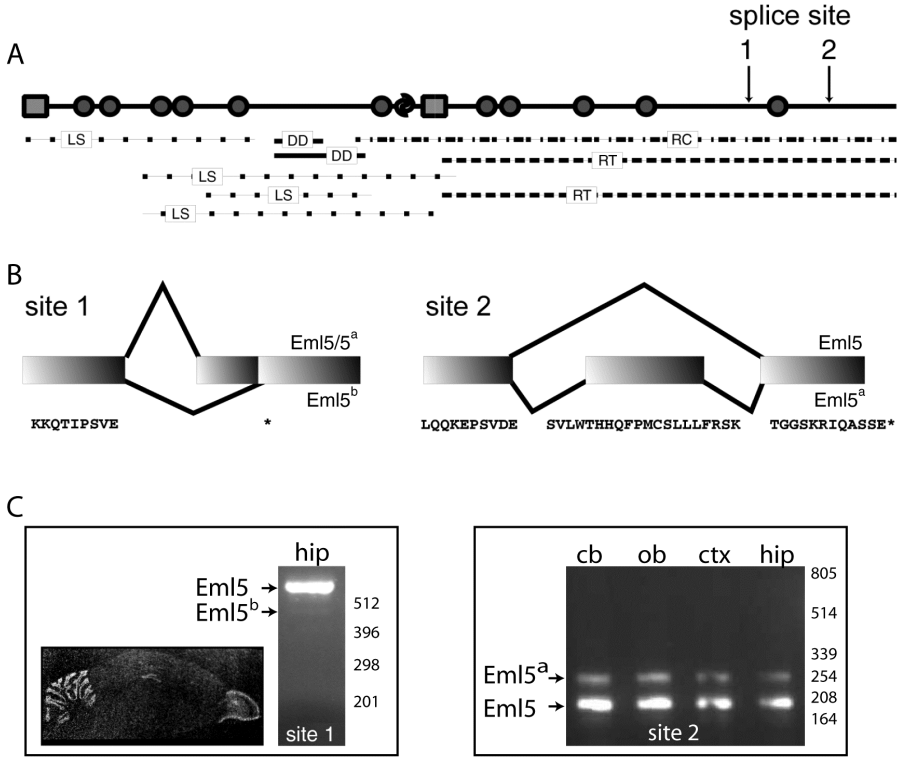

Figure 2. Alternative splicing of Eml5 leads to the formation of Eml5^{a} and Eml5^{b}. (A) Location of splice sites relative to the full-length Eml5 protein. Dashed lines indicate the individual clones isolated from the differential display screen (DD), RACE-PCR (RC), RT-PCR (RT) and library screens (LS). (B) Model of splice variants' origin based on comparison with the completed human genome sequence. Eml5^{b} is likely to be generated by an alternative splice acceptor site whereas Eml5^{a} is likely to be generated by insertion of an additional exon. (C) RT-PCR showing relative expression levels of Eml splice variants. Expected and identified PCR fragments are indicated with arrows. At splice site 1 (left panel), the expected fragment size is 583 and 473 bp for Eml5/Eml5^{a} and Eml5^{b}, respectively. In situ hybridization shows Eml5b expression in adult brain confirming expression of this splice variant. Expected fragments at splice site 2 (right panel) are 251 and 191 bp for Eml5^{a} and Eml5, respectively. cb: cerebellum, ob: olfactory bulb, ctx: cortex, hip: hippocampus.

The largest continuous open reading frame as shown in Figure 1A (Eml5) therefore uses the first splice acceptor site at exon 25 and does not contain the insertion at the second splice site. The shortest isoform truncates the protein at position 1167 resulting in a protein with a predicted MW of 130 kDa. The other isoform results in a protein of 1367 aa with a predicted MW of 150 kDa. We next performed RT-PCR to estimate the relative levels of all identified Eml5 splice variants. Our results show that all splice variants can be detected by RT-PCR, and that the ratio of expression between Eml5^{b} and Eml5/Eml5^{a} is estimated at 1:20. At splice site 2, the ratio of expression levels between Eml5^{a} and Eml5 is estimated to be 1:2. All brain regions tested express both splice variants as determined by RT-PCR (depicted for splice site 2 in Figure 2C, data not shown for splice site 1). Although the use of the alternative splice sequence at splice site 1 (resulting in Eml5^{b}) can be detected using RT-PCR, this transcript is expressed at low levels and we therefore performed in situ hybridization as an alternative approach to verify its expression. As can be seen in Figure 2C, in situ hybridization confirmed our RT-PCR data that demonstrated that Eml5^{b} is expressed in cerebellum, hippocampus, cortex and olfactory bulb. Eml5^{b} is expressed in brain regions similar to those that express Eml5 (see Figure 4).

Eml5 mRNA and protein expression

Northern blot analysis revealed that Eml5 is expressed in most regions of the adult rat brain (Figure 3). Highest levels of expression are found in hippocampus and olfactory bulb, moderate levels in the enthorinal cortex. No expression of Eml5 was detected in the striatum. Three distinct bands at ~6.0, 8.0 and 12 kb were detected; the smallest corresponds to the length of the complete cloned Eml5 sequence described in this paper. Because, on the DNA level, no other sequences homologous to Eml5 can be found in the public domain databases, it is likely that the three bands are products derived from a single gene. It is possible that the splice variants shown in Figure 2 are the cause of the three transcripts detected on the Northern blot. However, these splice variants result from small (<120 bp) modifications. Therefore, for these splice variants to give rise to up to 4 kb differences in transcript size, they would also have to differ in the untranslated region. KIAA0828, a 5.1-kb mRNA transcript expressed at high levels throughout the brain (Nagase *et al.*, 1998), was used as loading control.

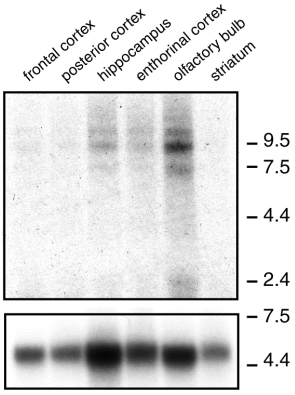

Figure 3. Northern blot analysis of Eml5 expression in adult rat brain. Northern blot containing 20 µg total RNA extracted from distinct regions of brain. Highest levels of expression are detected in the olfactory bulb whereas hippocampus and enthorinal cortex show moderated levels of expression. Lower panel shows expression of equivalent loading as judged by KIAA0828, a 5.1-kb mRNA transcript expressed at high levels throughout the brain.

In situ hybridization confirmed the expression pattern detected by Northern blot analysis. It revealed *Eml5* is expressed at high levels in the cerebellum, olfactory bulb and the dentate gyrus of the hippocampus. Transcripts are also detected in the cortex and in the CA1 and CA3 regions of the hippocampus (Figure 4). The high levels of expression in the cerebellum, olfactory bulb and dentate gyrus may reflect the high density of cells in these regions. To estimate relative expression levels between individual neurons, we performed a nonradioactive in situ hybridization using digoxigenin-labeled cRNA probes. Although this method is less quantitative than radioactive-labeled probes, staining intensity within one section is related to the mRNA expression level. Using this method, we find that the cells with highest *Eml5* expression are the Purkinje neurons of the cerebellum. Bearing in mind the quantitative limitations of this technique, a similar staining intensity was found in cortical neurons, CA1 pyramidal cells, granule cells of the cerebellum and thalamic neurons. Intermediate *Eml5* expression levels are found in granule cells of the dentate gyrus. No specific staining was observed using the sense (control) probe.

During development, *Eml5* transcripts are detected as early as embryonic day 13, E13 (Figure 5A), where they are expressed in regions of the developing brain. At E17, *Eml5* is expressed in most regions of the developing brain as well as the developing kidney (Figure 5B). At this stage, transcripts are also detected in regions surrounding the intestine, consistent with *Eml5* expression in the enteric nervous system. At postnatal day 1 and 10, P1 and P10, *Eml5* is expressed in most regions of the developing brain (Figure 5C,D). All in situ data presented were generated using oligo I but identical expression patterns were observed using the independent oligonucleotide II (data not shown). No hybridization signal was detected using either the sense probe or the antisense probe competed with a 50-fold excess of unlabeled oligo (not shown).

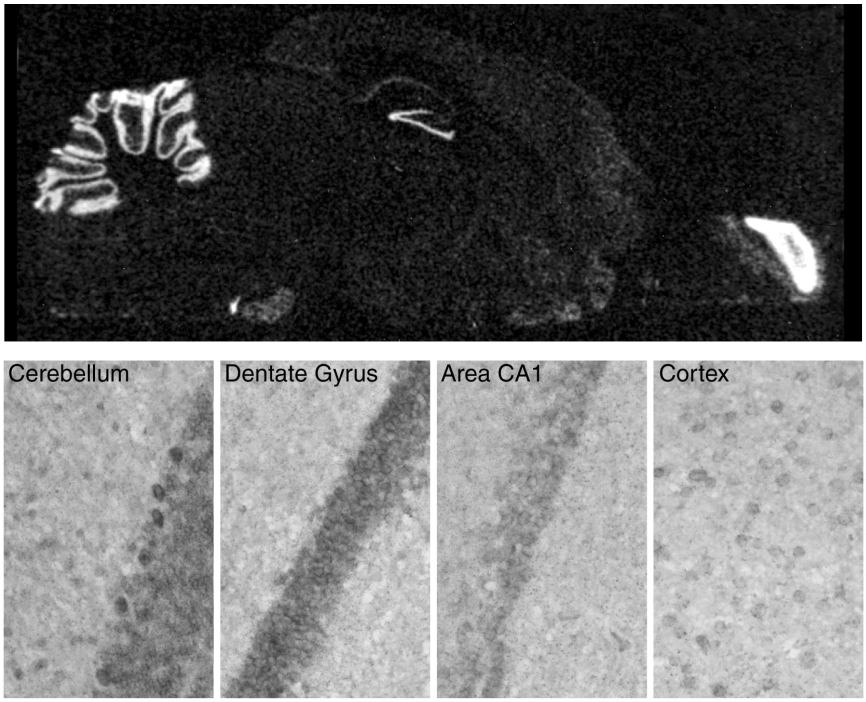

Figure 4. *Eml5* expression in the adult rat brain. In situ hybridization on a sagittal section (upper panel) demonstrating high levels of *Eml5* expression in the olfactory bulb, cerebellum and dentate gyrus region of the hippocampus. Transcripts are also detected in the cortex and the CA1 and CA3 regions of the hippocampus. Lower panels show examples of experiments using digoxigenin-labeled antisense cRNA probes to examine *Eml5* expression on a cellular level. Using this method, we find that the cells with highest *Eml5* expression are the Purkinje neurons of the cerebellum. Cortical neurons show a roughly similar staining intensity compared to the CA1 pyramidal cells, granule cells of the cerebellum and thalamic neurons. Intermediate *Eml5* expression levels are found in the granule cells of the dentate gyrus.

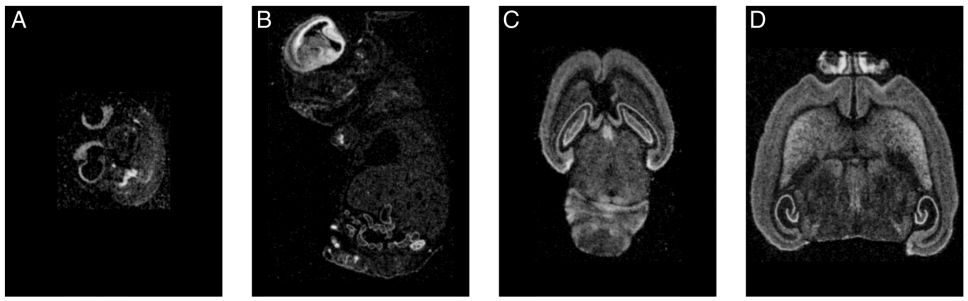

Figure 5. Developmental expression of *Eml5*. (A) At E13, *Eml5* is expressed in regions of the developing brain. (B) At E17, *Eml5* is expressed in most regions of the developing brain as well as the developing kidney. At this stage, transcripts are also detected in regions surrounding the intestine, consistent with *Eml5* expression in the enteric nervous system. At (C) P1 and (D) P10, *Eml5* is expressed in most regions of the developing brain.

To examine Eml5 protein expression, we have generated antibodies directed against aa 469–674. This region, containing the putative dimerization domain, was chosen for its predicted antigenicity as well as its low homology to other EML family members. For example, the 206 aa antigenic protein has 25% identity and 41% similarity to EMAP over its entire region. We first characterized these antibodies on Cos-7 cells that were transiently transfected with an Eml5^{b} construct C-terminally fused to GFP. As can be seen in Figure 6B, transient transfection of the Eml5^{b}-GFP construct shows an antibody staining pattern that is virtually identical to the GFP signal.

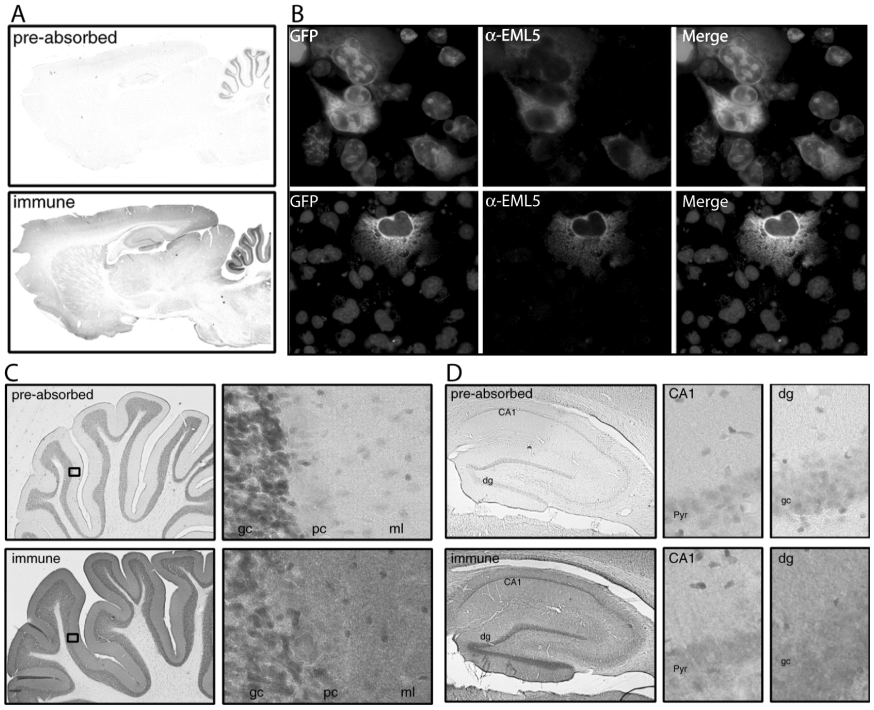

Figure 6. Distribution of Eml5 protein in neurons. (A) Immunocytochemistry using antibodies directed against Eml5$_{468–664}$ shows Eml5 immunoreactivity in the rat brain. Virtually no signal is detected using antibody preabsorbed with Eml5$_{468–664}$ protein (upper panel) compared to the immune serum (lower panel). (B) Specificity of the antibody was confirmed in Cos7 cells transfected with an Eml5^{b}-GFP construct. Transfected cells were visualized by GFP fluorescence (GFP) and were counterstained with our Eml5 antibody (a-Eml5). Overlay (merge) shows an identical staining between GFP and anti-Eml5 stained cells and demonstrates the specificity of the antibody. Nontransfected cells, visualized by the DAPI nuclear stain (blue signal) show no detectable Eml5-antibody signal. (C) In the cerebellum, Eml5 expression can be observed in the granule cells, the molecular layer and in Purkinje cells. Because the molecular layer receives axonal and dendritic projections from granule cells and Purkinje cells, respectively, Eml5 expression may not be restricted to either subtype of cellular process. (D) Eml5 immunoreactivity can also be observed in the hippocampus in all major cell layers and projection areas. No specific staining was observed when the antibodies have been competed with antigen (preabsorbed).

The fact that our antibodies recognize the Eml5 protein was further demonstrated by the fact that no specific staining was observed on rat brain sections incubated with preimmune serum (not shown) or with Eml5 antibodies preabsorbed on immobilized antigen (Figure 6A,C,D). These experiments demonstrate that our antibodies recognizes the Eml5 protein. Immunocytochemistry using these antibodies revealed that presumptive Eml5 expression is most pronounced in the molecular layer of the cerebellum (Figure 6A,B).
At higher magnification, Eml5 expression can be observed in the granule cells of the granule layer, and in Purkinje cells. Because the molecular layer receives axonal and dendritic projections from granule cells and Purkinje cells, respectively, Eml5 expression appears not to be restricted to either subtype of cellular process. Eml5 immunoreactivity can also be observed in the hippocampus in all major cell layers and projection areas.

Discussion

Eml5 primary sequence analysis

We have isolated and characterized a novel member of the EMAP-like family of proteins, Eml5, and two alternative spliced products, Eml5^{a} and Eml5^{b}, both of which are C-terminal truncations of Eml5. In humans, three other EML proteins have been identified, EML1 (Eudy *et al.*, 1997), EML2 (Lepley *et al.*, 1999) of which the rat homologue has also been cloned (Ly *et al.*, 2002), and EML4/Ropp120 (Heidebrecht *et al.*, 2000). An additional EML, EML3, can be predicted from the human genomic sequence. Eml5 is thus far the largest EML family member and is the most closely related to the archetypical member, EMAP (Figure 1B).
Interestingly, Eml5 appears to contain a 2.5-fold repeat of the complete EMAP protein, as both the N-terminal, middle and C-terminal parts are homologous to EMAP. A region that is strongly predicted to form an alpha-helical coiled coil, a putative dimerization domain, separates the N-terminal and the middle parts. Eml5 may therefore form homodimers or heterodimers with itself or one of its splice variants Eml5^{a} or Eml5^{b}. Alternatively, Eml5 may form a heterodimer with Eml3 or 4 as these family members also contain a predicted dimerization domain. It has been proposed that the microtubule-binding domain of EML proteins consists of a highly conserved hydrophobic stretch of 43 aa, the HELP domain (Eichenmuller *et al.*, 2002). EML proteins do not share the microtubule-binding domain of map1a and map1b/map5, the consensus being multiple copies of imperfect KKEX repeats (Noble *et al.*, 1989), or of other maps like MAP2, Tau and MAP4, the consensus being three to four copies of GSX2NX2HXPG3 (Lee *et al.*, 1989). Both N-terminal, middle and C-terminal parts of Eml5 contain a HELP domain, making Eml5 the only member

that contains three such domains. It remains to be determined whether these HELP domains actually participate in microtubule binding.
Eml5 contains, like other EML protein family members, several WD40 domains. WD40 repeats are putative protein–protein interaction domains that are usually present in 4–16 copies within a single protein (reviewed in Smith *et al.* 1999). Structurally, these repeats combined form a β propeller. Among the broad spectrum of functions of WD40 domain proteins are those involved in the regulation of cytoskeletal dynamics like coronin (de Hostos *et al.*, 1991), and mitotic spindle formation like CDC40 (Vaisman *et al.*, 1995). Besides the above-mentioned features, Eml5 is unique among the EML protein family in that it is the only member that lacks a consensus site for an EF hand (for review, see Lewit-Bentley and Rety, 2000). However, these calcium-binding motifs mainly occur in adjacent pairs (Lewit-Bentley and Rety, 2000) and the functional significance of a single motif within other EML proteins remains to be established.

Cellular functions of Eml proteins

Both EMAP and EML2 have shown to co-localize with mitotic spindles (Eichenmuller *et al.*, 2002; Suprenant *et al.*, 1993). Furthermore, EMAP was isolated as the major microtubule-associated protein in dividing sea urchin embryos (Suprenant *et al.*, 1993) and EML4/Ropp120 is strongly expressed during mitosis (Heidebrecht *et al.*, 2000). These observations suggest that the EML family of proteins is a class of MAPs that associate with mitotic spindles of dividing cells. Furthermore, both EMAP and EML2 have been reported to destabilize microtubules (Eichenmuller *et al.*, 2002; Hamill *et al.*, 1998); EMAP increases microtubule dynamics and inhibits the frequency of rescue (the transition from shortening to growing microtubules; Hamill *et al.*, 1998) whereas EML2 reduces the growth rate and promotes frequency of catastrophes (the transition from growing to shortening; Eichenmuller et al., 2002). Although it remains to be determined whether Eml5 destabilizes microtubules, a growing picture is emerging that the EML protein family is a novel class of microtubule-destabilizing proteins. Other microtubule-destabilizing proteins include Op18/Stathmin and its family members SCG10, SCLIP, RB3 and Katanin, a microtubule-severing protein. All of these, like Eml5, are expressed in the nervous system (Ahmad *et al.*, 1999; Cassimeris, 2002).
In the hippocampus, *Eml5* mRNA expression is confined to the neuronal layers whereas Eml5 immunoreactivity is found in all layers. This suggests that Eml5 protein is expressed in neuronal processes of the hippocampus. Similarly, in the cerebellum, Eml5 immunoreactivity is found over the molecular layer. Because both Purkinje cells and granule cells express Eml5, the staining in the molecular layer apparently may be derived from both Purkinje cell dendrites

and granule cell axons, suggesting that Eml5 regulates microtubule dynamics of neuronal processes. Moreover, because Eml5 is expressed during development, it may be involved in processes underlying the large-scale cytoskeletal rearrangements during neuronal development. As the majority of brain regions express Eml5 during development, it can be hypothesized that this expression is associated with the increased cytoskeletal dynamics of neurons during this time period. It remains to be determined why only a subset of brain regions express Eml5 in adult animals but it is tempting to speculate that these neurons show an increase in microtubule dynamics when compared to non-Eml5 expressing neurons. The granule cells of the dentate gyrus are associated with relatively high levels of neurogenesis. This may suggest Eml5 expression is related to their mitogenic potential and it will be interesting to test this hypothesis using other markers of neurogenesis and early neurite expansion.

In the adult brain, it has been suggested that microtubules can contribute to the morphological changes that have been reported in dendritic spines (van Rossum and Hanisch, 1999). Dendritic spines are the primary post-synaptic targets of excitatory glutamatergic synapses in the mature brain. Recent evidence suggests that the microtubule network is linked to the postsynaptic density (PSD), a specialized structure below the post-synaptic membrane of glutamatergic synapses, via certain scaffold proteins (for review, see van Rossum and Hanish, 1999). The PSD contains linker proteins like Cript (Niethammer *et al.*, 1998) that associates with both the NMDA receptor binding protein PSD95/Sap90 and tubulin. Furthermore, the NMDA receptor multiprotein complex associates with both tubulin and Map2B (Husi *et al.*, 2000). Inhibitory synapses are also associated with the microtubule network (for review, see Kneussel and Betz, 2000). For example, the linker protein Gephyrin associates with tubulin and binds and localizes $GABA_A$ and glycine receptors (Kneussel and Betz, 2000). Similarly, the $GABA_A$ receptor γ2 and $GABA_C$ receptor ρ1 subunits interact with GABARAP, a scaffold protein containing a tubulin-binding motif (Wang and Olsen, 2000) and MAP1B (Hanley *et al.*, 1999), respectively. The presence of tubulin and associated proteins within dendritic spines raises the possibility that Eml5 may aid in regulating tubulin-related dynamics of dendritic spines. Interestingly, recent observations have demonstrated an association between rat-Emap, the rat homologue of EML2/huEMAP2, and the synaptic δ2 glutamate receptor (Ly *et al.*, 2002) known to be required for the expression of cerebellar long-term depression (Kashiwabuchi *et al.*, 1995). The identity of Eml5-associated proteins remains to be established. Nevertheless, the broad neuronal expression and putative activity of Eml5 and its variants described in this

paper highlight their potential significance for neuronal function in the mature and developing nervous system.

Conclusions

We have cloned fifth member of the EML protein family, Eml5, and two alternative spliced products splice variants Eml5^{a} and Eml5^{b}, both of which are C-terminal truncations of Eml5. Eml5 contains a 2.5-fold repeat of the complete EMAP protein, the archetypical member of the EML protein family, and is its largest member. Because Eml5 is expressed in post-mitotic neurons (in adult animals and during development) and the EML protein family is likely to represent a novel class of microtubule destabilizing proteins, we hypothesize that Eml5 plays a role in the cytoskeletal rearrangements observed during neuronal development and in adult brain.

Acknowledgements

The initial observation leading to this work was made during a search for genes regulated by the induction of long-term potentiation in the hippocampus of awake rats. We thank the members of the consortium, funded by EC grant BIO4-96-0478, for their cooperation, in particular Dr. Serge Laroche and Dr. Sabrina Davis who provided the hippocampal tissue for the differential display screen. Part of this work was funded by the Dutch Science Foundation NWO grant 810-38.002.

References

Ahmad, F.J., W. Yu, F.J. McNally, and P.W. Baas. 1999. An essential role for katanin in severing microtubules in the neuron. *J Cell Biol*. 145:305-15.

Baas, P.W. 1999. Microtubules and neuronal polarity: lessons from mitosis. *Neuron*. 22:23-31.

Bornens, M. 2002. Centrosome composition and microtubule anchoring mechanisms. *Curr Opin Cell Biol*. 14:25-34.

Buee, L., T. Bussiere, V. Buee-Scherrer, A. Delacourte, and P.R. Hof. 2000. Tau protein isoforms, phosphorylation and role in neurodegenerative disorders. *Brain Res Brain Res Rev*. 33:95-130.

Cassimeris, L. 2002. The oncoprotein 18/stathmin family of microtubule destabilizers. *Curr Opin Cell Biol*. 14:18-24.

de Hostos, E.L., B. Bradtke, F. Lottspeich, R. Guggenheim, and G. Gerisch. 1991. Coronin, an actin binding protein of Dictyostelium discoideum localized to cell surface projections, has sequence similarities to G protein beta subunits. *Embo J*. 10:4097-104.

Eichenmuller, B., P. Everley, J. Palange, D. Lepley, and K.A. Suprenant. 2002. The human EMAP-like protein-70 (ELP70) is a microtubule destabilizer that localizes to the mitotic apparatus. *J Biol Chem*. 277:1301-9.

Eudy, J.D., M. Ma-Edmonds, S.F. Yao, C.B. Talmadge, P.M. Kelley, M.D. Weston, W.J. Kimberling, and J. Sumegi. 1997. Isolation of a novel human homologue of the gene coding for echinoderm microtubule-associated protein (EMAP) from the Usher syndrome type 1a locus at 14q32. *Genomics*. 43:104-6.

French, P.J., T.V. Bliss, and V. O'Connor. 2001. Ntab, a novel non-coding RNA abundantly expressed in rat brain. *Neuroscience*. 108:207-15.

Hamill, D.R., B. Howell, L. Cassimeris, and K.A. Suprenant. 1998. Purification of a WD repeat protein, EMAP, that promotes microtubule dynamics through an inhibition of rescue. *J Biol Chem*. 273:9285-91.

Hanley, J.G., P. Koulen, F. Bedford, P.R. Gordon-Weeks, and S.J. Moss. 1999. The protein MAP-1B links GABA(C) receptors to the cytoskeleton at retinal synapses. *Nature*. 397:66-9.

Heidebrecht, H.J., F. Buck, M. Pollmann, R. Siebert, and R. Parwaresch. 2000. Cloning and localization of C2orf2(ropp120), a previously unknown WD repeat protein. *Genomics*. 68:348-50.

Heidemann, S.R., J.M. Landers, and M.A. Hamborg. 1981. Polarity orientation of axonal microtubules. *J Cell Biol*. 91:661-5.

Husi, H., M.A. Ward, J.S. Choudhary, W.P. Blackstock, and S.G. Grant. 2000. Proteomic analysis of NMDA receptor-adhesion protein signaling complexes. *Nat Neurosci*. 3:661-9.

Joshi, H.C. 1998. Microtubule dynamics in living cells. *Curr Opin Cell Biol*. 10:35-44.

Kashiwabuchi, N., K. Ikeda, K. Araki, T. Hirano, K. Shibuki, C. Takayama, Y. Inoue, T. Kutsuwada, T. Yagi, Y. Kang, and et al. 1995. Impairment of motor coordination, Purkinje cell synapse formation, and cerebellar long-term depression in GluR delta 2 mutant mice. *Cell*. 81:245-52.

Kneussel, M., and H. Betz. 2000. Clustering of inhibitory neurotransmitter receptors at developing postsynaptic sites: the membrane activation model. *Trends Neurosci*. 23:429-35.

Kozak, M. 1987. An analysis of 5'-noncoding sequences from 699 vertebrate messenger RNAs. *Nucleic Acids Res*. 15:8125-48.

Lee, G., R.L. Neve, and K.S. Kosik. 1989. The microtubule binding domain of tau protein. *Neuron*. 2:1615-24.

Lepley, D.M., J.M. Palange, and K.A. Suprenant. 1999. Sequence and expression patterns of a human EMAP-related protein-2 (HuEMAP-2). *Gene*. 237:343-9.

Lewit-Bentley, A., and S. Rety. 2000. EF-hand calcium-binding proteins. *Curr Opin Struct Biol*. 10:637-43.

Ly, C.D., K.W. Roche, H.K. Lee, and R.J. Wenthold. 2002. Identification of rat EMAP, a delta-glutamate receptor binding protein. *Biochem Biophys Res Commun*. 291:85-90.

Nagase, T., K. Ishikawa, M. Suyama, R. Kikuno, M. Hirosawa, N. Miyajima, A. Tanaka, H. Kotani, N. Nomura, and O. Ohara. 1998. Prediction of the coding sequences of unidentified

human genes. XII. The complete sequences of 100 new cDNA clones from brain which code for large proteins in vitro. *DNA Res*. 5:355-64.

Niethammer, M., J.G. Valtschanoff, T.M. Kapoor, D.W. Allison, R.J. Weinberg, A.M. Craig, and M. Sheng. 1998. CRIPT, a novel postsynaptic protein that binds to the third PDZ domain of PSD-95/SAP90. *Neuron*. 20:693-707.

Noble, M., S.A. Lewis, and N.J. Cowan. 1989. The microtubule binding domain of microtubule-associated protein MAP1B contains a repeated sequence motif unrelated to that of MAP2 and tau. *J Cell Biol*. 109:3367-76.

Sanchez, C., J. Diaz-Nido, and J. Avila. 2000. Phosphorylation of microtubule-associated protein 2 (MAP2) and its relevance for the regulation of the neuronal cytoskeleton function. *Prog Neurobiol*. 61:133-68.

Smith, T.F., C. Gaitatzes, K. Saxena, and E.J. Neer. 1999. The WD repeat: a common architecture for diverse functions. *Trends Biochem Sci*. 24:181-5.

Suprenant, K.A., K. Dean, J. McKee, and S. Hake. 1993. EMAP, an echinoderm microtubule-associated protein found in microtubule-ribosome complexes. *J Cell Sci*. 104:445-50.

Vaisman, N., A. Tsouladze, K. Robzyk, S. Ben-Yehuda, M. Kupiec, and Y. Kassir. 1995. The role of Saccharomyces cerevisiae Cdc40p in DNA replication and mitotic spindle formation and/or maintenance. *Mol Gen Genet*. 247:123-36.

van Rossum, D., and U.K. Hanisch. 1999. Cytoskeletal dynamics in dendritic spines: direct modulation by glutamate receptors? *Trends Neurosci*. 22:290-5.

Walczak, C.E. 2000. Microtubule dynamics and tubulin interacting proteins. *Curr Opin Cell Biol*. 12:52-6.

Wang, H., and R.W. Olsen. 2000. Binding of the GABA(A) receptor-associated protein (GABARAP) to microtubules and microfilaments suggests involvement of the cytoskeleton in GABARAPGABA(A) receptor interaction. *J Neurochem*. 75:644-55.

Chapter 4

The expression of A Specific Synaptopodin Splice Variant is Associated with Activity and Induces Remodeling of the Actin Cytoskeleton.

S.H. Houtman[1*], M.A. Schlager[1], C.I. De Zeeuw[1,2], P.J. French[3]

[1] Dept. of Neuroscience, Erasmus MC, Rotterdam, the Netherlands
[2] Netherland Institute for Neuroscience, Royal Academy of Arts & Sciences (KNAW), Amsterdam, the Netherlands
[3] Dept. of Neurology, Erasmus MC, Rotterdam, the Netherlands

Prepared for submission

Abstract
Synaptopodin is an activity dependent, actin-associated protein that is localized in the spine neck of telencephalic neurons. Two distinct splice variants of Synaptopodin have been described in human and mouse. In this study, we have used RT-PCR and *in situ* hybridisation to determine the expression of both splice variants (Synaptopodin I and II) in rat brain (cortex and hippocampus) following electrical stimulation. Our results indicate that only one Synaptopodin splice variant (rat Synaptopodin II) shows activity associated expression. The activity-associated splice variant is distinct from human and mouse Synaptopodin II with respect to the 3' end. Interestingly, this activity associated splice variant lacks a domain that, in human Synaptopodin, binds to a-actinin and is associated with remodeling of the actin cytoskeleton. Although rat Synaptopodin II lacks such a domain, our results demonstrate that transient overexpression does induce a marked remodeling of the actin cytoskeleton. We next used deletion constructs to identify two distinct regions in Synaptopodin II (aa144-489 and aa461-692) that are sufficient for colocalization with actin and one region (aa144-489) that induces rearrangement of the actin cytoskeleton. Point mutation of two PPXY protein-protein interacting domains does not appear to affect cytoskeletal remodeling. Our results are suggestive of a causal role of Synaptopodin II in the remodeling of the actin cytoskeleton in dendritic spines of neurons following electrical stimulation.

Introduction
Long-term potentiation (LTP) is the strengthening of synaptic efficacy in hippocampal and cortical structures (Bliss and Collingridge, 1993). The early phase of LTP (E-LTP) lasts up to 6 hours and is not affected by protein and RNA synthesis inhibitors. In contrast, the late phase of LTP (L-LTP) can last for hours or days and is dependent on *de novo* RNA and protein synthesis (Bradshaw *et al.*, 2003; Frey *et al.*, 1988; Krug *et al.*, 1984; Nguyen *et al.*, 1994; Nguyen and Kandel, 1996; Otani *et al.*, 1989). Examples of transcripts that are associated with L-LTP, include transcription factors (e.g. *Zif268*) (Wisden *et al.*, 1990; Worley *et al.*, 1993), kinases (Konietzko *et al.*, 1999; Thomas *et al.*, 1994), phosphodi-esterases (e.g. PDE10A) (O'Connor *et al.*, 2004a) and cytoskeletal proteins (e.g. *Homer 1a, Synaptopodin*) (Brakeman *et al.*, 1997; Kato *et al.*, 1997; Matsuo *et al.*, 1998; Yamazaki *et al.*, 2001). As the expression of many of these transcripts are necessary for the establishment of L-LTP, functional studies of the encoded proteins will help elucidate the underlying molecular mechanism of L-LTP.
Synaptopodin is a gene that is upregulated after the induction of LTP (Yamazaki *et al.*, 2001). Similar to other LTP-associated transcripts (Capani *et*

al., 2001; Guzowski *et al.*, 2000; Guzowski *et al.*, 1999; Hall *et al.*, 2000; Jones *et al.*, 2001; Moita *et al.*, 2002), mice lacking Synaptopodin show a reduced L-LTP (Deller *et al.*, 2003). Synaptopodin is expressed in renal podocytes, olfactory bulb, cerebral cortex, striatum and hippocampus (Czarnecki *et al.*, 2005; Deller *et al.*, 2000a; Mundel *et al.*, 1997). Within neurons, Synaptopodin is localized in the neck of mature dendritic spines, where it is associated with F-actin, a-actinin and the spine apparatus (Deller *et al.*, 2000b).
Two Synaptopodin splice variant have been described in human and mouse (Asanuma *et al.*, 2005; Kremerskothen *et al.*, 2005). These two splice variants differ in both their 5'- and 3'-end. As splice variant-specific expression has been described for other LTP-associated transcripts (Brakeman *et al.*, 1997; Inoue *et al.*, 2004; Kato *et al.*, 1997; O'Connor *et al.*), we examined such splice variant-specific expression in rat Synaptopodin. Our results demonstrate that, similar to human Synaptopodin, two Synaptopodin splice variant are expressed in rat. Only one of these shows activity-associated expression. Because this activity associated splice variant in rat is distinct from human Synaptopodin splice variants, we determined its cellular function.

Methods

All animal experiments were performed in accordance with the recommendations by the European Communities Council Directive of 24 November 1986 (86/609/EEC) and were conducted with the approval of the Dutch Ethical Committee for animal experiments. All efforts were made to minimize animal suffering.

Electroconvulsive shock (ECS)

ECS was induced in 4 adult Sprague-Dawley (SD) rats following light halothane anaesthesia as described (O'Connor *et al.*, 2004a). In short, ear-clip electrodes were used to deliver a 200 V (sine wave) at 50 mA for 2 seconds to induce clonic seizure according to published protocols (Steward, 1994). Animals were sacrificed 12 hrs post ECS (n = 5 per group). Control rats (n = 3) were subjected to equivalent handling without subsequent stimulation. All brains were removed, frozen on dry ice and stored at –80 ˚C prior to subsequent analysis by *in situ* hybridisation (French *et al.*, 2001).

***In situ* hybridization**

In situ hybridizations were performed essentially as described (French *et al.*, 2001) using ^{35}S radiolabelled oligonucleotides. A 50-fold excess of unlabelled oligonucleotide was used as negative control. 45-mer antisense oligonucleotides of unique sequence (Invitrogen, Paisley, Scotland) were

designed against rat sequences that are homologous to exons of human Synaptopodin (see supplementary data).

RT-PCR

Total RNA was isolated from naive adult rat hippocampus or cortex using Trizol (Invitrogen) according to manufacturers instructions as described (Houtman *et al.*, 2007). 10-15 µg RNA was DNAse treated by adding 2U DNAse (RNAse free; Roche), 2 µl transcription buffer and dH_2O till a total volume of 20µl and 15 minutes incubation at 37°C. RNA was precipitated with 100 µl TE, 10 µl 4M LiCl and 300 µl ethanol (100%), in the presence of 2 µl glycogen (10 µg/µl), washed in 75% ethanol and dissolved in 20 µl TE (RNAse free). RNA samples (1 µg) were then reverse transcribed for 1 hr at 50°C in the presence of 200U Superscript III (Invitrogen), 150 ng oligo dT(18) primer, 0.5 mM dNTP's, 50 mM DTT and RNase inhibitor in a total volume of 20 µl. A control reaction was performed in absence of reverse transcriptase; control samples were otherwise treated identically. From the reverse transcribed cDNA 0.2 µl was used for each RT-PCR reaction. PCR primer pairs are stated in the supplementary data.

Constructs

Full-length Synaptopodin was amplified from rat hippocampal cDNA using gene-specific primers 5'-AAAGGGGGGACAAGACAGGC-3' and 5'-AAGCACTCCAGCTCCCAAAGCC-3', sequence verified and cloned into the pEGFP-C2 vector (Invitrogen). Synaptopodin gene-fragments were amplified on the cloned Synaptopodin construct using the expand high fidelity PCR kit (Roche; Basel, Switzerland). For primer sequences see supplementary data table 1. All constructs were cloned into pEGFP-C1, pEGFP-C2 or pEGFP-C3 (BD Biosciences; Franklin Lakes, NJ).

Transient transfection

Transient transfections were performed using DEAE-dextran as described (O'Connor *et al.*, 2004b). Sixteen hours following transient transfection, cells were fixed in ice-cold 4% PFA. Cells were then permeabilized in 0.1% Saponin/PBS, blocked in PBS containing 1% BSA, 10% fetal calf serum and incubated overnight with a primary antibody mixture.

Antibodies

The following primary antibodies were used: monoclonal anti-a-actinin (mouse IgM; 1:200 (v/v); Sigma), monoclonal anti-a-actinin mouse IgG; 1:200 and monoclonal anti-synaptopodin mouse IgG; 1:2 (Progen Biotechnik GmbH, Heidelberg, Germany). Secondary antibodies were goat-anti-mouse

Alexa488, goat-anti-mouse Alexa594, goat-anti-mouse Alexa680 or goat-anti-mouse IgM (all 1:300; Invitrogen). F-actin was visualized using Alexa Fluor 350 phalloidin, Alexa Fluor 594 phalloidin or Alexa Fluor 680 phalloidin (1:50; Invitrogen). Slides were mounted in Vectashield mounting medium containing dapi (Vector laboratories).

Imaging

Fluorescent images where made using either a Leica (Wetzlar, Germany) DMRBE microscope with a 40X oil immersion objective coupled to a Hamamatsu (Hamamatsu Photonics K.K.; Hamamatsu City, Japan) C4880 CCD camera, or using a Zeiss (Jena, Germany) LSM510 confocal laser-scanning microscope using a 63X oil immersion objective The latter was also used to perform live imaging during which cells and objective were kept at 37 °C, 5% CO_2. Images, with an optical slice of ~1 μm, were taken every 10 minutes for 2 - 6 hours.

Western blot

Proteins were isolated from transiently transfected Cos7 cells. Isolations were performed in ice-cold PBS containing 1% SDS and protease inhibitor cocktail (Sigma). Lysed cells were incubated on ice for 20 minutes and centrifuged to eliminate protein insoluble fractions. Protein concentrations were measured using BCA (Pierce, Perbio Science, The Netherlands) according to the manufacturer's guidelines. Samples diluted in Laemmli sample buffer (LSB; 50 mM Tris-HCl, pH 6.8, 2.5 % v/v SDS, 12.5% v/v glycerol, 0.01% w/v bromophenol blue, 100 mM DTT, β-mercaptoethanol) were denatured for 5 minutes at 95°C, after which 20 μg of protein was transferred to 10% acryl-amide gels. Following electrophoresis, gels were blotted on nitrocellulose (Bio-rad) using Transblot SD semi dry transfer cell (Biorad). The nitrocellulose was blocked in TBS containing 5% milk (Nutricia, Cuijk, The Netherlands) and 1% tween. Anti-GFP (Abcam, Cambridge, UK; 1:5000) was added to the blots in TBS containing 2% milk and 1% tween (TBS-T). Next day the blots were washed and incubated with secondary antibody (Rabbit-anti-Mouse-HRP, 1:5000 Dako, Denmark) in TBS-T. The blots were then washed in TBS/1% tween and protein signals on the blot were visualized using chemiluminescence (Amersham) according to the manufacturer's instructions.

Results

Isoform-specific activity-associated regulation of rat Synaptopodin

Two distinct human splice variants of Synaptopodin have thus far been described (accession numbers NM_007286 and AL831818)(Asanuma *et al.*, 2005). We have plotted the regions on the rat genome that correspond to

these human Synaptopodin splice variants. A model of splicing of these variants is given in figure 1a. Our first experiments were designed to examine which of these isoforms are expressed in naive rat brain (cortex and hippocampus). RT-PCR using exon-spanning primers indicated that most Synaptopodin exons that are homologous to human Synaptopodin exons are expressed in rat brain (figure 1b). However, we failed to find evidence of expression for the last exon, exon 5, in 4 independent RT-PCR reactions using 8-different primer combinations. These exon 5 primers did amplify the correct genomic Synaptopodin fragments, confirming their specificity. We did not design primers for exon 1, as this exon is not a part of the open reading frame of Synaptopodin I. Our experiments indicate that at least two distinct isoforms are expressed in adult rat brain. Based on the RT-PCR experiments, we suggest that the first isoform (Synaptopodin I) consists of exons 1, 2, 4a and 4b whereas the second isoform (Synaptopodin II) is likely to consist of exons 3, 4a and 4b. These isoforms are homologues of human Synaptopodin splice variants AL831818 and NM_007286 for Synaptopodin I and II respectively. Rat Synaptopodin II however differs from human Synaptopodin NM_007286 with respect to the 3' end: rat Synaptopodin II does not contain exon 5 (figure 1a).

It has been demonstrated that Synaptopodin expression is associated with activity (Kikuno *et al.*, 1999; Matsuo *et al.*, 1998; Roth *et al.*, 2001; Yamazaki *et al.*, 2001). To determine which isoform(s) show activity associated expression, we performed *in situ* hybridization on rat seizure brains using probes that are specific for each exon (figure 1C). *In situ* hybridization indicated that exons 3, 4a and 4b show activity associated expression whereas exons 1 and 2 do not. As Synaptopodin II consists of exons 3, 4a and 4b (see figure 1), these *in situ* hybridization results indicate that Synaptopodin II has an activity associated expression in rat hippocampus. Similar to RT-PCR experiments, *in situ* hybridization failed to provide evidence of expression for exon 5. Although no quantitative measurements were performed, both our RT-PCR and *in situ* hybridization experiments suggest that Synaptopodin II is expressed at higher levels than Synaptopodin I (Figure 1B,C).

Functional role of Synaptopodin II

Our results demonstrate that Synaptopodin II expression is upregulated following electrical activity. However, rat Synaptopodin II lacks a specific domain that, in human Synaptopodin is associated with a-actinin and is involved in remodeling of the actin cytoskeleton (Asanuma *et al.*, 2005; Kremerskothen *et al.*, 2005). Because Synaptopodin II lacks this functional domain, we examined the cellular effects of this activity associated isoform.

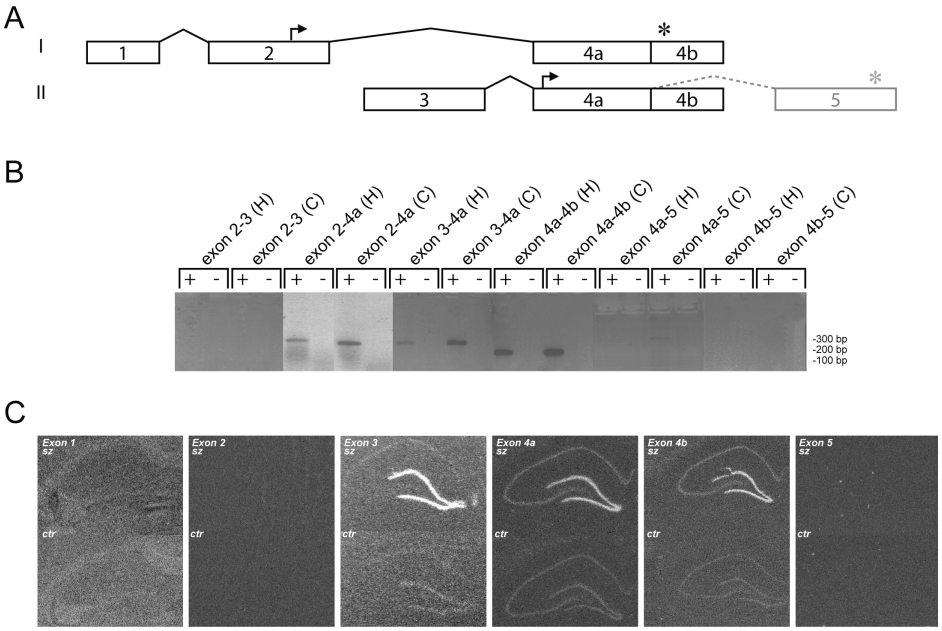

Figure 1 Synaptopodin splice variant expression in rat brain (A) Two distinct splice variants have been described in human: Synaptopodin I (short) consists of exons 1, 2, 4a and 4b; Synaptopodin II (long) consists of exons 3, 4a and 5. In rat, RT-PCR (B) and in-situ hybridization (C) failed to provide evidence for the expression of exon 5 (B) RT-PCR demonstrates expression of exons 2-4b but not 5 in rat cortex and hippocampus. Experiments were run in the presence (+) or absence (-) of reverse transcriptase. (C) *In situ* hybridization shows that all exons of splice variant II are up-regulated after activity (sz: seizure brain, ctr: control brain, C: cortex, H: hippocampus, arrows: startcodon, *: stopcodon)

We therefore transiently overexpressed rat Synaptopodin II, N-terminally fused to eGFP (GFP-Synaptopodin II) into Cos7 cells. In cells with a relatively low GFP-Synaptopodin II expression (based on the relative fluorescence intensity), we observed a filamentous staining pattern that colocalizes both with F-actin and a-actinin (figure 2B and 3B t=0). In cells with a relatively high expression of GFP-Synaptopodin II, we observed GFP-Synaptopodin II aggregates (typical aggregates are shown in figure 3B t>90). These aggregates also contain F-actin and a-actinin (data not shown). No such aggregates were observed following transient overexpression of GFP-actin (data not shown).
Time lapse imaging of GFP-Synaptopodin II demonstrated that Synaptopodin filaments, as observed in cells with low GFP-Synaptopodin II expression, became shorter and irregular overtime, and eventually formed aggregates (figure 2B and figure 3B). In all experiments, a complete colocalisation of F-actin and GFP-Synaptopodin II was observed (all transfected cells in 4 independent experiments). Our experiments therefore demonstrate that rat

Synaptopodin II, colocalizes with- and induces remodeling of the actin cytoskeleton.

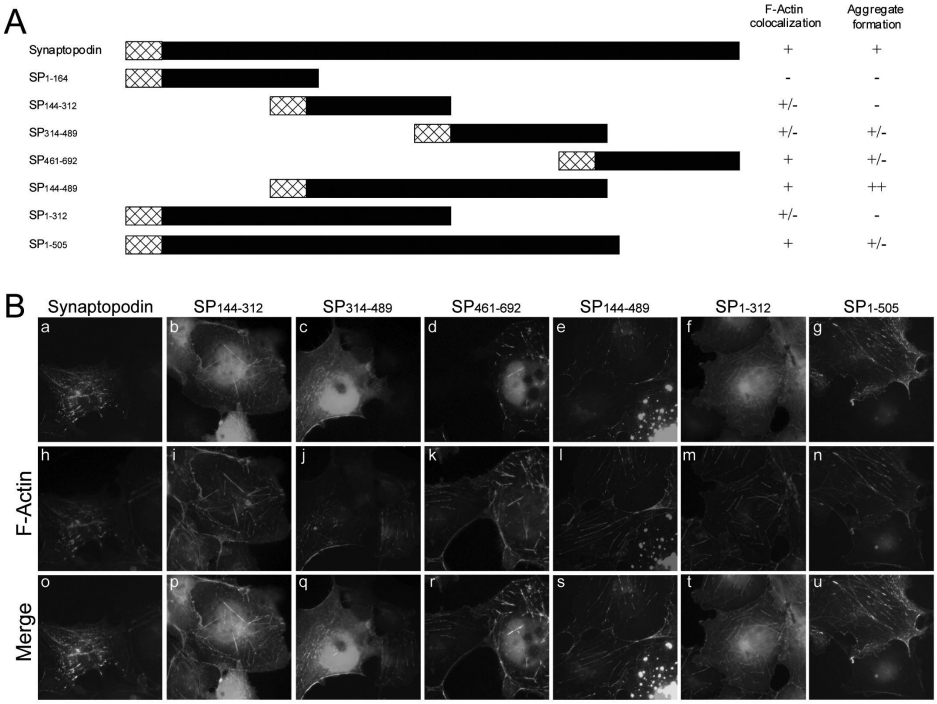

Figure 2 Synaptopodin deletion constructs designed to map regions that colocalize with F-actin and promote actin aggregate formation (A) Model of Synaptopodin deletion constructs. Indicated to the right are the levels of F-actin colocalization and aggregate formation (B) Full length Synaptopodin II (a, h and o) and $SP_{144-489}$ (e, l and s) induce and colocalize with actin aggregates. $SP_{314-489}$ (c, j and q) colocalizes with F-actin and causes the formation of short filaments. Actin aggregates are never observed with this construct. $SP_{461-692}$ (d, h and r) colocalizes with F-actin, induces a thickening of actin filaments without aggregates being formed. $SP_{144-312}$ (b, i and p), SP_{1-312} (f, m and t) and SP_{1-505} (g, n and u) colocalize with F-actin but do not affect the appearance of actin filaments.

Domains of Synaptopodin II involved in actin remodeling

Although rat Synaptopodin II lacks a domain that, in human Synaptopodin, binds to α-actinin, rat Synaptopodin II can still induce remodeling of the actin cytoskeleton (figure 2B and figure 3B). We therefore set out to determine which region of rat Synaptopodin II is involved in remodeling of the actin cytoskeleton. We generated a set of Synaptopodin II deletion constructs that were N-terminally fused to GFP (figure 2A) and transiently transfected them into Cos7 cells. Cell lysates of transiently transfected cells were used for

Western blot and confirmed correct expression of the deletion construct (data not shown).

The first 164 amino acids of Synaptopodin II (SP_{1-164}) show even distribution throughout the cytoplasm and in the nucleus (data not shown). This fragment does not colocalize with F-actin and does not induce remodeling of the actin cytoskeleton. SP_{1-312} does show some degree of filamentous staining that colocalizes with F-actin although significant GFP-SP_{1-312} staining is seen throughout the cytoplasm. This cytoplasmic staining may be indicative for a relatively low affinity for F-actin. (figure 2B; f, m, t). The actin cytoskeleton has normal appearance and therefore SP_{1-312} does not appear to remodel the actin cytoskeleton. Transient overexpression of SP_{1-505} shows a clear filamentous staining pattern that colocalizes with F-actin (figure 2B; g, n, u). Similar to the other 3' Synaptopodin II truncation constructs, SP_{1-505} does not appear to induce actin aggregate formation.
Our 3' deletion constructs therefore indicate that remodeling of the actin cytoskeleton requires the presence of the last 187 amino acids of Synaptopodin II. Indeed, transient overexpression of $SP_{461-692}$, containing the last 231 amino acids of Synaptopodin, shows not only colocalization with F-actin but F-actin bundles appear thicker and shorter (figure 2B; d, k, r). The last 231 amino acids are therefore sufficient to associate with F-actin and can induce remodeling of actin cytoskeleton. However $SP_{461-692}$ does not appear to induce dramatic remodeling (e.g. formation of aggregates) as observed with full-length Synaptopodin II (compare figures 2B, h and 2B, k). Transient overexpression of $SP_{144-489}$ (containing the central region of Synaptopodin II) does induce severe actin remodeling (figure 2B; e, l, s, aggregates in cell at lower left corner). Similar to full length Synaptopodin II, cells expressing low amounts of $SP_{461-692}$ show a filamentous staining pattern that co-localizes with F-actin (2B e, l, s, top cell).

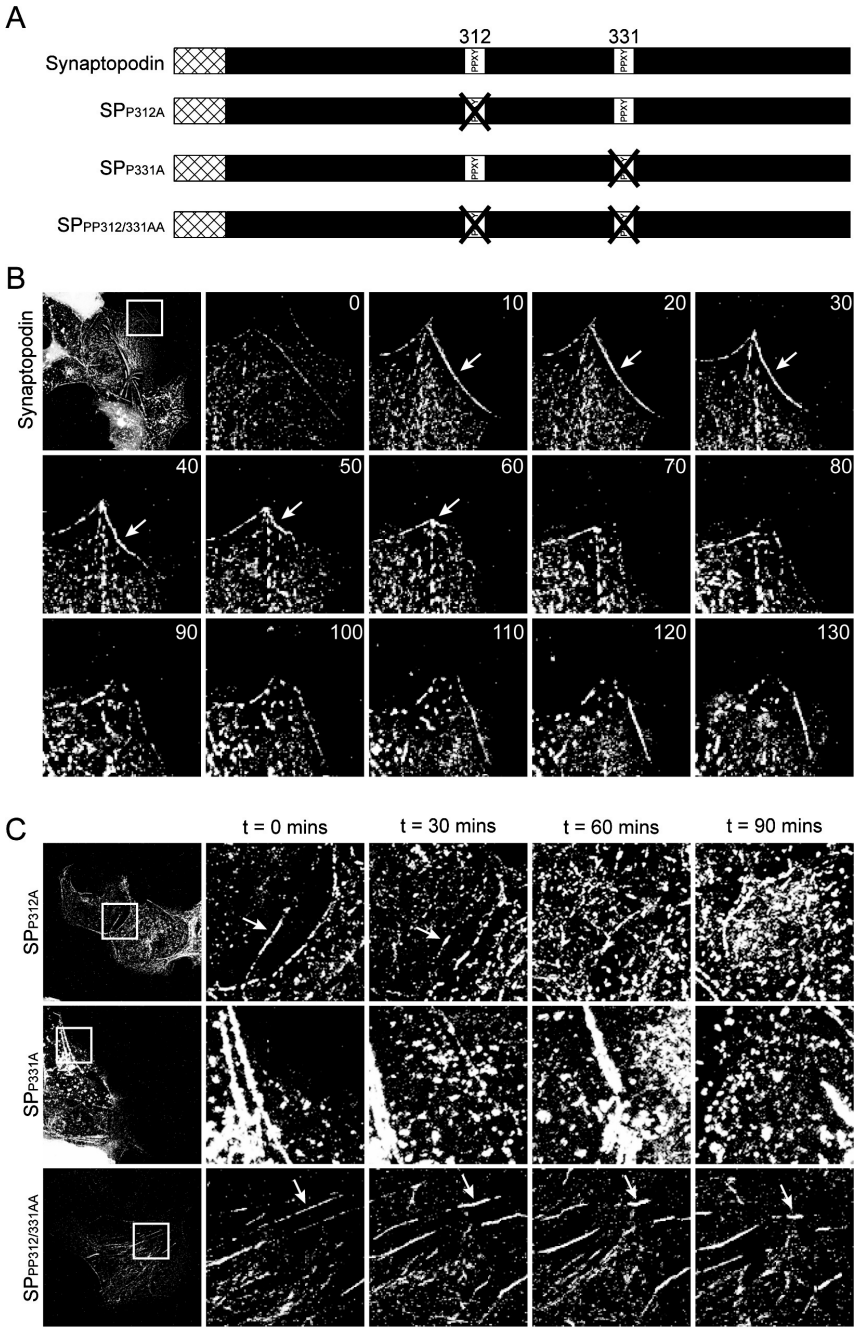
A
312
331
Synaptopodin
SPP312A
SPP331A
SPPP312/331AA
PPXY
B
Synaptopodin
0
10
20
30
40
50
60
70
80
90
100
110
120
130
C
t = 0 mins
t = 30 mins
t = 60 mins
t = 90 mins
SPP312A
SPP331A
SPPP312/331AA

Figure 3 Time lapse imaging of Synaptopodin II with or without point mutations of either or both PPXY motifs. In all experiments, Synaptopodin II showed complete colocalization with F-actin (A) Mutation constructs generated: In SP_{P312A} the first PPXY motif (aa 312) is changed to PATY, in SP_{P331A} the second PPXY motif (aa 331) is changed to PASY. $SP_{PP312/331AA}$ carries both mutations. (B) Live image showing the formation of Synaptopodin II (and F-actin) aggregates in a cell expressing Synaptopodin II-GFP (time indicated in minutes). (C) Point mutation in either or both of the PPXY protein-protein interaction domains do not affect the ability of Synaptopodin II to remodel the actin cytoskeleton or induce formation of Synaptopodin (and F-actin) aggregates. Arrows show Synaptopodin II filaments that shorten.

Our observations indicate that $SP_{144-489}$ is sufficient to associate with and remodel the actin cytoskeleton (3 independent experiments). The N-terminal part of this construct, $SP_{144-312}$ does colocalize with F-actin but also has a relatively high cytoplasmic distribution (figure 2B; b, i, p). This suggests that $SP_{144-312}$ can bind F-actin but with low affinity. In spite of this low affinity, $SP_{144-312}$ does induce remodeling of the actin cytoskeleton. Similarly, transient overexpression of $SP_{314-489}$, also shows colocalization with F-actin and a relatively high cytoplasmic staining (figure 2B; c, j, q). The actin cytoskeleton has a fragmented appearance suggesting this construct can remodel the actin cytoskeleton. Although thick, short actin bundles are observed following transient transfection with this construct, formation of actin aggregates was never observed. This suggests that actin bundling and aggregate formation are separate entities. In summary, transient transfection of Synaptopodin deletion constructs suggest two regions can associated with actin (amino acids 144-489 and 461-692) whereas one central region is involved in remodeling of the actin cytoskeleton (amino acids 144-489).

PPXY motifs involved in cytoskeleton remodeling

The central region of Synaptopodin ($SP_{144-489}$) that induces remodeling of the actin cytoskeleton contains two PPXY protein protein interaction domains. It has been hypothesized that these domains are required for remodeling the actin cytoskeleton (by recruiting proteins like α-actinin).

To test whether these domains are indeed involved in cytoskeletal remodeling, we generated GFP-Synaptopodin II constructs with point mutations in these motifs (SP_{P312A}, SP_{P331A} and $SP_{PP312/331AA}$). Similar to full length Synaptopodin, transient transfection of PPXY mutation constructs showed either a filamentous staining pattern that colocalized with F-actin (at low Synaptopodin expression levels) or aggregates containing Synaptopodin and F-actin (at high Synaptopodin expression levels). Live imaging was used to investigate the dynamics of these mutation constructs on the actin cytoskeleton. We observed actin remodeling with all constructs, with no gross differences with respect to actin aggregate formation. Our findings suggest

that mutation in PPXY motifs do not affect the cytoskeletal remodeling capability of Synaptopodin.

Discussion

Isoform specific expression and regulation

In this study we have used RT-PCR and *in situ* hybridization to demonstrate that at least two splice variants of Synaptopodin are expressed in rat brain, Synaptopodin I and II. One of these isoforms, Synaptopodin II, shows activity associated expression. When overexpressed, Synaptopodin II induces remodeling of the actin cytoskeleton.

Rat Synaptopodin I is similar to the human Synaptopodin isoform (Synaptopodin short; accession number: AL831818). However, rat Synaptopodin II and its human Synaptopodin isoform (Synaptopodin long; accession number: NM_007286) differ at the 3' end: Rat Synaptopodin II and human Synaptopodin long contain different 3' end exons. In rat, Synaptopodin I and II splice variants make use of the same 3' end exon whereas in human, Synaptopodin short and long use different 3' end exons (see figure 1). Genomic sequences between human and rat are identical in the region surrounding the alternative splice donor site of exon 4 (4a) and the splice acceptor site of exon 5. The similarity in primary sequence therefore does not explain differences in splice variants between rat and human. It remains possible that a splice variant of rat Synaptopodin containing exon 5 is expressed in rat kidney, as this tissue was not included in this study.

Expression of Synaptopodin is associated with electrical activity (Roth *et al.*, 2001; Yamazaki *et al.*, 2001). Here we demonstrate that Synaptopodin II, and not Synaptopodin I, is upregulated after electrical activity. These two rat isoforms differ with respect to their 5' ends suggesting that these two isoforms each have a specific promoter. The translational start of Synaptopodin II lies within the protein coding region of Synaptopodin I. On the protein level, Synaptopodin I therefore contains a unique N-terminus of 245 amino acids. This region of includes a leucine zipper and two consensus phoshorylation sites (CK2 and PKC). Whether these sites are important for functioning remains to be determined.

Colocalization and remodeling of the actin cytoskeleton

Rat Synaptopodin II lacks a domain that, in human Synaptopodin, can bind to a-actinin (Asanuma *et al.*, 2005; Kremerskothen *et al.*, 2005). Our results demonstrate that full-length rat Synaptopodin II, similar to human Synaptopodin long does show a colocalization with F-actin and a-actinin and induces remodeling of the actin cytoskeleton. The actin remodeling function of Synaptopodin therefore remains preserved in rat Synaptopodin II.

With our deletion constructs we identified two F-actin association domains in Synaptopodin II (located within amino acids 144-489 and 461-692) and one domain that is required for cytoskeletal remodeling (located within amino acids 144-489). Within this remodeling domain, two PPXY motifs are present. Mutation of these motifs showed no gross change in actin association and remodeling indicating that they are not required for cytoskeletal remodeling.
There are several ways in which Synaptopodin can affect the dynamics of the actin cytoskeleton. First, Synaptopodin can bind directly to actin and so affect the dynamics of the cytoskeleton. Alternatively, Synaptopodin can associate with several proteins that can induce changes in the actin cytoskeleton. For example, Synaptopodin can bind directly to both a-actinin and RhoA (Asanuma *et al.*, 2005; Asanuma *et al.*, 2006; Kremerskothen *et al.*, 2005).
In brain three isoforms of a-actinin are expressed, namely a-actinin 1, 2 and 4. They are abundantly expressed in the post-synaptic density (PSD) (Nakagawa *et al.*, 2004; Peng *et al.*, 2004). Where they form a link between NMDA receptors and the actin cytoskeleton (Wyszynski *et al.*, 1997). a-actinin 2 is not only localized in the PSD, but also shows colocalization with the spine apparatus (Wyszynski *et al.*, 1998). Interestingly, Synaptopodin knock-out mice lack both a spine apparatus and show a reduced a-actinin 2 expression (Asanuma *et al.*, 2005; Deller *et al.*, 2003).
RhoA is a small GTPase that induces changes in actin cytoskeletal dynamics (Ridley, 2006). RhoA is saved from degradation by binding to Synaptopodin following which RhoA is activated resulting in the formation of stress fibers (Asanuma *et al.*, 2006). RhoA is expressed, in hippocampus (O'Kane *et al.*, 2003) where activation is associated with a shorter spine neck length (Tashiro and Yuste, 2004).

Functional role of Synaptopodin in neurons

Our results indicate that a distinct splice variant, Synaptopodin II, is upregulated following electrical stimulation. In neurons Synaptopodin is localized to the neck of mature spines. In spines, actin is the major cytoskeletal component (Carlisle and Kennedy, 2005; Fischer *et al.*, 1998). Because Synaptopodin II has marked effects on the dynamics of the actin cytoskeleton, it is likely that the change in actin dynamics observed following electrical activity is mediated, at least partially, through Synaptopodin. Several studies indeed show that actin in spines undergoes a rapid turnover that is regulated by synaptic activity (Carlisle and Kennedy, 2005; Fischer *et al.*, 1998; Star *et al.*, 2002). Activation of the NMDA receptor results in a decrease of actin turnover (Carlisle and Kennedy, 2005; Okamoto *et al.*, 2004; Star *et al.*, 2002). Synaptopodin is expressed only in mature spines (i.e. those

that contain a spine apparatus). As lack of Synaptopodin expression in mouse is correlated with a lack of spine apparatus in the spine neck, and therefore a lack of mature spines (Deller *et al.*, 2003), upregulation of Synaptopodin II following electrical stimulation therefore may be associated with an increase in the number of mature spines (Yamazaki *et al.*, 2001).

Acknowledgements
We would like to thank Minetta Elgersma for technical assistence. Supported by ZON-MW (CDZ), NWO-ALW (CDZ) and NWO (PF).

References

Asanuma, K., K. Kim, J. Oh, L. Giardino, S. Chabanis, C. Faul, J. Reiser, and P. Mundel. 2005. Synaptopodin regulates the actin-bundling activity of alpha-actinin in an isoform-specific manner. *J Clin Invest*. 115:1188-98.

Asanuma, K., E. Yanagida-Asanuma, C. Faul, Y. Tomino, K. Kim, and P. Mundel. 2006. Synaptopodin orchestrates actin organization and cell motility via regulation of RhoA signalling. *Nat Cell Biol*. 8:485-91.

Bliss, T.V., and G.L. Collingridge. 1993. A synaptic model of memory: long-term potentiation in the hippocampus. *Nature*. 361:31-9.

Bradshaw, K.D., N.J. Emptage, and T.V. Bliss. 2003. A role for dendritic protein synthesis in hippocampal late LTP. *Eur J Neurosci*. 18:3150-2.

Brakeman, P.R., A.A. Lanahan, R. O'Brien, K. Roche, C.A. Barnes, R.L. Huganir, and P.F. Worley. 1997. Homer: a protein that selectively binds metabotropic glutamate receptors. *Nature*. 386:284-8.

Capani, F., M.E. Martone, T.J. Deerinck, and M.H. Ellisman. 2001. Selective localization of high concentrations of F-actin in subpopulations of dendritic spines in rat central nervous system: a three-dimensional electron microscopic study. *J Comp Neurol*. 435:156-70.

Carlisle, H.J., and M.B. Kennedy. 2005. Spine architecture and synaptic plasticity. *Trends Neurosci*. 28:182-7.

Czarnecki, K., C.A. Haas, C. Bas Orth, T. Deller, and M. Frotscher. 2005. Postnatal development of synaptopodin expression in the rodent hippocampus. *J Comp Neurol*. 490:133-44.

Deller, T., M. Korte, S. Chabanis, A. Drakew, H. Schwegler, G.G. Stefani, A. Zuniga, K. Schwarz, T. Bonhoeffer, R. Zeller, M. Frotscher, and P. Mundel. 2003. Synaptopodin-deficient mice lack a spine apparatus and show deficits in synaptic plasticity. *Proc Natl Acad Sci U S A*. 100:10494-9.

Deller, T., T. Merten, S.U. Roth, P. Mundel, and M. Frotscher. 2000a. Actin-associated protein synaptopodin in the rat hippocampal formation: localization in the spine neck and close association with the spine apparatus of principal neurons. *J Comp Neurol*. 418:164-81.

Deller, T., P. Mundel, and M. Frotscher. 2000b. Potential role of synaptopodin in spine motility by coupling actin to the spine apparatus. *Hippocampus*. 10:569-81.

Fischer, M., S. Kaech, D. Knutti, and A. Matus. 1998. Rapid actin-based plasticity in dendritic spines. *Neuron*. 20:847-54.

French, P.J., V. O'Connor, M.W. Jones, S. Davis, M.L. Errington, K. Voss, B. Truchet, C. Wotjak, T. Stean, V. Doyere, M. Maroun, S. Laroche, and T.V. Bliss. 2001. Subfield-specific immediate early gene expression associated with hippocampal long-term potentiation in vivo. *Eur J Neurosci*. 13:968-76.

Frey, U., M. Krug, K.G. Reymann, and H. Matthies. 1988. Anisomycin, an inhibitor of protein synthesis, blocks late phases of LTP phenomena in the hippocampal CA1 region in vitro. *Brain Res*. 452:57-65.

Guzowski, J.F., G.L. Lyford, G.D. Stevenson, F.P. Houston, J.L. McGaugh, P.F. Worley, and C.A. Barnes. 2000. Inhibition of activity-dependent arc protein expression in the rat hippocampus impairs the maintenance of long-term potentiation and the consolidation of long-term memory. *J Neurosci*. 20:3993-4001.

Guzowski, J.F., B.L. McNaughton, C.A. Barnes, and P.F. Worley. 1999. Environment-specific expression of the immediate-early gene Arc in hippocampal neuronal ensembles. *Nat Neurosci*. 2:1120-4.

Hall, J., K.L. Thomas, and B.J. Everitt. 2000. Rapid and selective induction of BDNF expression in the hippocampus during contextual learning. *Nat Neurosci*. 3:533-5.

Houtman, S.H., M. Rutteman, C.I. De Zeeuw, and P.J. French. 2007. Echinoderm microtubule-associated protein like protein 4, a member of the echinoderm microtubule-associated protein family, stabilizes microtubules. *Neuroscience*. 144:1373-82.

Inoue, Y., N. Honkura, A. Kato, S. Ogawa, H. Udo, K. Inokuchi, and H. Sugiyama. 2004. Activity-inducible protein Homer1a/Vesl-1S promotes redistribution of postsynaptic protein Homer1c/Vesl-1L in cultured rat hippocampal neurons. *Neurosci Lett*. 354:143-7.

Jones, M.W., M.L. Errington, P.J. French, A. Fine, T.V. Bliss, S. Garel, P. Charnay, B. Bozon, S. Laroche, and S. Davis. 2001. A requirement for the immediate early gene Zif268 in the expression of late LTP and long-term memories. *Nat Neurosci*. 4:289-96.

Kato, A., F. Ozawa, Y. Saitoh, K. Hirai, and K. Inokuchi. 1997. vesl, a gene encoding VASP/Ena family related protein, is upregulated during seizure, long-term potentiation and synaptogenesis. *FEBS Lett*. 412:183-9.

Kikuno, R., T. Nagase, K. Ishikawa, M. Hirosawa, N. Miyajima, A. Tanaka, H. Kotani, N. Nomura, and O. Ohara. 1999. Prediction of the coding sequences of unidentified human genes. XIV. The complete sequences of 100 new cDNA clones from brain which code for large proteins in vitro. *DNA Res*. 6:197-205.

Konietzko, U., G. Kauselmann, J. Scafidi, U. Staubli, H. Mikkers, A. Berns, M. Schweizer, R. Waltereit, and D. Kuhl. 1999. Pim kinase expression is induced by LTP stimulation and required for the consolidation of enduring LTP. *Embo J*. 18:3359-69.

Kremerskothen, J., C. Plaas, S. Kindler, M. Frotscher, and A. Barnekow. 2005. Synaptopodin, a molecule involved in the formation of the dendritic spine apparatus, is a dual actin/alpha-actinin binding protein. *J Neurochem*. 92:597-606.

Krug, M., B. Lossner, and T. Ott. 1984. Anisomycin blocks the late phase of long-term potentiation in the dentate gyrus of freely moving rats. *Brain Res Bull*. 13:39-42.

Matsuo, R., A. Kato, Y. Sakaki, and K. Inokuchi. 1998. Cataloging altered gene expression during rat hippocampal long-term potentiation by means of differential display. *Neurosci Lett*. 244:173-6.

Moita, M.A., R. Lamprecht, K. Nader, and J.E. LeDoux. 2002. A-kinase anchoring proteins in amygdala are involved in auditory fear memory. *Nat Neurosci*. 5:837-8.

Mundel, P., H.W. Heid, T.M. Mundel, M. Kruger, J. Reiser, and W. Kriz. 1997. Synaptopodin: an actin-associated protein in telencephalic dendrites and renal podocytes. *J Cell Biol*. 139:193-204.

Nakagawa, T., J.A. Engler, and M. Sheng. 2004. The dynamic turnover and functional roles of alpha-actinin in dendritic spines. *Neuropharmacology*. 47:734-45.

Nguyen, P.V., T. Abel, and E.R. Kandel. 1994. Requirement of a critical period of transcription for induction of a late phase of LTP. *Science*. 265:1104-7.

Nguyen, P.V., and E.R. Kandel. 1996. A macromolecular synthesis-dependent late phase of long-term potentiation requiring cAMP in the medial perforant pathway of rat hippocampal slices. *J Neurosci*. 16:3189-98.

O'Connor, V., A. Genin, S. Davis, K.K. Karishma, V. Doyere, C.I. De Zeeuw, G. Sanger, S.P. Hunt, G. Richter-Levin, J. Mallet, S. Laroche, T.V. Bliss, and P.J. French. 2004a. Differential amplification of intron-containing transcripts reveals long term potentiation-associated up-regulation of specific Pde10A phosphodiesterase splice variants. *J Biol Chem*. 279:15841-9.

O'Connor, V., S.H. Houtman, C.I. De Zeeuw, T.V. Bliss, and P.J. French. 2004b. Eml5, a novel WD40 domain protein expressed in rat brain. *Gene*. 336:127-37.

O'Kane, E.M., T.W. Stone, and B.J. Morris. 2003. Distribution of Rho family GTPases in the adult rat hippocampus and cerebellum. *Brain Res Mol Brain Res*. 114:1-8.

Okamoto, K., T. Nagai, A. Miyawaki, and Y. Hayashi. 2004. Rapid and persistent modulation of actin dynamics regulates postsynaptic reorganization underlying bidirectional plasticity. *Nat Neurosci*. 7:1104-12.

Otani, S., C.J. Marshall, W.P. Tate, G.V. Goddard, and W.C. Abraham. 1989. Maintenance of long-term potentiation in rat dentate gyrus requires protein synthesis but not messenger RNA synthesis immediately post-tetanization. *Neuroscience*. 28:519-26.

Peng, J., M.J. Kim, D. Cheng, D.M. Duong, S.P. Gygi, and M. Sheng. 2004. Semiquantitative proteomic analysis of rat forebrain postsynaptic density fractions by mass spectrometry. *J Biol Chem*. 279:21003-11.

Ridley, A.J. 2006. Rho GTPases and actin dynamics in membrane protrusions and vesicle trafficking. *Trends Cell Biol*. 16:522-9.

Roth, S.U., C. Sommer, P. Mundel, and M. Kiessling. 2001. Expression of synaptopodin, an actin-associated protein, in the rat hippocampus after limbic epilepsy. *Brain Pathol*. 11:169-81.

Star, E.N., D.J. Kwiatkowski, and V.N. Murthy. 2002. Rapid turnover of actin in dendritic spines and its regulation by activity. *Nat Neurosci*. 5:239-46.

Steward, O. 1994. Electroconvulsive seizures upregulate astroglial gene expression selectively in the dentate gyrus. *Brain Res Mol Brain Res*. 25:217-24.

Tashiro, A., and R. Yuste. 2004. Regulation of dendritic spine motility and stability by Rac1 and Rho kinase: evidence for two forms of spine motility. *Mol Cell Neurosci*. 26:429-40.

Thomas, K.L., S. Laroche, M.L. Errington, T.V. Bliss, and S.P. Hunt. 1994. Spatial and temporal changes in signal transduction pathways during LTP. *Neuron*. 13:737-45.

Wisden, W., M.L. Errington, S. Williams, S.B. Dunnett, C. Waters, D. Hitchcock, G. Evan, T.V. Bliss, and S.P. Hunt. 1990. Differential expression of immediate early genes in the hippocampus and spinal cord. *Neuron*. 4:603-14.

Worley, P.F., R.V. Bhat, J.M. Baraban, C.A. Erickson, B.L. McNaughton, and C.A. Barnes. 1993. Thresholds for synaptic activation of transcription factors in hippocampus: correlation with long-term enhancement. *J Neurosci*. 13:4776-86.

Wyszynski, M., V. Kharazia, R. Shanghvi, A. Rao, A.H. Beggs, A.M. Craig, R. Weinberg, and M. Sheng. 1998. Differential regional expression and ultrastructural localization of alpha-actinin-2, a putative NMDA receptor-anchoring protein, in rat brain. *J Neurosci*. 18:1383-92.

Wyszynski, M., J. Lin, A. Rao, E. Nigh, A.H. Beggs, A.M. Craig, and M. Sheng. 1997. Competitive binding of alpha-actinin and calmodulin to the NMDA receptor. *Nature*. 385:439-42.

Yamazaki, M., R. Matsuo, Y. Fukazawa, F. Ozawa, and K. Inokuchi. 2001. Regulated expression of an actin-associated protein, synaptopodin, during long-term potentiation. *J Neurochem*. 79:192-9.

Supplementary Data:

Exon 1	5'-AGCTGGACTCTGCACACACTGGAGAGGAAGTCGGCGGTGCCC-3'
Exon 2	5'-ATGGTTGACTCTGCTCTTGCTGGTCCCCTCTTCTTCCAAGTCCAC-3'
Exon 3	5'-CCTGGCCGACAAAGAGAGGAAAAATCCCACCTTGACAGTACCCGG-3'
Exon 4a	5'-ACTGTGTCTCAGATGAATTTTGTTGGACAGGGGTGATAGTGGCTG-3'
Exon 4b	5'-AAGACAGGCACTGGGATGTGTTACTTGAAGCAGAAGGAAGGTTTC-3'
Exon 5	5'-CCAAAGCTAAGGGTCAAAGACTACAGTACAGGCTCTTCCTCAGAG-3'

Table 1: Exon specific in situ hybridisation probes

	Forward	**Reverse**
Exon 2	5'-ATGGGACACCACCACTATCCAGAG-3'	5'-GACGCTGGCTGTCATCACTTTC-3'
Exon 3	5'-CAAGGTGGGATTTTTCCTC-3'	5'-CTCAAAGCCTCTGGAACAG-3'
Exon 4a	5'-ACCAGCTTCACAGAAAAGGATCTG-3'	5'-CTCTTGGCTGAGCTTTGGTGAC-3'
Exon 4b	5'-AAGTAACACATCCCAGTGCCTGTC-3'	5'-TGCCAGACCTTGAACCGTAGAC-3'
Exon 5	5'-TAGGCTACAACATCTGTCCTCGGG-3'	5'-TTCCTTGACCCCCCTTTTCTC-3'

Table 2: Exon specific PCR primers

	Forward	**Reverse**
Exon 2 - 3	5'-ATGGGACACCACCACTATCCAGAG-3'	5'-CTCAAAGCCTCTGGAACAG-3'
Exon 3 – 4a	5'-CAAGGTGGGATTTTTCCTC-3'	5'-CTCTTGGCTGAGCTTTGGTGAC-3'
Exon 4a – 4b	5'-TTCCTTCTCCACCCGGAATG-3'	5'-ATGGTCCACCTACAGTCACATGC-3'
Exon 4b - 5	5'-GGTCCTGCCTCCTGTTCTCAATAC-3'	5'-CGTTGATGATGTTGCGTGCC-3'

Table 3: Interexonal PCR primers

Construct	**Forward Primer**	**Reverse Primer**
SP 1-164	5'-AAGCACTCCAGCTCCCAAAGCC-3'	5'-CAATCAGGAGAATGCTGGACCTC-3'
SP 1-312	5'-AAGCACTCCAGCTCCCAAAGCC-3'	5'-GGTGGGGTAAAGTTTCCTAAGGG-3'
SP 1-505	5'-AAGCACTCCAGCTCCCAAAGCC-3'	5'-CGTATTTCTCCATCCGTGACTGG-3'
SP 144-312	5'-GAGGTCCAGCATTCTCCTGATTG-3'	5'-GGTGGGGTAAAGTTTCCTAAGGG-3'
SP 144-489	5'-GAGGTCCAGCATTCTCCTGATTG-3'	5'-CGTATTTCTCCATCCGTGACTGG-3'
SP 314-489	5'-CCACCTATGCGGAGACTTTGTC-3'	5'-CGTATTTCTCCATCCGTGACTGG-3'
SP 461-692	5'-GCCCAAACCCAACCAGAATC-3'	5'-GAAGGTACCACTTGAAGCAGAAGGAAGGTT-3'
SP P319A 1	5'-CACCAAGCACTCCAGCTCCCAAAGCC-3'	5'-CATAGGTGGCGGGTGGGGTAAAGTTTC-3'
SP P319A 2	5'-TTTACCCCACCCGCCACCTATGCGGAG-3'	5'-AAAGGGGGGACAAGACAGGC-3'
SP P338A 1	5'-CACCAAGCACTCCAGCTCCCAAAGCC-3'	5'-GTAGAATAAGAGGCAGGAGACCTAACCTGG-3'
SP P338A 2	5'-GGTTAGGTCTCCTGCCTCTTATTCTACTG-3'	5'-AAAGGGGGGACAAGACAGGC-3'

Table 4: Primers used for deletion and mutation constructs

Chapter 5

General Discussion

5.1 Introduction

Many processes within a cell depend on an intrinsic network of filaments called the cytoskeleton. This cytoskeleton is required to determine and maintain cell shape, it is required for cell migration, and for intracellular transport of proteins and organelles. The cytoskeleton exist of microtubules, intermediate filaments and actin filaments (microfilaments). In neurons, microtubules are especially important for the delivery of organelles and proteins to the periphery, while the actin cytoskeleton is the major cytoskeleton component of spines. The cytoskeleton of cells is highly dynamic to be able to respond to e.g. migratory stimuli and adapt to changes in the environment. Cytoskeletal dynamics is regulated by proteins that associate with the cytoskeleton. One of such associated proteins in sea urchins (Echinoidea) is the Echinoderm Microtubule Associated Protein (EMAP). EMAP is the major microtubule associated protein in sea urchins and several mammalian homologs have been identified (Eml1-5). In chapter 2 we have characterized one of the mammalian homologs of EMAP, Eml4. In Chapter 3 we describe the identification of Eml5. Chapter 4 describes a functionally characterization study of Synaptopodin, an actin associated protein. Below we will discuss the main findings of this thesis.

5.2 Echinoderm Microtubule Associated Protein like proteins.

Echinoderm microtubule associated protein (EMAP) is the major microtubule associated protein (MAP) in dividing sea urchin eggs. Four mammalian homologs of EMAP are previously identified, Eml1-4 (Eudy *et al.*, 1997; Heidebrecht *et al.*, 2000; Jin *et al.*, 2004; Lepley *et al.*, 1999; Pollmann *et al.*, 2006; Pozuelo Rubio *et al.*, 2004) whereas a fifth Eml family member, Eml5 is described in Chapter 3.

5.2.1 Eml domains and splice variants

The protein sequences of all five mammalian Emls are highly conserved and contain several distinctive domains. All Eml family members contain a hydrophobic EMAP like (HELP) domain, a domain that is unique for this family. In addition, Emls always contain a coiled coil dimerization domain and multiple WD40 protein protein interacting domains (Hamill *et al.*, 1998; Li *et al.*, 1998; Pollmann *et al.*, 2006; Suprenant *et al.*, 2000). It has been suggested that the HELP domain is required for microtubule binding (Eichenmuller *et al.*, 2002), but in a recent study by Pollmann *et al.* (2006) the HELP domain of Eml4, fused to GFP, failed to colocalize with microtubules. Instead, these authors show that the first 249 amino acids of Eml4 are sufficient to bind microtubules. The exact function of the HELP domain therefore remains to be determined.

Protein domain databases (http://pfam.sanger.ac.uk/family?acc=PF03451) show a predicted transmembrane helix within the HELP domain. However, no localization of any Eml family member to the membrane has been described. The presence of a coiled coil in all Eml family members suggests that homo- or heterodimers can be formed (Beck and Brodsky, 1998). Whether such dimers exist remains to be determined. The third domain present in all Eml family members is the WD40 domain. In general, WD40 domains consist of approximately 4 to 16 WD repeats. These repeats are 40 amino acids in length and often end with a Tryptophan-Aspartic acid (W-D) dipeptide. Each repeat forms a blade of a propeller like structure that functions as a protein-protein interaction domain. These WD40 domains are present in many proteins of all eukaryotes, and are involved in a variety of functions.
Apart of these domains, Eml1, 2 and 4 contain a single EF hand, a domain involved in the binding of calcium. However, EF hands mainly occur in adjacent pairs and the functional significance of a single motif remains to be established (Lewit-Bentley and Rety, 2000).

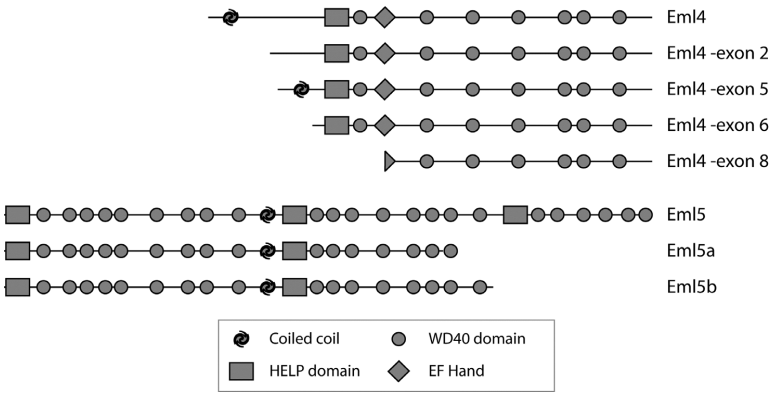

Figure 1 Protein structures of Eml4 and Eml5 splice-variants.

In chapter 2 and 3 we show that similar to many other mammalian proteins, Eml4 and Eml5 are both alternatively spliced. On protein level, the effect of splicing is different for Eml4 and Eml5 (see figure 1). Eml4 splice variants show differences in domain structure on the N-terminal whereas, Eml5 splice variants (Eml5a and Eml5b) have a premature stopcodon, resulting in truncated proteins. Given these results in Eml4 and Eml5 it can be expected that other Emls may also undergo alternative splicing.

5.2.2 Eml4 and Eml5 expression

Following the identification of the domains of the Eml family we investigated the spatio-temporal expression of two family members in chapter 2 and 3. Our

results indicate that *Eml4* and *Eml5* are mainly expressed in the CNS. *Eml4* is highly expressed during development after which the transcript is down regulated (Chapter 2). This developmentally regulated expression suggests that Eml4 plays an important role during development. In contrast *Eml5* expression was not detected in early stages of development (Chapter 3). *Eml5* expression levels increased during development and maintained at high levels in hippocampus, cerebellum and olfactory bulb. Non radioactive *in situ* hybridization showed that both *Eml4* and *Eml5* are expressed in post-mitotic neurons. Similar to *Eml4* and *Eml5*, *Eml1* is also expressed in the CNS. Other regions that express *Eml1* include PNS, liver and lung of mouse embryo (Blackshaw *et al.*, 2004). Our unpublished results confirm the expression pattern of Eml1. To date, no data have been published on the expression of Eml2 and Eml3 during development. Our unpublished observations indicate that *Eml2* expression during development is low and can be observed from E15 in mouse in some regions of the mouse. In contrast, the expression of *Eml3* appears to be mainly expressed during development in most regions of the mouse.

As *Eml4* and *Eml5* are mainly expressed in the CNS we further studied postnatal expression of these Emls in young (p10) and adult brain sections. Both *Eml4* and *Eml5* expression is restricted to the olfactory bulb, hippocampus and cerebellum in adult brain.

Interestingly, the expression of other *Emls* are also mainly restricted to these areas: *Eml1* in cerebellum, cortex, hippocampus and hindbrain (Blackshaw *et al.*, 2004), *Eml2* in olfactory bulb, hippocampus, cortex and brainstem, and *Eml3* is expressed in the hippocampus, thalamus and cerebellum (unpublished observations; www.brain-map.org). Our results also indicate that on the cellular level *Eml1* is expressed in Purkinje cells of the cerebellum (unpublished observation). Persistent expression of Emls in the adult brain suggests that they are required in post-mitotic neurons.

The role of Emls during development and in post-mitotic neurons is not know. However Eml4 is a microtubule stabilizing protein, which might ensure stable microtubules during axonal outgrowth. In the adult brain there is some evidence suggesting that Eml proteins can be involved in synaptic plasticity. For example Eml2 can bind to the delta2-glutamate receptor (Ly *et al.*, 2002). This receptor is only expressed in the cerebellar Purkinje cell, where it is required for long-term depression (LTD). Interestingly, the binding site within Eml2 for the δ2-glutmate receptor is conserved between the family members suggesting that other Emls, like Eml4 or Eml5, may also associate with this receptor. Another example is that Eml4 expression is down-regulated following nicotine stimulation (Dunckley and Lukas, 2003). The mechanism of Eml protein involvement with synaptic plasticity remains to be determined.

5.2.3 Microtubule interaction

We and others have demonstrated that Eml proteins can associate with microtubules (Chapter 2, Pollmann *et al.,* 2006). Furthermore, several members of the Eml family also affect the dynamics of microtubules. For example, Eml2 destabilizes the microtubule cytoskeleton by reducing the growth rate and promoting the frequency of catastrophes, while EMAP increases the microtubule dynamics and inhibits the frequency of rescue (Eichenmuller *et al.*, 2002; Hamill *et al.*, 1998). The results of both Emls is a shortening of microtubules. It was therefore hypothesized that the Eml protein family destabilizes microtubules. However, in chapter 2 we demonstrate that Eml4 does not destabilize the microtubules. In fact, Eml4 increased microtubule stability. Because Eml4 was first described as a restrictedly overexpressed proliferation-associated protein (Ropp-120) in mitotic cells and is highly expressed during development, Eml4 is likely to play a role in the stabilization of the microtubule cytoskeleton during cell division.
Despite the proposed microtubule stabilizing effect of Eml4, the function of the other members of the Eml family is not clear yet. The function of Eml1, Eml3 and Eml5 still has to be determined.

5.3 Synaptopodin

Synaptopodin is the founding member of a proline rich protein family. Other members of this family are Myopodin and Fesselin. Synapotopodin is expressed in renal podocytes, olfactory bulb, cerebral cortex, striatum and hippocampus. Myopodin is expressed in skeletal muscle and heart, and Fesselin is expressed in avian smooth muscle (Leinweber *et al.*, 1999; Weins *et al.*, 2001). With diverse protein domain searching (PFAM, SMART and PROSITE) machines no domains could be found in Synaptopodin. However, in Myopodin one PDZ domain could be identifies. The protein sequence of Fesselin is so far unknown, and mammalian homologs are not described (Schroeter and Chalovich, 2005).
In podocytes, Synaptopodin is involved in cell migration and in the formation of stress fibers (Asanuma *et al.*, 2006). In addition, Synaptopodin interacts with CD2AP and MAGI-1, thereby linking the cell surface receptors of the split diaphragm and the glomerular basement membrane (Faul *et al.*, 2007). This tight actin system is needed to form a protein barrier in the kidney. Mice lacking Synaptopodin may have proteinuria and/or focal segmental glomerulosclerosis (Huber *et al.*, 2006; Yanagida-Asanuma *et al.*, 2007).

5.3.1 Splice variants of Synaptopodin

Two splice variants of mouse Synaptopodin have been described: Synaptopodin long (isoform A; GenBank accession number NP_796314.2) and

Synaptopodin short (isoform B; GenBank accession number NP_001103445.1) (Asanuma *et al.*, 2005). In chapter 4 we show that, in rat brain, also two isoforms of Synaptopodin are also present. Synaptopodin II is the rat homolog of Synaptopodin short, while Synaptopodin I appears to be a novel isoform (GenBank accession number rat: Q9Z327; mouse: Q8CC35) and consists of exon 2, 4a and 4b (figure 2). Both isoforms are expressed in hippocampus and cortex, but only Synaptopodin II expression is associated with activity. As Synaptopodin I and Synaptopodin II differ in their 5'-end it is likely that each variant has its own specific promoter.

In mice, Synaptopodin long is a splice variant containing exon 5. This isoform is reported not to be expressed in mouse brain tissue (Asanuma *et al.*, 2005). These observations are in line with our findings, as we were not able to show exon 5 expressed in rat brain (Chapter 4). The rat homolog of Synaptopodin long therefore does not appear in rat brain, thought it is possible that this homolog is expressed in rat kidney.

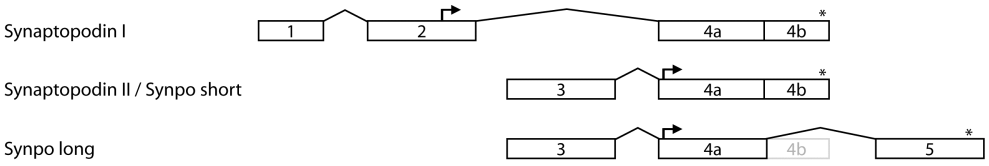

Figure 2. Three splice variants of Synaptopodin. The arrow is a startcodon, and the * a stopcodon.

5.3.2 Actin interaction

In chapter 4 we describe that Synaptopodin II and not Synaptopodin I is associated with electrical activation in rat brain. In mice, Synaptopodin long has been described to remodel the actin cytoskeleton (Kremerskothen *et al.*, 2005). However, Synaptopodin long and Synaptopodin II differ in their domain architecture as Synaptopodin II does not contain a putative a-actinin binding site. We therefore studied the cellular function of rat Synaptopodin II to determine whether this isoforms can also remodel the actin cytoskeleton.

Indeed, overexpression of Synaptopodin II in Cos7 cells, showed a colocalization with both F-actin and a-actinin and induces remodeling of the actin cytoskeleton.

To elucidate the functional domains in Synaptopodin II, we generated a series of deletion constructs. Our results indicate that two specific regions of Synaptopodin II colocalized with F-actin, namely SP144-489 and SP461-692 of which SP144-489 also induced remodeling of the actin cytoskeleton. Within this domain two PPXY motifs are present. PPXY motifs are putative protein interaction domains (Patrie *et al.*, 2002). However, disruption of one or both PPXY motifs did not significantly affect the remodeling capacity of

Synaptopodin II. We conclude from this data that these two putative protein interaction domains are not necessary for the remodeling capacity of Synaptopodin.

5.3.3 Function of Synaptopodin in neurons

In neurons, Synaptopodin is expressed in the spine neck and the axon initial segment. In the spine neck it is associated with the spine apparatus, while in the axon initial segment is associates with the cisternal organelle (Bas Orth *et al.*, 2007; Deller *et al.*, 2000). Although the cellular function of Synaptopodin in neurons is unknown, mice lacking Synaptopodin have a reduced LTP, impaired memory formation and spines without a spine apparatus (Deller *et al.*, 2003).

Synaptopodin has a marked effects on the dynamics of the actin cytoskeleton, therefore changes in actin dynamics observed following electrical activity could be mediated, at least partially, through Synaptopodin. Several studies indeed show that actin in spines undergoes a rapid turnover that is regulated by synaptic activity (Carlisle and Kennedy, 2005; Fischer *et al.*, 1998; Star *et al.*, 2002). Upregulation of Synaptopodin II following electrical stimulation therefore may be associated with an increase in actin dynamics.

5.4 Future plans

The current thesis presents data on Eml4 and Eml5 expression patterns during development and in the mature brain. In addition, we found that Eml4 is a microtubule stabilizing protein. Although Emls associate with microtubules and modify their dynamics, several key questions remain. These questions involve domain architecture and cellular function of Eml proteins.

The next step in understanding the function of Emls therefore is to investigate the interaction of Emls with other proteins. For instance, do the Emls form hetero- or homodimers? In what situations and are these dimers functional? An overexpression study of constructs without the coiled coil could show the functionality of this domain.

The functional role of the two other domains within Eml proteins, the HELP domain and WD40 domains, should also be investigated. First, the conserved HELP domain, thought to bind the microtubules, must be required for the functioning of Emls. So by using a microtubule binding protein spin-down kit in combination with full-length and/or deletion constructs of Eml proteins would show whether the HELP domain is required for microtubule binding.

Second, to understand the function of each Eml, a conditional knock-out mouse model will provide good insights. A conditional model should be used to prevent compensatory mechanisms, as we have already identified 5 Emls.

Third, a more general approach, is using techniques like yeast-2-hybrid, GST-pull down or biotin-streptavidin pull down assays. These techniques could show interaction of full-length Emls, or specific domains (HELP domain or WD40 domains) with proteins. The results of these experiments will show a functional network for the mammalian Emls.
To understand the effect of Eml1, 3 and 5 on microtubule dynamics a functional analysis should be performed. Such functional analysis can be done either by using overexpression studies, equal to described in chapter 2, by using RNAi in cells, and/or by *in vitro* polymerization studies as performed using Eml2 and EMAP (Eichenmuller *et al.*, 2002; Hamill *et al.*, 1998).
Chapter 4 of this thesis describes the function of Synaptopodin II on the dynamics of the actin cytoskeleton and the involvement in synaptic plasticity. However several questions remain to be answered. For example, what is the functional role of Synaptopodin splice variants? This question could be answered by 1). using splice variant specific antibodies to determine the cellular localization of Synaptopodin I and Synaptopodin II in neurons and 2) by generating splice variant specific knock outs to investigate the effect on hippocampal LTP and learning.
The second question that arises, is what are the binding partners of Synaptopodin; by using yeast-2-hybrid, GST-pull down or biotin-streptavidin pull down assays we could answer which splice variant can bind a-actinin, RhoA, MAGI-1 and other proteins that have to be identified.
Next we would like to investigate the role of Synaptopodin upregulation following electrical stimulation. Where are the Synaptopodin proteins expressed? And are they only in the spines that have been potentiated? To answer this question a combination of bleaching Synaptopodin-GFP, Ca^{2+} imaging and stimulation of cultured hippocampal neurons should be tried.
The last question that remains to be answered is what the role of Synaptopodin is in the axonal initial segment. In the absence of Synaptopodin, the cisternal orangelle, which is a Ca^{2+}-storage, is lost. The lost of this cisternal organelle may affect the excitability of pyramidal cells (Benedeczky *et al.*, 1994).

Together, these experiments could unravel the function and the network of both Eml family members and Synaptopodin in neuronal development and plasticity.

5.5 References

Asanuma, K., K. Kim, J. Oh, L. Giardino, S. Chabanis, C. Faul, J. Reiser, and P. Mundel. 2005. Synaptopodin regulates the actin-bundling activity of alpha-actinin in an isoform-specific manner. *J Clin Invest*. 115:1188-98.

Asanuma, K., E. Yanagida-Asanuma, C. Faul, Y. Tomino, K. Kim, and P. Mundel. 2006. Synaptopodin orchestrates actin organization and cell motility via regulation of RhoA signalling. *Nat Cell Biol*. 8:485-91.

Bas Orth, C., C. Schultz, C.M. Muller, M. Frotscher, and T. Deller. 2007. Loss of the cisternal organelle in the axon initial segment of cortical neurons in synaptopodin-deficient mice. *J Comp Neurol*. 504:441-9.

Beck, K., and B. Brodsky. 1998. Supercoiled protein motifs: the collagen triple-helix and the alpha-helical coiled coil. *J Struct Biol*. 122:17-29.

Benedeczky, I., E. Molnar, and P. Somogyi. 1994. The cisternal organelle as a Ca(2+)-storing compartment associated with GABAergic synapses in the axon initial segment of hippocampal pyramidal neurones. *Exp Brain Res*. 101:216-30.

Blackshaw, S., S. Harpavat, J. Trimarchi, L. Cai, H. Huang, W.P. Kuo, G. Weber, K. Lee, R.E. Fraioli, S.H. Cho, R. Yung, E. Asch, L. Ohno-Machado, W.H. Wong, and C.L. Cepko. 2004. Genomic analysis of mouse retinal development. *PLoS Biol*. 2:E247.

Carlisle, H.J., and M.B. Kennedy. 2005. Spine architecture and synaptic plasticity. *Trends Neurosci*. 28:182-7.

Deller, T., M. Korte, S. Chabanis, A. Drakew, H. Schwegler, G.G. Stefani, A. Zuniga, K. Schwarz, T. Bonhoeffer, R. Zeller, M. Frotscher, and P. Mundel. 2003. Synaptopodin-deficient mice lack a spine apparatus and show deficits in synaptic plasticity. *Proc Natl Acad Sci U S A*. 100:10494-9.

Deller, T., T. Merten, S.U. Roth, P. Mundel, and M. Frotscher. 2000. Actin-associated protein synaptopodin in the rat hippocampal formation: localization in the spine neck and close association with the spine apparatus of principal neurons. *J Comp Neurol*. 418:164-81.

Dunckley, T., and R.J. Lukas. 2003. Nicotine modulates the expression of a diverse set of genes in the neuronal SH-SY5Y cell line. *J Biol Chem*. 278:15633-40.

Eichenmuller, B., P. Everley, J. Palange, D. Lepley, and K.A. Suprenant. 2002. The human EMAP-like protein-70 (ELP70) is a microtubule destabilizer that localizes to the mitotic apparatus. *J Biol Chem*. 277:1301-9.

Eudy, J.D., M. Ma-Edmonds, S.F. Yao, C.B. Talmadge, P.M. Kelley, M.D. Weston, W.J. Kimberling, and J. Sumegi. 1997. Isolation of a novel human homologue of the gene coding for echinoderm microtubule-associated protein (EMAP) from the Usher syndrome type 1a locus at 14q32. *Genomics*. 43:104-6.

Faul, C., K. Asanuma, E. Yanagida-Asanuma, K. Kim, and P. Mundel. 2007. Actin up: regulation of podocyte structure and function by components of the actin cytoskeleton. *Trends Cell Biol*. 17:428-37.

Fischer, M., S. Kaech, D. Knutti, and A. Matus. 1998. Rapid actin-based plasticity in dendritic spines. *Neuron*. 20:847-54.

Hamill, D.R., B. Howell, L. Cassimeris, and K.A. Suprenant. 1998. Purification of a WD repeat protein, EMAP, that promotes microtubule dynamics through an inhibition of rescue. *J Biol Chem*. 273:9285-91.

Heidebrecht, H.J., F. Buck, M. Pollmann, R. Siebert, and R. Parwaresch. 2000. Cloning and localization of C2orf2(ropp120), a previously unknown WD repeat protein. *Genomics*. 68:348-50.

Huber, T.B., C. Kwoh, H. Wu, K. Asanuma, M. Godel, B. Hartleben, K.J. Blumer, J.H. Miner, P. Mundel, and A.S. Shaw. 2006. Bigenic mouse models of focal segmental glomerulosclerosis involving pairwise interaction of CD2AP, Fyn, and synaptopodin. *J Clin Invest*. 116:1337-45.

Jin, J., F.D. Smith, C. Stark, C.D. Wells, J.P. Fawcett, S. Kulkarni, P. Metalnikov, P. O'Donnell, P. Taylor, L. Taylor, A. Zougman, J.R. Woodgett, L.K. Langeberg, J.D. Scott, and T. Pawson. 2004. Proteomic, functional, and domain-based analysis of in vivo 14-3-3 binding proteins involved in cytoskeletal regulation and cellular organization. *Curr Biol*. 14:1436-50.

Kremerskothen, J., C. Plaas, S. Kindler, M. Frotscher, and A. Barnekow. 2005. Synaptopodin, a molecule involved in the formation of the dendritic spine apparatus, is a dual actin/alpha-actinin binding protein. *J Neurochem*. 92:597-606.

Leinweber, B.D., R.S. Fredricksen, D.R. Hoffman, and J.M. Chalovich. 1999. Fesselin: a novel synaptopodin-like actin binding protein from muscle tissue. *J Muscle Res Cell Motil*. 20:539-45.

Lepley, D.M., J.M. Palange, and K.A. Suprenant. 1999. Sequence and expression patterns of a human EMAP-related protein-2 (HuEMAP-2). *Gene*. 237:343-9.

Lewit-Bentley, A., and S. Rety. 2000. EF-hand calcium-binding proteins. *Curr Opin Struct Biol*. 10:637-43.

Li, Q., M. Callaghan, and K.A. Suprenant. 1998. The 77-kDa echinoderm microtubule-associated protein (EMAP) shares epitopes with the mammalian brain MAPs, MAP-2 and tau. *Biochem Biophys Res Commun*. 250:502-5.

Ly, C.D., K.W. Roche, H.K. Lee, and R.J. Wenthold. 2002. Identification of rat EMAP, a delta-glutamate receptor binding protein. *Biochem Biophys Res Commun*. 291:85-90.

Patrie, K.M., A.J. Drescher, A. Welihinda, P. Mundel, and B. Margolis. 2002. Interaction of two actin-binding proteins, synaptopodin and alpha-actinin-4, with the tight junction protein MAGI-1. *J Biol Chem*. 277:30183-90.

Pollmann, M., R. Parwaresch, S. Adam-Klages, M.L. Kruse, F. Buck, and H.J. Heidebrecht. 2006. Human EML4, a novel member of the EMAP family, is essential for microtubule formation. *Exp Cell Res*. 312:3241-51.

Pozuelo Rubio, M., K.M. Geraghty, B.H. Wong, N.T. Wood, D.G. Campbell, N. Morrice, and C. Mackintosh. 2004. 14-3-3-affinity purification of over 200 human phosphoproteins reveals new links to regulation of cellular metabolism, proliferation and trafficking. *Biochem J*. 379:395-408.

Schroeter, M.M., and J.M. Chalovich. 2005. Fesselin binds to actin and myosin and inhibits actin-activated ATPase activity. *J Muscle Res Cell Motil*. 26:183-9.

Star, E.N., D.J. Kwiatkowski, and V.N. Murthy. 2002. Rapid turnover of actin in dendritic spines and its regulation by activity. *Nat Neurosci*. 5:239-46.

Suprenant, K.A., J.A. Tuxhorn, M.A. Daggett, D.P. Ahrens, A. Hostetler, J.M. Palange, C.E. VanWinkle, and B.T. Livingston. 2000. Conservation of the WD-repeat, microtubule-binding protein, EMAP, in sea urchins, humans, and the nematode C. elegans. *Dev Genes Evol*. 210:2-10.

Weins, A., K. Schwarz, C. Faul, L. Barisoni, W.A. Linke, and P. Mundel. 2001. Differentiation- and stress-dependent nuclear cytoplasmic redistribution of myopodin, a novel actin-bundling protein. *J Cell Biol*. 155:393-404.

Yanagida-Asanuma, E., K. Asanuma, K. Kim, M. Donnelly, H. Young Choi, J. Hyung Chang, S. Suetsugu, Y. Tomino, T. Takenawa, C. Faul, and P. Mundel. 2007. Synaptopodin protects against proteinuria by disrupting Cdc42:IRSp53:Mena signaling complexes in kidney podocytes. *Am J Pathol*. 171:415-27.

Summary

Summary

Many processes within a cell depend on an intrinsic network of filaments called the cytoskeleton. The cytoskeleton exists of microtubules, intermediate filaments and actin filaments (microfilaments) and is highly dynamic. Both microtubule and actin dynamics are regulated by proteins that associate with these filaments. In sea urchins, EMAP is the major microtubule associated protein and several mammalian homologs have been identified (Eml1-5).
Chapters 2 and 3 of this thesis focus on Eml4 and Eml5 respectively. Chapter 2 functionally characterizes Eml4. With *in situ* hybridization data we show that the overall expression of *Eml4* decreases during development. However within the CNS, PNS, and intestine the expression persists. Furthermore we describe that *Eml4* expression in the adult brain is restricted to the olfactory bulb, hippocampus, and cerebellum. Within these brain areas *Eml4* is expressed in post-mitotic neurons, e.g. pyramidal cells of the hippocampus and Purkinje cells in the cerebellum. Importantly, we are the first to demonstrate that Eml4 affects microtubule dynamics. In Cos7 cells, we show that overexpression of a GFP-tagged Eml4 results in elongated microtubules. Therefore we conclude that Eml4 is a microtubules stabilizing protein.
In Chapter 3 we describe the cloning and characterization of *Eml5*, a novel member of the EMAP protein family. Eml5 differs from other Eml family members as it is a 2.5-fold repeat of the complete EMAP protein. With *in situ* hybridization, we show that during development *Eml5* expression can be observed and expression persist in the adult brain. Here *Eml5* is expressed the cerebellum (Purkinje cells and granule cells), hippocampus (CA1 pyramidal cells and granule cells) and thalamus.

In chapter 4 we focus on Synaptopodin, an actin binding protein, that is regulated by neuronal activity. Our results indicate that two splice variants of Synaptopodin are expressed in rat hippocampus and cortex, namely Synaptopodin I and Synaptopodin II. Interestingly, we show that only one of these splice variants, Synaptopodin II, is regulated following electrical stimulation. Similar to mouse Synaptopodin, overexpression of full-length rat Synaptopodin II induces a clear rearrangement of the actin cytoskeleton. Because no known domains are described in Synaptopodin, we generated a nested set of deletion constructs to examine functional domains. Our results indicate that $SP_{144-489}$, is sufficient to colocalize and remodel the actin cytoskeleton. A second domain $SP_{461-692}$, is sufficient to colocalize with F-actin cytoskeleton but does not induce remodeling. Although, $SP_{144-489}$, contains two putative protein protein interacting domains (PPXY motifs), actin association and remodeling still occurs when both motifs are disrupted.

In summary, the effect of cytoskeleton associated proteins on the cytoskeleton dynamics during development and plasticity help us elucidate role of the cytoskeleton during these events.

Samenvatting

Samenvatting

Elk zoogdier bestaat uit miljoenen cellen. Hoewel deze cellen kunnen verschillen in functie is de opbouw van iedere cel vergelijkbaar. Elementen zoals de kern, het golgi apparaat, de mitochondrien en het cytoskelet komen voor in iedere cel. Het cytoskelet, oftewel skelet van de cel, is nodig om de vorm van de cel te behouden en is van belang voor de bewegelijkheid van een cel. Ook zorgt het cytoskelet voor het transport in de cel en kan worden vergeleken met een "wegennetwerk". Dit wegennetwerk bestaat uit actine filamenten (microfilamenten), intermediaire filamenten en microtubuli. In neuronen vormen de microtubuli de "snelwegen" die zorgen voor het transport naar alle uithoeken van de cel. Terwijl de actine filamenten zich bevinden aan de periferie en vormen daar de "locale wegen". Het cellulaire "wegennetwerk" is zeer dynamisch. Deze dynamiek wordt gereguleerd door eiwitten die binden aan de verschillende onderdelen van het netwerk. Om deze dynamiek te kunnen begrijpen is het van belang deze cytoskelet bindende eiwitten te bestuderen. Dit proefschrift beschrijft twee microtubuli bindende eiwitten en het effect dat zij hebben op de dynamiek van microtubuli en een actine bindend eiwit.

In hoofdstuk 2 en 3 richten we ons op twee microtubuli bindende eiwitten, namelijk Eml4 en Eml5. In hoofdstuk 2 beschrijven we waar *Eml4* mRNA tot expressie komt, zo laten we met behulp van *in situ* hybridisatie zien dat *Eml4* expressie gedurende de embryonale ontwikkeling afneemt. Ook laten we zien dat ondanks deze afname in specifieke gebieden de expressie van *Eml4* aanwezig blijft (CNS, PNS en darmen). In het volwassen brein komt *Eml4* voor in niet-delende neuronen van de bulbus olfactorius, hippocampus en cerebellum. Aangezien Eml4 tot expressie komt gedurende de ontwikkeling en in neuronen speelt Eml4 waarschijnlijk een rol in zowel de ontwikkeling als in neuronen.
Naast de expressie van Eml4 hebben we ook gekeken naar het effect van Eml4 op de microtubuli dynamiek. Dit hebben we gedaan door Eml4 te fuseren met GFP (groen fluorescerend eiwit) en tot overexpressie te brengen in Cos7 cellen. Uit dit experiment bleek dat de microtubuli circulaire structuren werden. Hieruit bleek voor het eerst dat Eml4 een microtubuli stabiliserend eiwit is.
In hoofdstuk 3 beschrijven we een nieuw lid van de Eml familie, Eml5. Het verschil tussen Eml5 en de andere leden van de familie is dat Eml5 ongeveer 2,5x de gehele Eml sequentie blijkt te bevatten. Hierdoor zijn domeinen die normaal gesproken maar 1 keer voorkomen (bijvoorbeeld het HELP domein), nu 3 keer aanwezig. Verder laten we zien dat *Eml5* mRNA voorkomt in de

granulaire cellen en Purkinje cellen van het cerebellum, de CA1 piramidale en granulaire cellen van de hippocampus en in neuronen van de thalamus. Hieruit blijkt dat er waarschijnlijk een belangrijke rol voor Eml5 is weggelegd in neuronen.
Verder laten we zien in hoofdstuk 2 en 3 dat zowel Eml4 als Eml5 alternatieve splicing ondergaan, waardoor meerdere eiwit isovormen van elke Eml tot expressie kunnen komen.

Na heb bestuderen van deze microtubuli bindende eiwitten hebben we ook gekeken naar een actine bindend eiwit, Synaptopodin (Hoofdstuk 4). Van dit eiwit is al bekend dat het verhoogd tot expressie komt bij specifieke activering van neuronen. Bij muizen die geen Synaptopodin tot expressie brengen is een vorm van synaptische plasticiteit (LTP) verminderd en ze scoren lager in een geheugen test. In hoofdstuk 4 laten we zien dat er in de hersenen twee isovormen van Synaptopodin aanwezig zijn (Synaptopodin I en Synaptopodin II), waarvan alleen Synaptopodin II verhoogd tot expressie komt na neuronale stimulatie. Verder laten we, met behulp van het tot overexpressie brengen van Synaptopodin II, zien dat Synaptopodin II colocaliseerd met het actine cytoskelet en deze moduleert. Om inzicht te krijgen welk gedeelte van Synaptopodin II hiervoor nodig is hebben we deletie constructen gemaakt. Deze deletie constructen laten zien dat een gedeelte van Synaptopodin, $SP_{144-489}$, voldoende is om de colocalizeren met actine en de dynamiek te veranderen. Een tweede domein, $SP_{461-692}$, blijkt ook te kunnen colocalizeren met actine, maar dit domein heeft geen effect op de dynamiek. In het eerste domein, $SP_{144-489}$, blijken twee eiwit bindende motieven te zitten. Echter, de colocalisatie en het effect op de dynamiek veranderde niet na het verstoren van deze motieven.
Uit deze resultaten kan geconcludeerd worden dat na neuronale stimulatie Synaptopodin II verhoogd tot expressie komt in neuronen. Door deze verhoogde expressie van Synaptopodin zal het actine cytoskelet moduleren, en op deze manier zal Synaptopodin II een bijdrage kunnen leveren aan het stabiliseren van synaptische contacten.

De resultaten als beschreven in dit proefschrift helpen ons bij het begrijpen van het effect van deze cytoskelet bindende eiwitten op de dynamiek van het cytoskelet. In het centrale zenuwstelsel zal dit een bijdrage leveren in het begrijpen van de rol van het cytoskelet en de dynamiek daarvan gedurende de embryonale ontwikkeling en in niet-delende neuronen. Daarnaast levert dit proefschrift een bijdrage aan de rol die het cytoskelet speelt in neuronale plasticiteit.

List of Publications

List of publications

Houtman SH*, Schonewille M*, Badura A, Amerika W, Cupido A, Boele HJ, Othsuki G, Belmeguenai A, Hosy E, Elgersma Y, Koekkoek SK, Hansel CH, De Zeeuw CI. The role of calcineurin mediated PF-PC LTP in cerebellar motor learning. *(in preparation)*.

Houtman SH, Schlager MA, De Zeeuw CI, French PJ. The expression of A Specific Synaptopodin Splice Variant is Associated with Activity and Induces Remodeling of the Actin Cytoskeleton. *(prepared for submission)*.

Houtman SH, Rutteman M, De Zeeuw CI, French PJ. (2007) Echinoderm microtubule-associated protein like protein 4, a member of the echinoderm microtubule-associated protein family, stabilizes microtubules. *Neuroscience 144:1373-82.*

Hansel C, de Jeu M, Belmeguenai A, **Houtman SH**, Buitendijk GH, Andreev D, De Zeeuw CI, Elgersma Y. (2006) alphaCaMKII Is essential for cerebellar LTD and motor learning. *Neuron 51(6):835-43.*

Roelofs RF, Fischer DF, **Houtman SH**, Sluijs JA, Van Haren W, Van Leeuwen FW, Hol EM. (2005) Adult human subventricular, subgranular, and subpial zones contain astrocytes with a specialized intermediate filament cytoskeleton. *Glia 52(4) 289-300.*

Meijer OC, Kalkhoven E, van der Laan S, Steenbergen PJ, **Houtman SH**, Dijkmans TF, Pearce D, de Kloet ER. (2005) Steroid receptor coactivator-1 splice variants differentially affect corticosteroid receptor signaling. *Endocrinology 146(3): 1438-48.*

O'Connor V, **Houtman SH**, De Zeeuw CI, Bliss TV, French PJ. (2004) Eml5, a novel WD40 domain protein expressed in rat brain. *Gene 336 (1):127-37.*

* Contributed equally

Curriculum Vitae

Curriculum Vitea

(door Gjalt Reitsma)

Het was op 10 juni 1977 dat Simone Hendrika Houtman werd geboren als eerste kind van Jannie en Kees Houtman. Als snel verhuisde de familie Houtman naar Dussen, waar Simone haar lagere school deed.

Toen Simone in 1989 naar het Atheneum in Raamsdonkveer ging was zij thuis in het gezelschap van een jongere broer en zus. Na een korte overstap naar de HAVO heeft Simone haar Atheneum diploma in september 1996 gehaald aan het Strabrecht College in Geldrop. Inmiddels was ze ook naar Geldrop verhuisd en had ze nog een broer gekregen. Ook had ze Judith leren kennen, met wie ze nog steeds veel contact heeft.

Ze moest weer verhuizen toen ze als student Biomedische Wetenschappen aan de Universiteit Leiden ging studeren. Als student heeft ze veel plezier gehad met haar vrienden Carlijn, Diana, Marissa, Eric en nog vele anderen. In diezelfde tijd heeft zij als student-assistent onder leiding van Mark Kruit aan de afdeling Radiologie van het Leids Universitair Medisch Centrum gewerkt. Hier heeft Simone meegeholpen een databank met genetisch materiaal aan te leggen van mensen met migraine. Als stagiair voor Roel Ophof en Arn van de Maagdenberg aan de afdeling Humane en Klinische Genetica van de Universiteit Leiden heeft zij vervolgens onderzoek gedaan naar de erfelijke eigenschappen van migraine met aura.

Een stage waar Simone met veel plezier op terug kijkt was aan de afdeling Medische Farmacologie van Ron de Kloet van de Universiteit Leiden. Hier heeft zij onderzoek gedaan onder begeleiding van Onno Meijer naar het effect van corticosteroïden op transcriptiefactoren in aanwezigheid van co-factoren. Als afsluitende stage heeft zij onderzoek gedaan naar de expressie van een eiwit, GFAP delta, op verschillende plaatsen in de hersenen aan het Nederlands Hersen Instituut onder leiding van Reinko Roelofs en Elly Hol.

In 2002 kreeg Simone van Chris de Zeeuw een baan aangeboden als AIO. Ik zal mij niet wagen aan een beschrijving van wat zij hier gedaan heeft. Dat kan elders in dit proefschrift gevonden worden.

Sinds 1 januari 2006 woont Simone samen met haar vriend. Wij zijn in blijde verwachting van een zoon die als alles goed gaat eind juli 2008 geboren zal worden.

Dankwoord

Dankwoord

Nu, na bijna 6 jaar is het zover; mijn promotie is in zicht en de laatste pagina's kunnen geschreven worden. Het dankwoord is een belangrijk onderdeel van dit proefschrift, aangezien dit boekje niet tot stand had kunnen komen zonder de hulp en steun van vele diverse mensen.

Als allereerste wil ik Chris, mijn promotor, bedanken. Bedankt voor alle vrijheid die je me de afgelopen jaren gegeven hebt. Hierdoor heb ik veel dingen geleerd en kunnen doen, zoals basale moleculaire biologie, het opereren en injecteren van muizen, gedragsproeven, histologie en uiteindelijk ook elektrofysiologie. Je was altijd enthousiast, en er waren altijd leuke proeven te doen. Bedankt voor deze dynamische en diverse tijd.

Pim, ook jij hebt als co-promoter een belangrijke bijdrage geleverd aan dit proefschrift. Ik ben (te) makkelijk afgeleid van de hoofdweg. Jij liet me afdwalen, maar zorgde dat ik uiteindelijk altijd weer terugkwam op die hoofdweg, zodat uiteindelijk toch dat geliefde artikel geschreven kon worden. Bedankt voor je eindeloze geduld en dat ik altijd m'n ei bij je kwijt kon (privé of werk, dat maakte niet uit).

Nou Mandy, nu ben jij dan eindelijk aan de beurt. Ik weet dat je liever wat hoger had gestaan, maar helaas... Ik wil jou graag bedanken in eerste instantie voor alle koffies, theeën en etentjes. Maar natuurlijk ook voor alle western blotjes, celkweekjes, muizenbusiness etc. Je bent van een gewaardeerde collega een goed vriendin geworden. Wat al wel blijkt uit het feit dat men al eerder dacht dat je m'n paranimf zou worden dan dat ik er zelf uit was. Maar geloof me ik vind het heel erg fijn dat je naast me staat.

Voornamelijk de eerste 4 jaar heb ik doorgebracht in Ee1271, het moleculaire lab. In het begin veel te ruim voor die paar mensen, maar wel gezellig met altijd leuke discussies. Bedankt Phebe, Jenn, Bjorn, Minetta, Hikke, Dmitri, Ruben, Eva en Rik. Een speciale dank gaat uit naar Max, je was een leuke en gemotiveerde student. Je wilde graag dingen weten die ik voor lief nam (zoals hoe het milliQ apparaat werkt) en ik vind het erg leuk dat je AIO bent geworden bij Casper. Heel veel succes met jouw boekje! De tweede student die ik graag bedank is Sahar, je hebt me geleerd dat het leven niet voor iedereen makkelijk is. Ik ben erg blij dat jij en je familie verder kunnen met jullie leven in Nederland. Geeske, ook jij verdient een apart stukje, alhoewel je dit waarschijnlijk overdreven vind. Ook jij loopt al erg lang rond op de afdeling en begon ooit in Ee1271. Je bent een bijzonder mens, en dat is iets heel positiefs! Ik vind het altijd erg gezellig om met je kletsen over van alles en nog

wat en hoop dat we contact houden. En natuurlijk ook jij heel veel succes met je boekje, het dankwoord schrijven is erg leuk!

Niemand begrijpt een vrouw beter dan een vrouw, we moeten "ventileren". Ook ik heb behoefte hieraan en gelukkig kon ik daarvoor terecht op het histo-lab (en natuurlijk ook voor het serieuze werk). Erika en Elize bedankt. Ook Loes, Edith en Ria wil ik graag bedanken voor alle gezelligheid, de snoepjes/koekjes en natuurlijk ook alle administratieve rompslomp waar jullie me mee geholpen hebben.

Bij de diverse onderzoeken die ik gedaan heb zijn er vele mensen die me geholpen hebben. Tom, in het begin van m'n AIO periode heb je me geleerd hoe ik injecties kon maken in de olijf en in de cerebellaire kernen. En met veel geduld heb je me de daarbij behorende anatomie proberen te leren, bedankt voor alle wijze lessen (inclusief die over de anatomie van het hart en de longen). Ype, jou wil ik graag bedanken voor de ondersteuning bij het fokken en "maken" van muizen. En natuurlijk Dick, bij het gebruiken van antilichamen kun je niet om jou heen. Bedankt voor je adviezen over de westerns, immuno's en natuurlijk voor al je humor. Casper, ook met jou heb ik heel kort een project gedaan, en ik hoop dat er nog wat met de resultaten gedaan wordt, bedankt.

Het laatste jaar heb ik voornamelijk door gebracht in het Hansel lab. Christian, volgens mij duurt het nog wel even voor je een "all-women" lab hebt, maar ik wens je heel veel succes in Chicago! Of course to all the (former) members of the Hansel lab thanks! Martijn (de R), het was altijd gezellig om met jou op een kamer te zitten, hoewel de gesprekken natuurlijk altijd maar over een ding gingen... Raghu, it was nice to get to know you, I enjoyed our time together on the Hansel lab, and how you learned me to use your set-up. Amor, also for you a thank you, especially for the (special) baseball lessons. And of course Gen, Boeke and Gao, I would also like to thank you all for tolerating my "I hate patching" moods.

Verder wil ik graag Martijn (S.) bedanken voor de fijne samenwerking en de gezellige gesprekken. Freek bedankt voor alle uitleg over electrofysiologie en waarom je dingen wel of niet wil corrigeren. En ik hoop dat je mooie resultaten boekt met de Nr2b muizen. Rob, Marcel en Tom (S) ook jullie wil ik hier graag even noemen. Het was altijd gezellig als ik met jullie derde jaars probeerde iets bij te brengen over de anatomie van de mens. Erik, ook jou wil ik graag bedanken, altijd gezellig om met je te kletsen als Pim er niet was om de telefoon op te nemen. En natuurlijk ook voor alle cellen die je voor me klaar hebt gezet! Jos, ook jij bedankt voor de gezellige tijd in de trein (of op het station). Hans bedankt voor alle gezellige gesprekken! Eddy, bedankt

voor alle ondersteuning met m'n computer en met plaatjes die nog even snel afgedrukt moesten worden. Ineke, ook jij bedankt, jouw oplettendheid bij alle dingen die ik via AMS aanvroeg heeft mij een hoop tijd en fouten gescheeld. Je bent voor al mijn muisproeven onmisbaar geweest. Iemand die ook zeker niet vergeten moet worden is Kees, je bent al een tijdje met pensioen, maar ik ging altijd met veel plezier naar jouw borrels. Eerst waren die achter de klapdeuren, en later beneden. Hier belde de baas dan wel eens naartoe als hij vond dat de afdeling wel erg rustig werd voor een vrijdagmiddag. Bedankt voor alle bitterballen en biertjes!

De afdeling Neurowetenschappen kent veel te veel mensen om allemaal te kunnen noemen in dit dankwoord. Het voordeel echter van zoveel collega's is dat je onderzoek erg divers is en je veel leert van andere methodes en gedachtenwijzes in de maandagochtend werkbesprekingen, hiervoor wil ik graag iedereen bedanken. Ik had nooit gedacht zoveel te leren over onder andere "grasping", RSI of whiplashes.

Naast alle collega's wil hier graag meteen gebruik maken om een aantal bijzondere mensen in mijn leven te bedanken. Te beginnen met twee zeer belangrijke mensen in mijn leven. Lieve papa en mama, bedankt voor jullie onvoorwaardelijke steun en liefde. Ook het feit dat jullie geen blad voor jullie mond nemen is uiteindelijk altijd erg fijn. Jullie hebben mij zeer liefdevol opgevoed en daar ben ik jullie (ondanks alle protest in m'n jeugd) nu erg dankbaar voor. Sebastiaan, je hebt het als mijn broertje niet altijd makkelijk gehad, maar ja ruzie met je maken stond in m'n takenbeschrijving. Je bent een schat van een vent en ik wens je heel veel moois en goeds toe. M'n enige zusje, Chantelle, je bent heel bijzonder en we lijken helemaal niet op elkaar hoor! Ik wens jou heel veel succes toe met KI en ik vind het heel leuk dat je me wilt bijstaan bij m'n verdediging. Christiaan, als jongste telg van de familie heb je wel wat te verduren, maar je bent er goed tegen bestand. Ik vond het erg leuk dat je stage bij me kwam lopen en hoop dat de toekomst je veel goeds brengt (je zult er misschien wel hard voor moeten werken hoor!). Oma ook u wil ik graag bedanken voor alle steun en gezelligheid.

Judith, ik ken je al vanaf het Strabrecht College en onze levens hebben er sinds die tijd heel anders uitgezien, jij in Maastricht, ik in Leiden en toch heeft onze vriendschap altijd stand gehouden. Bedankt voor alle gezellige bezoekjes en natuurlijk de geweldige skivakanties! Carlijn, jou ken ik al vanaf de El Cid en natuurlijk de Ravenhorst. Bedankt voor alle goede zorgen in die lange tijd, we wonen misschien niet meer in dezelfde flat, maar ik vind het erg leuk dat we nu allebei in Den Haag wonen. Diana, ook jou wil ik graag bedanken voor alle gezellige etentjes en stapavondjes en ik wens jou en Bart

9 mei de mooiste dag van jullie leven toe! Marissa, jou wil ik bedanken voor alle gezelligheid, etentjes en lunches. Ik wens jou nog veel succes met het afronden van jouw boekje, en dan natuurlijk met de opleiding! Caroliene, Allard en Jelle ook voor jullie een stukje hier. Jullie ken ik het kortst van allemaal, maar dat is ook alweer ruim drie jaar. Bedankt voor alle tosti's en gezelligheid. Jullie staan altijd voor ons klaar en ik verwacht dat dit over 40 jaar nog steeds zo zal zijn. En ik kan niet wachten tot we gezellig met z'n zevenen op vakantie gaan!

Lieve Piet en Paulien, jullie hebben me drie jaar geleden met veel liefde opgenomen in jullie familie. Bedankt hiervoor en natuurlijk ook voor alle gezellige avonden, voor de informatie die jullie ons opsturen en alle raad die jullie ons geven. Hugo, de eerste keer dat je het vriendinnetje van je broer ontmoette vertelde we dat we gingen samenwonen. Het moet voor jou een rare gewaarwording zijn geweest, maar je bent een geweldige zwager.

Gjalt, als laatste wil ik jou graag bedanken. Je bent mijn grote liefde en ik bof met jou! Je vind het niet nodig dat ik je noem in dit dankwoord, maar je hebt dan zelf niet door hoeveel je voor mij betekent en dus ook hebt betekend voor dit boekje. De avondjes samen achter de computer in de Chasséstraat, of de lieve woorden als ik er even helemaal doorheen zat. Met andere woorden jouw onvoorwaardelijke liefde en steun betekenen heel veel voor mij. En ook ik kan niet wachten tot onze zoon er is! Ik heb zoveel zin in de rest van ons leven.

Simone